2022

Endogenous Neurosteroid Hormone Production and Early Oligodendricyte Development

Paige Winokur

ENDOGENOUS NEUROSTEROID HORMONE PRODUCTION AND EARLY OLIGODENDROCYTE DEVELOPMENT

A Thesis Presented to the Faculty of
The Rockefeller University
in Partial Fulfillment of the Requirements for
the degree of Doctor of Philosophy

by
Paige Winokur
June 2022

ENDOGENOUS NEUROSTEROID HORMONE PRODUCTION AND EARLY OLIGODENDROCYTE DEVELOPMENT

Paige Winokur, Ph.D.
The Rockefeller University 2022

The field of neuroendocrinology grew immensely with the realization that steroid hormone production is not confined to the adrenal and reproductive glands, but also occurs in the central nervous system (CNS). Steroids synthesized de novo in the brain and spinal cord are referred to as neurosteroid or neuroactive hormones, and encompass estrogens, androgens, glucocorticoids, and mineralocorticoids. Though all substrates and enzymes required for neurosteroid biosynthesis exhibit CNS expression, a thorough comprehension of their functionality is lacking. In addition to mediating stress responses, neurosteroids influence CNS-specific processes known to regulate neural development and pathology. Multiple sclerosis (MS), a debilitating neurodegenerative disorder classified by rampant demyelination, exemplifies the neuroendocrine crosstalk facilitated by CNS-resident steroids. Local steroid production from cholesterol, which also happens to be the primary lipid component of myelin sheaths, is critical to myelin repair.

Progesterone in particular is implicated in expediting remyelination following demyelinating insults in animal models via an unknown mechanism. Despite the established effect of progesterone on myelin regeneration, its impact on early myelinogenesis remains unclear. This observation inspired the work presented here, in which I investigated a potential role for progesterone in embryonic oligodendrocyte development. Applying the synthetic progestin Nestorone to mouse cerebellar slice cultures, I found that progesterone stimulates expression of the mature myelin protein, myelin basic protein. Curious as to whether this phenomenon mirrors progesterone-induced remyelination at the molecular level, I implemented the same experimental system in mice genetically altered to delete expression of the nuclear progesterone receptor. Unexpectedly, removal of this receptor from cerebellar slices led not only to an increase in myelin basic protein expression, but more robust oligodendrocyte maturation into myelinating cells actively extending processes to axons and participating in fiber formation.

The fact that this surprising effect could not be mediated by the nuclear progesterone receptor prompted me to examine potential caveats to studying individual hormones like progesterone in isolation. Due to the existence of multiple non-canonical progesterone receptors expressed in the CNS, the rapid metabolism of progesterone under physiological conditions, and endogenous astrocytic progesterone production, I opted to transition to a mouse devoid of all neurosteroid hormones. To this end, I obtained a transgenic strain with a mutation inhibiting activity of the enzyme that initiates steroid hormone biosynthesis from cholesterol. Histological analyses of E18.5 embryos revealed no differences between wild-type and knockout general anatomy, CNS architecture, or oligodendrocyte quantity and distribution in the brain and spinal

cord. I therefore concluded that access to maternal steroid hormones is sufficient to sustain the knockout mice until inevitable perinatal lethality.

Unconvinced that the apparent histological normalcy of the knockout CNS represented the full extent of oligodendrocyte functionality, I performed spinal cord explant experiments in which uniform segments of spinal cords dissected from E12.5 embryos were cultured for four days with no exposure to steroid hormones. In this protocol, fluorescent staining with oligodendrocyte transcription factor Nkx2.2 and myelin basic protein revealed a novel CNS phenotype attributed to neurosteroid deficiency. Diffuse Nkx2.2 and myelin basic protein staining was evident across genotypes. However, the explants from knockout embryos also contained a significantly elevated concentration of myelin basic protein-positive cells along the entirety of the midline in the tissue. While further studies are necessary to determine the nature of this abnormality, the results described here suggest excess oligodendrocyte production and/or proliferation defects in spinal cord tissue deprived of neurosteroid hormones may be at play. With our limited understanding of the intricacies governing oligodendrocyte development from neural precursors, relevant neurosteroid activity undoubtedly warrants ongoing pursuit.

Taken together, the data holds diverse implications for neurosteroid involvement in oligodendrocyte development, distinct from the myelin repair so urgently needed in MS patients. Spontaneous remyelination proceeds relatively normally in early acute lesions, but progressively declines over time as lesions become chronic and prone to glial scarring and accumulation of inflammatory cellular debris. My finding that unlike in myelin regeneration, progesterone-induced effects on developmental myelin formation do not rely on signaling through the nuclear progesterone receptor, reaffirms the notion that simply recapitulating the process of early oligodendrocyte maturation is inadequate to treat degenerative disorders like MS. The capacity of a sex hormone like progesterone to exert such remarkable effects on oligodendrocyte behavior is in accordance with the striking gender differences characterizing MS, which is nearly three times more common in women but typically more severe in men. Gender-based variations in steroid hormone levels over the course of a lifetime certainly must be considered. Conceivably, men and women may respond uniquely to various pharmacological interventions; thus, MS treatment modalities cannot be approached with a “one size fits all” mentality. Future therapeutic improvements are incumbent on accounting for the explicit sexual dimorphism of MS, to which neurosteroid hormones assuredly contribute.

In loving memory of a biological pioneer with the purist of hearts, Dr. Bruce McEwen, the driving force behind the inquisitive and collaborative spirit this work embodies.

ACKNOWLEDGMENTS

I was originally drawn to Rockefeller by the unparalleled opportunities for collaboration and lack of barriers to the scientific enterprise. The culmination of my graduate studies here is truly a manifestation of a team effort in every sense of the phrase. It is my privilege and honor to acknowledge those who have given of themselves to champion my path thus far.

To my advisors, Bruce McEwen and Don Pfaff, and my co-advisor, Tim Vartanian: your collective willingness to first and foremost indulge my scientific curiosity throughout the (numerous) iterations of my thesis work is a testament to your belief in my capabilities as a researcher. When I first met with Bruce in his office to propose a collaboration, the collage of Schnauzer faces adorning the open door was all the reassurance I needed. I immediately knew Bruce was good people. This instinct could not have been more accurate. Against the backdrop of a pressure-filled and occasionally intimidating atmosphere within a city that constantly runs at an overwhelming pace, Bruce's authentic love of learning for the sole purpose of learning was refreshing, to say the least. I could rarely predict the trajectory of our discussions, but knew I would walk away somehow more intrigued and captivated by neuroendocrinology than before. Those conversations, though sorely missed, will never be forgotten. I would like to take a moment to express my gratitude towards Karen Bulloch for inviting me into her life after Bruce's passing. It is an absolute joy to be in her company when she is in the city. Don didn't hesitate to step in to fill Bruce's shoes as advisor, allowing my work to proceed as smoothly as possible amid such tragic loss and grief. His optimism was cautious, but his criticism always constructive.

Tim is ambition personified, his enthusiasm for each of his many roles as clinician, mentor, lab head, and father palpable. Upon initially contacting him to discuss a rotation in his lab at Weill Cornell, my expectation was that my email would be lost in a sea of more pressing emails, and at best, glanced at and ignored. Instead, Tim immediately invited me into his lab with open arms and never looked back. I am equally grateful for his academic direction and insistence on prioritizing the important things in life, most of which lie outside the lab.

To my thesis committee members, Shai Shaham and Sid Strickland: thank you for keeping me on track, even and especially when I felt no end was in sight. Shai's insights simultaneously propelled my project through periods of seeming stagnation and facilitated my recognition of the 'big picture' value of my data. Sid was eager to join my committee late in the game when I was suddenly in need of a third member. His encouragement and complimentary response to the narrative of my data along with my personal story will have a lasting impact on my confidence in myself as a scientist and beyond. Many thanks to Teresa Wood for her time and intellectual prowess serving as the external examiner for my thesis defense.

To the Dean's Office: Your attentiveness to my individual circumstances throughout my time at Rockefeller was a solace. Emily Harms has been reliably accessible and open to hearing and addressing my concerns. Sid and Emily are the reasons I was able to forge such a fruitful collaboration between Rockefeller and Weill

Cornell labs studying a disease about which I am passionate. I have had the pleasure of knowing Andrew Morris for about a decade at this point. From neuroscience professor to undergraduate thesis advisor to life mentor and, to be completely honest, resident Rockefeller therapist, Andrea has become one of my fiercest advocates. With each passing year, my appreciation for our relationship deepens, as she seamlessly morphs into the exact resource I require in the moment. Cris Rosario was the first person to greet me upon my arrival to the 2015 prospective student interview weekend. He is more than a friendly face around campus; he has mastered the art of meticulously organizing a diverse group of students and postdocs while maintaining his cordial and comforting demeanor. Thank you to the Dean's office for managing such a unique and transformative graduate program.

To the McEwen lab members: you went out of your way to ensure I felt at home in the lab despite the majority of my benchwork being done at Weill Cornell. Special thanks to Lucy Apicello for introducing me to everyone and including me in all of the lab events and celebrations. I have particularly fond recollections of the end of year festivities in 2019, specifically the Secret Santa exchange and the holiday luncheon. Bruce drew my name for Secret Santa, and gifted me a bottle of Frangelico with a coffee press, innocently oblivious to the fact that I do not drink alcohol or coffee. The box is still sitting untouched in my pantry, as I can't bring myself to give it away for sentimental reasons. The holiday lunch at Tony's is another cherished memory, marking the last time I interacted with Bruce. He would be proud to witness his lab members upholding his collegiality and avidity for neuroendocrinological research.

To the Vartanian lab members: you have shaped my daily life for the past seven years, first as colleagues, and now, as friends. Baohua Zhao's assistance was essential to the success of this work. Her generosity of time, treating my experiments with the same level of painstaking care given to her own, did not go unnoticed. Jenni Linden offered experimental advice, training sessions for unfamiliar protocols, and an objective voice of reason when troubleshooting was required. And troubleshooting was definitely required! Yinghua Ma's commitment to performing sound science and healthy skepticism when interpreting results influenced my approach to experimental design and enhanced my critical thinking skills. My many and varied discussions with Kiel Telesford, covering lab-related issues, philosophy, and everything in between, helped to humanize the at with a times mechanical aspect of benchwork. More often than not, he was simply reassuring me that I would, in fact, graduate Ph.D., and here we are.

To the Rockefeller BIRC: you brought my data to life in ways I never could have imagined. Christina Pyrgaki far exceeded her responsibilities as the 'operations manager' of the BIRC. Our hours spent together hunched over the confocal were rife with laughter, story-telling, and aspirational dialogues sharing our lifelong ambitions. Christina's innovative solutions to the imaging obstacles I encountered were certainly paramount to my work. Equally so was her solicitude and relatability as an academic, but more importantly, as a person. Ved Sharma provided me with the image processing and programming tools necessary to convey my data in an accurate and digestible manner. The time he took to explain his analytical rationales amplified my ability to

engage with and interpret the imaging data I collected. Together, Christina's camaraderie and Ved's ingenuity enriched my growth as a student, scientist, and human being.

To all of our collaborators: it goes without saying that the following body of work only exists due to your contributions. John Lydon of the Baylor College of Medicine provided the PRKO mice that were crucial to my progesterone experiments in cerebellar slices. Eric Schmidt of the Heintz lab at Rockefeller assisted with accessing and analyzing existing bacTRAP data to determine progesterone-related gene expression in oligodendrocytes. Narender Kumar of the Population Council offered his expertise on the progestin Nestorone and *in vivo* work with steroid hormones. Robert Miller of the George Washington School of Medicine and Health Sciences disclosed his vast knowledge of spinal cord explant culture, which proved critical to my troubleshooting efforts and eventual success with this experimental paradigm. I am indebted to Elizabeth Chlipala and Mark Butters of Premier Laboratory LLC, as well as Brad Bolon of GEMpath Inc., who were responsible for the sectioning and histopathological assessment of the steroid-hormone deficient mouse embryos, respectively. The sheer time and zeal they devoted to my project yielded a highly productive collaboration.

To my previous mentors: I would be remiss without emphasizing the degree to which your involvement in my academic and personal growth has enabled me to reach this point. I attribute my desire to pursue laboratory research largely to Steve Crocker of UConn Health, who served as my first formal PI during a summer internship. Within a matter of three months, he nurtured my passion for oligodendrocyte biology, encouraged me to participate in scholarly writing resulting in multiple publications, and fostered an environment of companionship that convinced me I wouldn't have wanted to spend my summer any other way. If there was even a sliver of doubt left in my mind that I belonged in the lab, Rachel Hoang and Andrea Morris, my undergraduate thesis advisors at Haverford, effectively put it to rest. By granting me the freedom to develop my own thesis and follow the data wherever it led, they exposed me to the exhilaration of the scientific process at its best. But their involvement in my life extended far beyond the bench. They were academic advisors, innate teachers, maternal figures, and the personification of why science is so worthwhile, all in one small but mighty package of effervescent best friends. I'm not sure I would have happily abandoned the comforts of my bed in the middle of the night to inject frogs with pregnancy-inducing hormones in the company of anyone else. I count myself fortunate to have been inspired so early on in my career by Steve, Rachel, and Andrea, and to have been able to further connect with Andrea in different capacities here at Rockefeller.

To Jess, Laura, and Mittsi: your relentless compassion has upended my entire definition of my identity in ways I never deemed possible. Whether resisting my imposter syndrome or challenging my internal conception of worthiness, you all epitomize the mutual trust I've found so elusive in relationships past. Your gentle guidance and unwavering support have been imperative to my ability to navigate this life I have created for myself as a graduate student. I now wait in avid anticipation to see how the knowledge we attained together will inform my future endeavors.

To my chosen family: there is a strong case to be made for comic relief in the midst of high-stress situations, and you never failed to deliver in this arena. With the unpredictable nature of a lab-centric lifestyle, Siya's steadfast commitment to our friendship is one I never had to question. By far the most empathic person I have met, Siya is a phenomenal listener, and an even better dog-walking companion. Sam, for better or for worse, has seen me at my best and my worst, both in and out of the lab. Witnessing our parallel journeys of personal growth as we pursue our individual career goals is truly cathartic. Jeannette has this uncanny tendency to meet my often cynical mindset with a fresh perspective that neither trivializes my experience nor promises unreasonable optimism. Her thoughtful advice reminds me that not everything has to be complicated; the simplest solution is usually the most effective. Jeanee is that friend I can lose touch with for months at a time without the slightest worry we won't pick right up where we left off next time we talk. Given our similar personalities, I still find it difficult to believe the amount of time it took us to acknowledge our compatibility. Aside from being quite the comedian, Jeanee exudes a rare combination of grit and grace that I have yet to encounter in anyone else. Her tenacity in the face of challenge after challenge and loyalty as a friend are nothing short of extraordinary.

To my biological family: Your unconditional love is my greatest consolation. My parents never push me to be perfect, but feverishly push me to live my fullest life while maintaining my sense of self. Mom and Dad accept and embrace my idiosyncrasies without letting them define my identity, something I frequently struggle to do independently. I couldn't be more grateful for the myriad ways in which our at times tenuous relationship has evolved over the course of the past 31 years. My parents' insistence on prioritizing my wellbeing above all else quite literally enabled me to reach this milestone of completing graduate school, and continues to lay the foundation for my trajectory moving forward. Carly, your love and respect for me is tangible, and I hope you can feel that it is mutual. My sister's work ethic, devotion to those close to her, and fearlessness in charting her own path are traits I aspire to incorporate into my own actions on a daily basis. Carly's presence in my life as a role model and friend is something I find myself cherishing more and more with each passing year. It does not surprise me at all that she refused to settle in the husband department. Although I still remember the day Josh called to inform me of his plans to propose to Carly, it now feels as if he has always been a part of the immediate family. Together, Carly and Josh are not only an indispensable addition to my support system, but have also made me the proudest dog aunt to Fenway.

If I've learned anything during my time at Rockefeller, it has to be that puppy therapy is hands down the best medicine. And that I have never been alone in striving to fulfill my scholastic and personal potential. My sincerest thanks to everyone who has impacted my experience at Rockefeller, thereby paving the way for the next phase of my life.

TABLE OF CONTENTS

LIST OF FIGURES

LIST OF TABLES

LIST OF ABBREVIATIONS

AD	Alzheimer's disease
Akt	protein kinase B
ALLO	allopregnanolone
bacTRAP	bacterial artificial chromosome translating ribosome affinity purification
BBB	blood-brain barrier
BDNF	brain-derived neurotrophic factor
bFGF	basic fibroblast growth factor
CNPase	2',3'-cyclic nucleotide-3'-phosphodiesterase
CNS	central nervous system
Cyb5d2	neuferricin
CYP11A1	cytochrome P450 Family 11 Subfamily A Member 1
DAPI	4',6-diamidino-2-phenylindole
Dbi	diazepam binding inhibitor
DCC	dextran-coated charcoal
DHP	5α-dihydroprogesterone
DMSO	dimethyl sulfoxide
ECM	extracellular matrix
ERK	extracellular signal-regulated kinase
FGF2	fibroblast growth factor 2
GABA	gamma-aminobutyric acid
GC/MS	gas chromatography/mass spectrometry
GFAP	glial fibrillary acidic protein
GFP	green fluorescent protein
Het	heterozygote
HIER	heat-induced epitope retrieval
Hsd3b7	3β-hydroxysteroid dehydrogenase
H&E	hematoxylin and eosin
IGF	insulin-like growth factor
IHC	immunohistochemistry
KO	knockout
MAG	myelin-associated glycoprotein
MAL	myelin and lymphocyte protein
MAPK	mitogen-activated protein kinase
MAPR	membrane-associated progesterone receptor
MBP	myelin basic protein
MS	multiple sclerosis
Nenf	neudesin neurotrophic factor
Nes	Nestorone
NGF	nerve growth factor
Nkx2.2	homeobox protein Nkx2.2
NPC	neural progenitor cell
nPR	nuclear progesterone receptor

Olig1	oligodendrocyte transcription factor 1
Olig2	oligodendrocyte transcription factor 2
OPA1	optic atrophy 1
OPC	oligodendrocyte progenitor cell
P0	glycoprotein zero
PBMC	peripheral blood mononuclear cell
PBS	phosphate-buffered saline
PCR	polymerase chain reaction
PDGF	platelet-derived growth factor
PFA	paraformaldehyde
PGRMC	progesterone receptor membrane component
PIER	proteolytic-induced epitope retrieval
PMNT	phenylethanolamine-N-methyltransferase
PMP22	peripheral myelin protein 22
PNS	peripheral nervous system
Preg	pregnenolone
PRKO	progesterone receptor knockout (mouse)
P4	progesterone
P450scc	cholesterol side-chain cleavage enzyme
RRMS	relapsing-remitting multiple sclerosis
RT	room temperature
Srd5a1	5α-reductase 1
Srd5a3	5α-reductase 3
StAR	steroidogenic acute regulatory protein
SVZ	subventricular zone
TBI	traumatic brain injury
TH	tyrosine hydroxylase
THP	3α,5α-tetrahydroprogesterone
TMPR	seven-transmembrane class 2 progestin and adipoQ receptor
TSPO	translocator protein
TUJ1	class III beta-tubulin
VVZ	ventral ventricular zone
VZ	ventricular zone
WT	wild-type

CHAPTER 1: Background and Introduction

1.1 Neurosteroid Hormones

1.1.1 Classification

The discovery of de novo steroid biosynthesis in the brain in the early 1980's marked a critical milestone in the advancement of neuroendocrine biology[1]. Accumulating evidence such as consistent progesterone (P4) levels in castrated and adrenalectomized rats, higher concentrations of some sterols in the central nervous system (CNS) than in peripheral fluids, and high brain pregnenolone (Preg) levels in newborn rats in the absence of significant adrenal sterol synthesis, all supported the concept of the brain as an independent steroidogenic organ[2-5]. Such neuroactive steroids, colloquially dubbed 'neurosteroids,' refer to steroids specifically generated in the nervous system as opposed to endocrine glands, namely the gonads and adrenal glands, or the placenta. Neurosteroid production occurs through endogenous means and from circulating sterols in both the CNS and peripheral nervous system (PNS). Classical CNS-derived neurosteroids include androstane- and pregnane-derived steroids that influence neuronal excitability through neuronal plasma membrane receptors and ion channels. Hormones such as cortisol, estrogen, and testosterone, though neuroactive as well, are categorized as peripheral steroid hormones, and generally signal through intracellular nuclear hormone receptors[6]. The vast majority of the current literature utilizes the term 'neurosteroid' to encompass all steroid hormones that induce effects within the CNS. Recent and ongoing studies continue to blur the distinction between CNS-derived and peripheral neurosteroids, many of which are now known to signal through nuclear as well as membrane-associated receptors[7].

Baulieu's pioneering work in the field revealed that multiple cell types in the brain have the capacity to synthesize neurosteroids, particularly glia; astrocytes; and hippocampal, cerebellar, and pineal neurons[8-10]. While free neurosteroids unbound to albumin can transfer between the CNS and the blood via the blood-brain barrier (BBB), their high lipophilicity typically doesn't permit frequent secretion into the circulation[11]. Instead, these neuroactive steroids tend to be confined to the membranes of the cells in which they were synthesized, leading to predominantly local downstream effects. Conservation of neurosteroid synthesis across mammals, birds, amphibians, and fish indicates the essential nature of this biological process[12-14]. The extent of the roles for neurosteroids in local brain signaling remains largely unknown. That being said, one popular hypothesis maintains that neurosteroids are critical during times of low steroid hormone levels in the circulation such as menstruation in females, and/or to increase naturally lower levels of P4 in males[15].

1.1.2 Biosynthesis

Unlike the intricacies of the physiological relevance of neurosteroids, their biosynthetic pathway has been studied meticulously. As mentioned above, circulating sterols that traverse the BBB can potentially serve as precursor molecules in neurosteroid synthesis[16]. However, this is not believed to be the primary mechanism. Instead, neurosteroid synthesis typically first requires the transport of cholesterol, either directly from the endoplasmic reticulum or from endocytosis of lipoproteins, into the mitochondrial membrane[17,18]. Numerous enzymes in the cytochrome p450 family are required for this initial step[19]. Further cholesterol transport from the outer to inner mitochondrial membrane is facilitated by the formation of a complex between steroidogenic acute regulatory protein (StAR) and translocator protein (TSPO), the latter serving as a pore granting cholesterol access to the inner membrane[18,20]. The viability of TSPO knockout (KO) mice suggests the evolution of multiple molecular methods of cholesterol transport[21]. The p450 side chain cleavage enzyme (p450scc) is responsible for catalyzing three mono-oxygenation reactions that generate Preg from cholesterol. Technically speaking, the mere presence of p450scc is sufficient to classify a cell as steroidogenic[18]. Preg is the immediate precursor to P4 and 17-hydroxypregnenolone[22]. Following its passive diffusion across the outer mitochondrial membrane, enzymes with high expression throughout the brain, namely 5α-reductase and 3α- and 5α-hydroxysteroid dehydrogenase, convert P4 to various metabolites including allopregnanolone (ALLO) and pregnanolone[23]. Estrogens, androgens, glucocorticoids, and mineralocorticoids are all ultimately derived from the conversion of cholesterol to Preg[24]. The fate of a particular neurosteroid hormone is dictated by expression and activity of local enzymes, as illustrated in Figure 1.1.

The extent of extracellular mediation of neurosteroid biosynthesis is unclear at this point. Intracellular second messengers like cyclic adenosine monophosphate and protein kinase A stimulate 5α-reductase activity. Phosphorylation of StAR and TSPO upregulate the import of cholesterol into the mitochondrial membrane, and has been linked to the onset of ovulation[25,26]. In this prime example of tightly coordinated peripheral and neurosteroid signaling, circulating estradiol increases P4 synthesis in hypothalamic astrocytes. The absence of P4 in turn inhibits luteinizing hormone secretion[27].

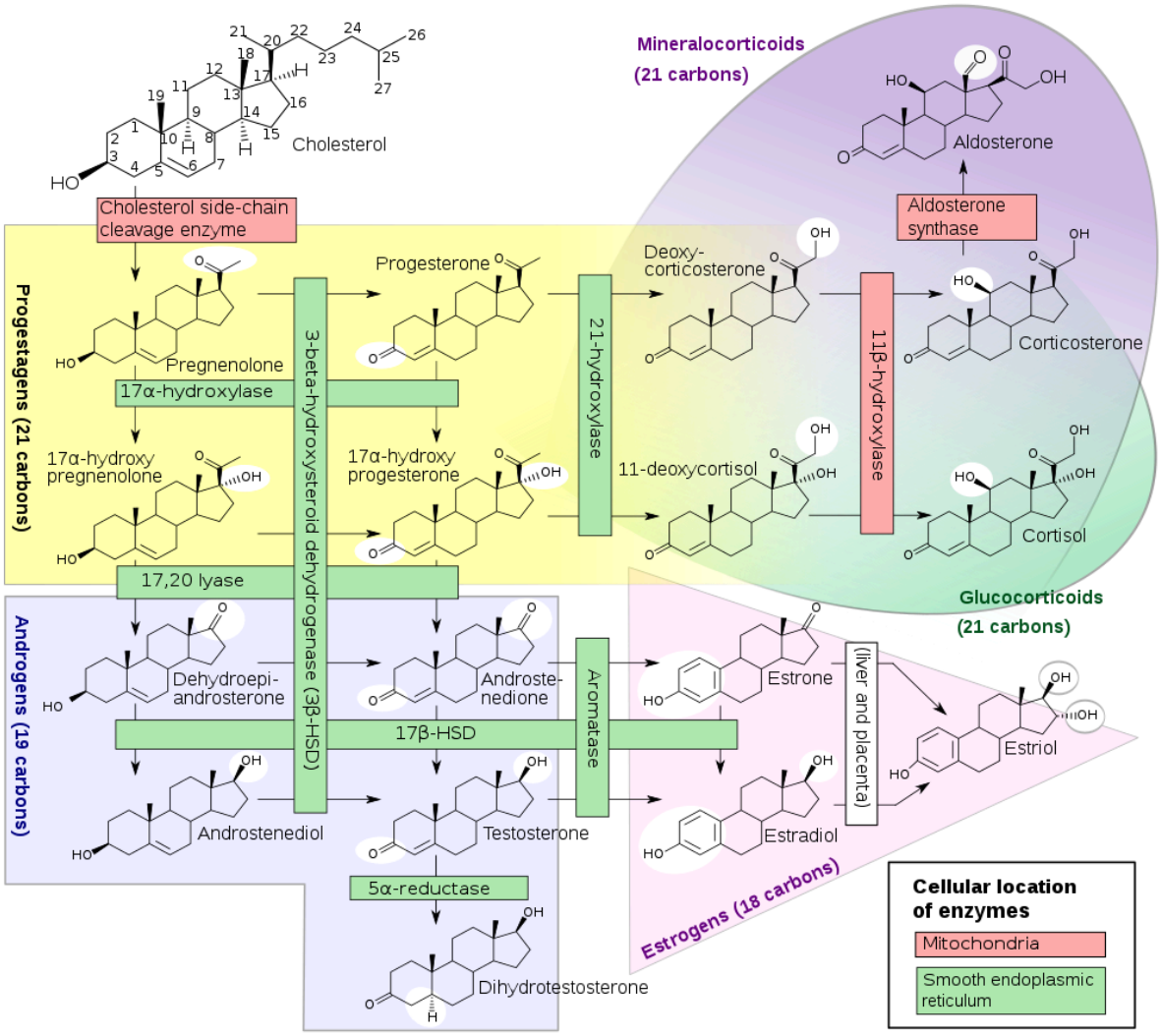

Figure 1.1: Neurosteroid biosynthetic pathway. All neurosteroid synthesis begins with the conversion of cholesterol that has been transported to the outer mitochondrial membrane into Preg. This step is required for the production of estrogens, androgens, glucocorticoids, and mineralocorticoids. Adapted from Häggström and Richfield, 2014[24].

1.2 Critical roles of the neurosteroid P4 in the CNS

1.2.1 Physiological functions

P4 is widely known to work in tandem with estradiol to mediate reproductive functions, such as uterine epithelial proliferation. However, these two hormones often exert CNS effects independently of each other[28]. Whereas estradiol has been shown to combat neuronal glutamate excitotoxicity, amyloid beta accumulation, and oxidative stress, emerging evidence suggests distinct roles for P4 in cognition and neuroprotection as well. P4 receptor expression identified by polymerase chain reaction

(PCR) throughout the brain does not exhibit strict localization to specific cell types[29]. The primary mechanisms by which P4 mediates CNS function include gene regulation at the expression level, direct effects on neurotransmitters, and stimulation of various signaling cascades. Prominent cascades involve activation of the mitogen-activated protein kinase (MAPK)/extracellular signal-regulated kinase (ERK) and protein kinase B (Akt) pathways, both associated with neuronal survival, especially in the context of ischemia[30,31].

In terms of memory, preliminary studies indicate a role for P4 in synaptic transmission and plasticity requisite for memory storage and learning. Under physiological conditions, P4 treatment may enhance hippocampal synaptic transmission as measured by increased field potential and population spike amplitude[32]. Interestingly, while both estrogen and P4 alone promote glutamate-mediated increases in intracellular calcium, combination treatment does not augment this effect, suggesting P4 can actually reduce the potency of estrogen action on synaptic transmission[33].

A prime example of the constant crosstalk between the nervous and endocrine systems is the modulation of mood and cognitive function throughout different phases of the menstrual cycle. Specifically, increased P4 levels during the luteal phase has repeatedly been linked to overall decline in mood[34,35]. In conditions such as premenstrual dysphoric disorder and postpartum depression, altered gamma-aminobutyric acid (GABA) receptor sensitivity is the chief biological factor at play[36]. P4 influences neuronal inhibition via augmentation of chloride conductance by GABA receptors, leading to postsynaptic membrane hyperpolarization[37].

The GABAergic system is also involved in cognitive tasks such as learning, memory accrual, face recognition, and reaction time. P4 diminishes acuity of memory-based performance in both humans and animal models[38-40]. Oral administration of P4 to women presented with a barrage of faces hindered their ability to accurately recognize the faces upon reintroduction. P4 appears to interfere with memory via the amygdala given the decreased amygdala and fusiform gyrus activity detected by magnetic resonance imaging[39]. Likewise, P4 treatment impedes the ability of rats to successfully navigate the Morris water maze[38,40]. In accordance with these observations of reduced cognitive capacity, P4 downregulates dendritic spine outgrowth to a similar extent as ovariectomization, thereby counteracting the pro-dendritic growth capacity of estrogen[41]. Signaling cascades initiated through P4 receptors found in hippocampal dendritic spines as well as GABA inhibition through GABA receptors provide evidence for indirect and direct P4 effects, respectively, on dendritic spine density indicative of synapse excitation. Corresponding variations in dendritic spine quantity over the course of the rodent estrous cycle are consistent with the suspected impact of P4 on general cognition[42].

The presence of P4 in all major glial cell types including astrocytes, microglia, and myelinating cells of the CNS (oligodendrocytes) and PNS (Schwann cells) has been thoroughly studied[28]. Astrocytic P4 modulates the production of proteins like ApoE that transport lipids to budding neurites, and thus enable synaptic plasticity, particularly during pregnancy upon the uterine introduction of maternal lipids[43]. This reserve of P4 can in turn stimulate macrophages to generate more ApoE in a cyclical manner. The

interplay between estrogens and P4 differs according to endocrine versus nervous system localization[44]. The lack of consensus regarding the relevance of P4 activity in isolation, especially in the CNS milieu, warrants further investigation.

Neurosteroid hormones were first identified in the PNS. Sciatic nerve Schwann cells express the classical nuclear P4 receptor (nPR), and contain the substrates needed to produce and metabolize P4. Several P4 derivatives, namely 5α-dihydroprogesterone (DHP) and 3α,5α-tetrahydroprogesterone (THP), control the expression of major PNS proteins glycoprotein zero (P0) via nPR and peripheral myelin protein 22 (PMP22) via the $GABA_A$ receptor[45]. Sex-dependent regulation of myelin proteins myelin-associated glycoprotein (MAG) and myelin and lymphocyte protein (MAL) are also attributed to activity of P4 and its derivatives[46]. The same metabolites were later shown to promote synthesis of CNS myelin proteins such as myelin basic protein (MBP) and 2',3'-cyclic nucleotide-3'-phosphodiesterase (CNPase). Although the mechanisms by which P4 and/or its metabolites regulate CNS myelination remain elusive, enhanced proliferation of oligodendrocyte progenitor cells (OPCs) has been proposed[15].

Indeed, P4 demonstrates positive effects on neurogenesis and neural progenitor proliferation, among other stages of neurodevelopment (Figure 1.2). Long-term P4 administration on the order of months significantly upregulate growth factors essential to endometrial cell proliferation in pregnant mares[47]. Similarly, growth factors in the brain like brain-derived neurotrophic factor (BDNF) increase with P4 levels and decrease with age after menopause[48]. The immediate P4 metabolite ALLO exhibits mitogenic behavior on par with that of basic fibroblast growth factor (bFGF) prior to OPC proliferation and migration[49,50]. Both CNS and plasma P4 stores fluctuate with menstrual cycle stage and age, providing yet another instance of the fluidity of CNS- and endocrine gland-derived steroid hormones[48].

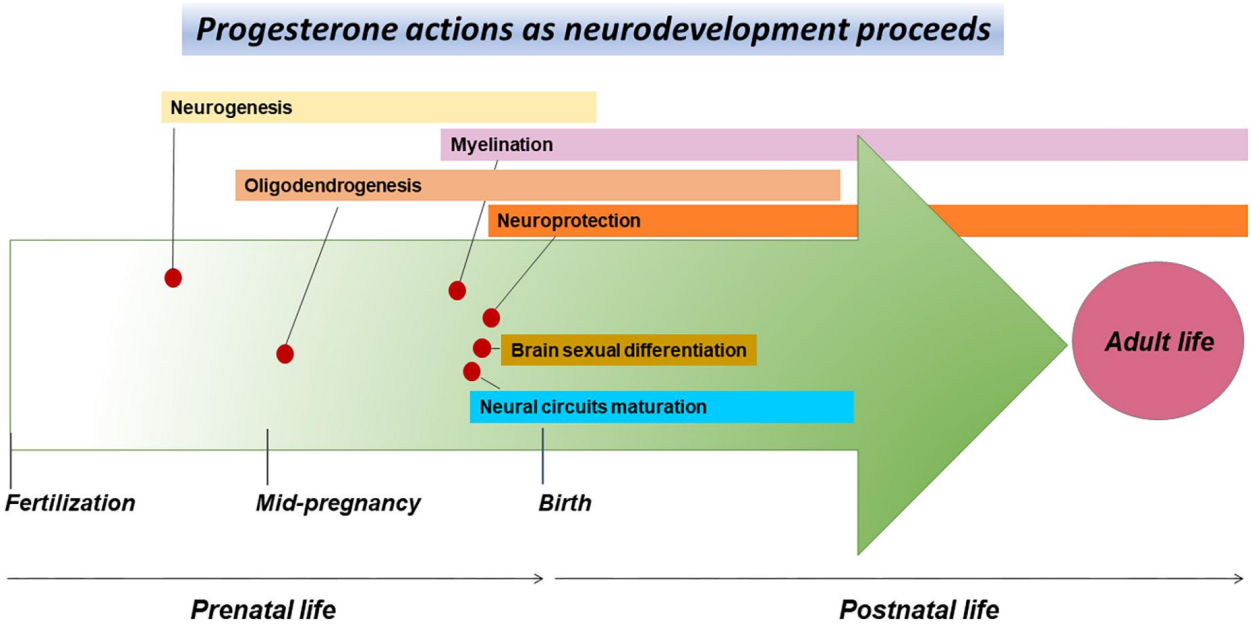

Figure 1.2: Influence of P4 throughout CNS development. P4 is essential to numerous neurodevelopmental milestones from prenatal to adult life. These events include neurogenesis, oligodendrogenesis, myelination, neuroprotection which later combats aging and disease, brain sexual differentiation, and maturation of neural circuits. Adapted from González-Orozco and Camacho-Arroyo, 2019[51].

Ample evidence in the literature supports the stimulatory effects of P4 signaling through nPR on OPC proliferation and morphogenesis into mature oligodendrocytes[28,52-56]. In fact, oligodendroglial production of P4 is tightly correlated with the maturation process itself. In a rather elegant model of the precisely orchestrated autocrine and paracrine signaling mechanisms implemented by P4, OPCs generate large quantities of P4, whereas myelinating oligodendrocytes are better equipped for P4 metabolism[57,58]. Briefly, OPCs produce P4, which promotes their vitality, thus cyclically allowing for further neurosteroid synthesis within mitochondrial membranes. P4 pre-treatment in yeast exposed to cytotoxic reactive oxygen species leads to mitochondrial uncoupling, a process associated with improved cellular fitness[59]. Considering the expansion and inefficiency of abnormal mitochondria characteristic of demyelinating disorders like multiple sclerosis (MS), patients may benefit from P4-induced mitochondrial maintenance.

1.2.2 Implications in CNS pathology

P4 has been proposed as a neuroprotective agent in a variety of CNS disorders including, but not limited to, epilepsy, ischemia, traumatic brain injury (TBI), Alzheimer's disease (AD), and MS[60]. The broad range of mechanisms by which P4 appears to confer its reparative properties demonstrates its versatility as a pro-survival factor in the brain. Experimental seizure paradigms involving kainate, pilocarpine, and pentylenetetrazole stimulation are quite sensitive to ALLO treatment. This P4 metabolite

simultaneously reduces the severity of seizure behaviors and attenuates neuronal injury in the hippocampus[61-64 65]. By directly enhancing chloride conductance through $GABA_A$ receptors, ALLO effectively dampens excitatory signaling, thereby preventing seizure activity[66].

Uncoupling the individual mechanisms through which P4 combats damage in the CNS is virtually impossible due to its rapid metabolism and diverse ligand interactions. In spinal cord injury models, for example, the hormone upregulates BDNF levels and greatly improves mitochondrial dysfunction[67,68]. The anti-inflammatory effects of P4 are especially prominent in ischemia, as is its ability to minimize oxidative stress by reducing production of free radicals like nitric oxide in the cerebrum[69]. Beyond neurons, P4-mediated signaling influences brain endothelial cells and glia, among other distinct cell populations. Reduced BBB permeability and microglial and astrocytic activation, in conjunction with increased myelination induced by P4, contribute to the amelioration of ischemic and other pathological insults on the CNS[70-72].

In depth studies of the restorative role of P4 in TBI confirm the benefits of both acute and long-term P4 administration. Immediate treatment with P4 diminishes cerebral edema, while consecutive days of P4 treatment up to one week leads to behavioral improvements as measured by spatial learning and additional sensory tasks[73]. P4 and ALLO, likely in tandem, modulate complement factors and inflammatory cytokines following TBI. The ensuing anti-inflammatory effect is particularly prevalent in models subjecting the medial frontal cortex to TBI[74].

Gender differences in the innate capacity for recovery from TBI are striking. Cerebral edema attributed to brain injury is significantly less pronounced in normally cycling female as opposed to male rats, and essentially non-existent in pseudopregnant females. Application of these studies to ovariectomized females suggests circulating P4 levels are inversely correlated with edema due to TBI[75]. As in many instances of CNS pathology, ALLO exhibits restorative capabilities comparable to those of P4. Both neurosteroids are anti-apoptotic via prevention of DNA fragmentation, inhibit lesion-induced astrocytic activation, and support retention of learning capacity and memory typically impacted by TBI[76,77]. Inspired by robust *in* vivo support for P4 as a therapeutic agent in brain injury, Stein et al. organized a clinical trial in comatose humans with TBI. Though less definitive in its findings than the rodent studies, this groundbreaking trial confirmed the possible healing properties of P4 in modern biomedical settings. This conclusion is based on the observation that surviving participants who received P4 had better diagnostic outcomes than those in the placebo cohort[78].

AD provides yet another example of the myriad ways in which P4 participates in pathological signaling cascades in the CNS. The widely accepted amyloid cascade hypothesis posits that an accumulation of soluble β-amyloid inevitably leads to the formation of insoluble clusters of aggravated β-amyloid peptides[79]. These fibrillar β-amyloid species then initiate a series of signaling cascades ultimately resulting in widespread neurodegeneration[80-84]. Gas chromatography/mass spectrometry (GC/MS) measurements of neurosteroids in several brain regions of aged AD versus non-demented human subjects revealed a correlation between low neurosteroid and high β-amyloid levels in AD patients. This trend lent credence to the hypothesis that

neurosteroids like P4 can regulate β-amyloid metabolism in the brain[85]. While estrogen has repeatedly been shown to impede β-amyloid pooling and memory loss in rodent AD models, neurosteroids rarely act in isolation[86-89]. Thus, of greater clinical interest are the synergistic effects of estrogen and P4 on AD pathology. Surprisingly, P4 seems to counteract the healing properties of estrogen in at least one mouse model of AD[90].

The benefits of P4 in demyelinating disorders like MS, unlike in AD, are well-established[54,91-94]. Myelin, the lipid-dense, oligodendrocyte-derived material ensheathing fast-conducting axons, is among the most compositionally and metabolically intricate structures in the vertebrate CNS[95]. In addition to its architectural complexity, myelin maintains axonal health and facilitates rapid saltatory conduction. Animals with larger brain volumes rely on CNS myelination to compensate for greater conduction distances[96]. The devastating consequences of myelin damage, especially in the brain as seen in MS, include cognitive decline, motor debilitation, and chronic pain[97].

Neurosteroid hormones like P4 offer a promising avenue for repair within a demyelinated microenvironment, i.e. an MS lesion, which becomes less permissive of myelin regeneration over time. P4 has been implicated in several dysmyelinating mouse phenotypes in addition to MS in humans. Notably, the brains of jimpy, shiverer, and wobbler mutant myelin mouse strains feature elevated P4 levels, suggesting P4 contributes to myelination[98]. Similarly, relapsing-remitting MS (RRMS) patients generate higher quantities of the P4 derivative, Preg, than do healthy, age-matched controls. The correlation between elevated Preg levels and MS pathogenesis suggests an endogenous response of the P4 synthesis pathway to CNS injury[99,100]. Examples of myelin regeneration stimulated by P4 are abundant in the literature where it is clear that P4 and synthetic derivatives like Nestorone (Nes) not only stimulate OPC migration and maturation in multiple demyelinating rodent models, but mitigate neurological and behavioral impediments associated with demyelination as well[46,54,57,92,93,100-107]. In fact, P4 synthesized in the CNS is generated from oligodendrocyte-derived cholesterol which comprises approximately 25% of the total myelin lipid profile[92,96,108,109].

Accordingly, ample evidence supports the stimulatory effects of P4 signaling through nPR on OPC proliferation and morphogenesis into mature oligodendrocytes[28,52-56]. This pro-differentiation effect has been described extensively[53,93,102,110-112]. Yet a coherent molecular mechanism connecting P4 receptors with their respective transcriptional and downstream targets is lacking. P4 appears to circumvent defective OPC maturation characteristic of MS lesions by upregulating pro-differentiation transcription factors including (oligodendrocyte transcription factors 1 and 2 (Olig1 and Olig2), and homeobox protein Nkx2.2 (Nkx2.2)[52]. Additional indirect mechanisms likely contribute substantially to myelin regeneration according to preliminary reports of P4-induced ERK1/2 activation and AKT phosphorylation, both of which in turn initiate signaling cascades favoring myelin regeneration and neuroprotection[107,112-117]. P4 synthesis itself may be neuroprotective, as evidenced by negative regulation of inflammatory responses in macrophages by TSPO, an essential actor in neurosteroidogenesis[118]. The profound impact of P4 on oligodendrocyte morphology and development is indubitably sufficient to challenge, if not overcome, the barrage of impediments to myelin regeneration within a lesioned microenvironment.

1.2.3 Therapeutic potential in MS

MS, the most prevalent demyelinating disease effecting neural transduction in the CNS, manifests clinically in heterogeneous motor, sensory, and cognitive symptoms[119]. Despite the widely accepted dogma that MS is an autoimmune disorder in which one's own immune cells attack and destroy myelin sheaths insulating axons of the brain and spinal cord, the origins of and explanations for many of the pathological hallmarks, namely failed myelin regeneration, remain unclear. Much like developmental myelination, successful remyelination of damaged axons requires proliferation, differentiation, and maturation of functional OPCs. In fact, demyelinated lesions that emerge in early stages of MS undergo rather robust myelin regeneration despite shorter myelin internodes that form fewer wraps than those characteristic of development. As the disease progresses, however, myelin regeneration predictably becomes increasingly inefficient, until it ceases entirely (Figure 1.3). Current treatment options are largely limited to immunosuppressants with adverse side effects that do not address the ultimate failure of myelin regeneration in a pathological context[120,121]. Investigators have documented an abundance of OPCs associated with lesions, thereby refuting theories based on OPC quantity and/or migration deficiencies[122-126]. An emerging relationship between endogenous sex hormones and the regenerative capacity of the CNS highlights the growing need to explore neurodegenerative diseases like MS from a neuroendocrine perspective[28,49,52,53,57,58,92,101-103,105,106,110,127-132].

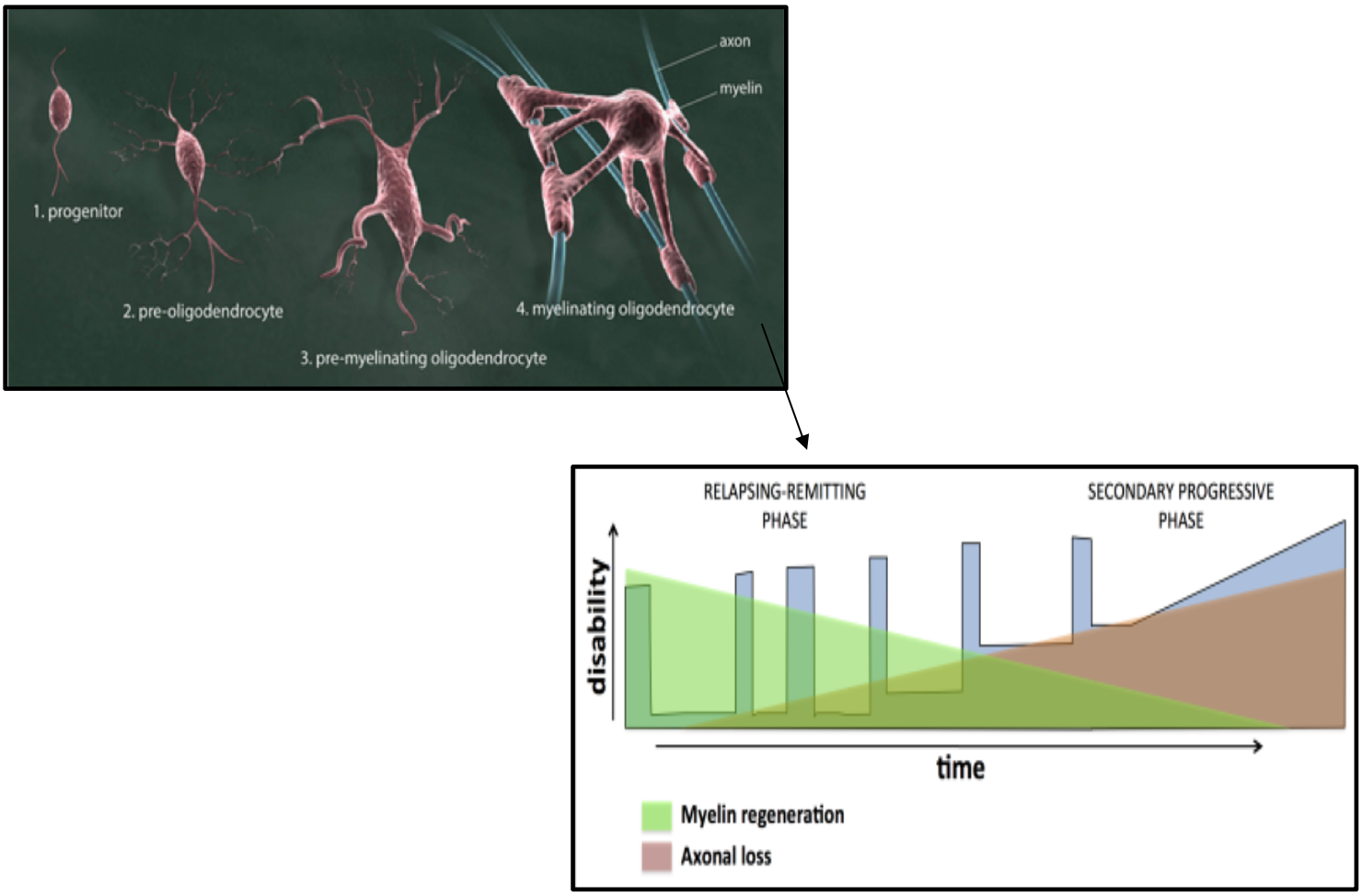

Figure 1.3: Myelin in physiology and disease. Developmental myelination requires proliferation, differentiation, and maturation of OPCs, as portrayed in the top image. While this is also true of myelin regeneration in demyelinating disorders, the disease course of MS, for example, suggests this is not the full story. The schematic on the right conveys the typical pattern of demyelinated lesions undergoing robust remyelination in early disease stages that progressively declines over time[133]. An abundance of OPCs surrounding lesions implies OPC migration and proliferation are normal, and the biological reasons for the differences between developmental and reparative myelination remain a mystery in the field.

The marked effects of P4 on myelin regeneration within the lesion environment offer compelling insight into the sexual dimorphism of MS[91,132]. As early as adolescence, white matter in males contains myelin with a higher g-ratio that is therefore thinner than white matter in females[134,135]. Note these data reflect a developmental stage during which sex hormones like P4 begin to differ significantly in concentration among males and females. While men are less susceptible to MS than women, they experience more rapid disease progression and heightened severity[136,137]. Speculative explanations for this phenomenon involve external factors such as smoking, low sunlight exposure and circulating vitamin D levels, higher childhood body mass index, and various contraceptive methods[138].

There is indeed precedent for sexual dimorphism of myelin protein gene expression in response to P4 and its metabolites DHP and THP in Schwann cells, the

myelinating cells of the PNS[139]. The aforementioned PNS proteins PMP22 and P0 vary in mRNA levels according to gender following treatment with P4, DHP, and THP, supporting neurosteroid effects on myelination as early as transcription[46]. Preliminary studies focused in the corpus callosum and cerebral cortex reveal that the synthetic, high-affinity nPR agonist Nes administered to female mice following cuprizone-induced demyelination increases the density of OPCs and mature oligodendrocytes, while stimulating production of MBP and proteolipid protein (PLP), and decreasing astrocytic and microglial activation[93,101]. Of particular interest, and depicted in Figure 1.4, is that increased estrogen and P4 levels during pregnancy exert beneficial effects on immune tolerance and correspond to reduced relapse rates in women with MS[140-143]. Based on the observation that P4 promotes remyelination, it is appropriate that women have a greater quantity of OPCs and turnover rate of oligodendrocytes[144]. High P4 levels in females in comparison to males may then enable more efficient remyelination of lesions.

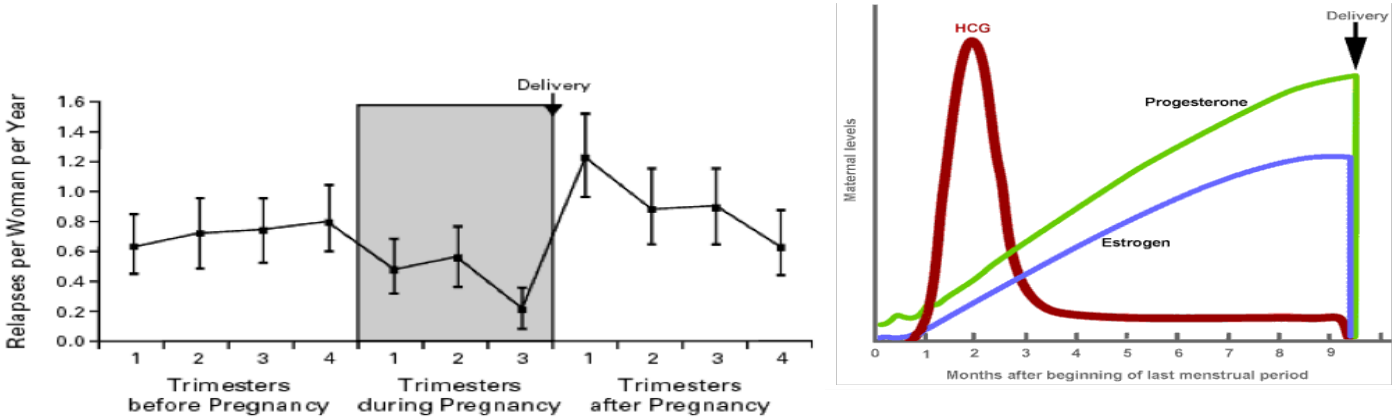

Figure 1.4: Correlation between P4 levels and MS relapse protection during pregnancy. As a sex hormone, P4 differs in abundance among genders and age groups within genders. Strikingly, MS exhibits clear sexual dimorphism in terms of prevalence and disease progression for as of yet undetermined reasons. Specifically, MS is an estimated two to five times more common in women, but generally more severe in men. Furthermore, relapse rates in women with MS drop significantly during pregnancy, but increase after delivery, as reflected in the graph on the left[145]. This trend is coincident with a surge and subsequent plummet in P4 shown in green on the right, supporting a correlation between P4 levels and MS symptoms.

1.3 Objectives

Emerging data highlighting the relevance of neuroendocrinology to neurodegenerative pathology depicts CNS-derived steroid hormones as potent regulators of disease progression and repair. A recent focus on the restorative properties of P4 and its metabolites in the context of demyelinating conditions mirroring those associated with MS provides a promising avenue for innovative treatment modalities fostering myelin restoration. Crucial to understanding the molecular mechanisms that account for P4-stimulated remyelination is determining the physiological relationship between neurosteroid hormones and myelin development.

Here, I describe my investigation of the contributions of endogenous neurosteroids to early CNS development by honing in on oligodendrocytes as an ideal cell type exhibiting a reproducibly robust response to P4 following myelin damage. *Ex vivo* cerebellar and spinal cord explant cultures performed in mice lacking nPR and the cytochrome P450 Family 11 Subfamily A Member 1 (CYP11A1) gene necessary for neurosteroid synthesis, respectively, have helped to elucidate P4 and overall neurosteroid functionality in early postnatal and embryonic CNS development. Accompanied by chemical staining and immunohistochemistry of basic neural as well as specific oligodendrocyte protein markers, these experiments reveal both the complexities of neurosteroid signaling and its vast potential to ameliorate, if not reverse, the biological and clinical manifestations of demyelination.

Chapter 3 explores the impact of a synthetic P4 derivative on early oligodendrocyte development via imaging of cerebellar, myelin-related proteins in the early neonatal mouse brain. Replicated in mice deficient in the classical nPR, these studies highlight the many nuances of neurosteroid signaling that complicate traditional molecular biology methods. A comprehensive review of these caveats follows.

Chapter 4 reassess the current understanding of neurosteroid functioning in the developing CNS using a model system devoid of all endogenous neurosteroid hormones. Late embryonic dissections of mice lacking an enzyme required for all neurosteroid synthesis complimented by histological analyses facilitates gross, anatomical, and molecular comparisons among the different genotypes. Follow-up histological and immunohistochemical efforts directed towards neuron- and oligodendrocyte-specific proteins hone in on putative roles for neurosteroid hormones like P4 in the CNS.

Chapter 5 incorporates an *ex* vivo spinal cord explant procedure in the same unique mouse strain introduced in Chapter 4 to probe the functional consequences of severe neurosteroid deficiency on embryonic CNS development, specifically oligodendrocyte progenitor maturation into myelinating oligodendroglial cells.

CHAPTER 2: MATERIALS AND METHODS

2.1 bacTRAP analysis

2.1.1 P4 genes in oligodendrocytes

Gene expression in oligodendrocytes was analyzed by the bacterial artificial chromosome translating ribosome affinity purification (bacTRAP) method as previously described[146,147]. Briefly, transgenic mice expressing eGFP-tagged ribosomal protein L10a (EGFP-L10a) in oligodendrocytes were used to affinity purify cell type specific polysomes from cortex. Polysome-bound mRNAs or mRNAs from whole tissue were analyzed by RNA sequencing. Evaluation of P4 receptor gene expression in oligodendrocytes versus whole brain was based on microarray data on Olig2-bacTRAP mice. This analysis was performed in collaboration with Dr. Eric Scmidt of the Heintz lab at Rockefeller University.

2.2 Animals

2.2.1 Mouse strains

All animal experiments were conducted in accordance with the guidelines of the United States National Institutes of Health Guide for the Care and Use of Laboratory Animals, and with approval from the Institutional Animal Care and Use Committee of Weill Cornell Medicine.

Two male mice heterozygous for the an nPR loss-of-function mutation on a C57BL/6 background were generously provided by Dr. John Lydon of Baylor College of Medicine in Houston, Texas. These mice were crossed with WT C57BL/6 female mice purchased from the Jackson Laboratory to initiate breeding. In the nPR knockout (PRKO) strain, female homozygotes, are sterile; therefore, in order to maintain the colony, male homozygotes were continually crossed with female heterozygotes (Hets). Wild-type (WT) littermates were used as controls in all experiments.

B6:129P-*Cyp11a1*$^{tm1(GFP/cre)Pzg}$/J transgenic mice, cryorecovered from the Jackson Laboratory (Stock No: 010988), contain a targeted, recombinase-expressing mutation in the first coding exon of the endogenous *Cyp11a1* locus. Mice heterozygous for the targeted mutation are viable, fertile, normal in size, and do not display any gross physical or behavioral abnormalities. Mice homozygous for the targeted mutation die shortly after birth presumably due to acute dehydration and electrolyte imbalances, not to mention their inability to convert cholesterol into Preg and produce neurosteroid hormones. WT littermates were used as controls in all experiments.

2.2.2 Genotyping

Genotyping of PRKO mice was performed using GoTaq® Green Master Mix (Promega, USA, M7122) with three PCR primers in the same reaction, the sequences of which were also provided by Dr. Lydon's lab. Primers 5'-CTT CAC CCA CCG GTA CCT TAC GCT TC-3' (L1) and 5'-GTG AGC ACT CCC CGA GGT A-3' (PZ4) identified the 140-base pair amplicon corresponding to the PRKO mutation allele. Primers 5'-CGG AGA AGG ACA GCA GAC TC-3' (PZ1) and PZ4 identified the 302-base pair amplicon corresponding to the WT P4 receptor allele. DNA for genotyping was isolated using the DNeasy Blood & Tissue Kit (Qiagen, Germany, 69506) from tail tissue. PCR results were visualized by gel electrophoresis on 1% agarose gels with ethidium bromide. PCR conditions are shown in Table 2.1.

Table 2.1: PCR conditions for genotyping of PRKO mice.

Step	Temperature (°C)	Time
Initial heat activation	95	5 min
Denaturing	94	50 s
Annealing	56	50 s
Extension	72	50 s
Cycles	Go to Step 2	30 times
Final extension	72	5 min
Hold	4	Forever

Genotyping of B6:129P-*Cyp11a1*$^{tm1(GFP/cre)Pzg}$/J transgenic mice was performed using GoTaq® Green Master Mix (Promega, USA, M7122) with three PCR primers in the same reaction. Primers 5'-GAG CTG CCT GCC AGT GTT TG-3' (Common) and 5'-GGA CCT AGG ACT GCT AGT AG-3' (WT) identified the 368-base pair amplicon corresponding to the WT allele, while the primers 5'-GTC CAG CTC GAC CAG GAT GG-3' (Mut) and Common identified the 296-base pair amplicon corresponding to the mutant allele. DNA for genotyping embryos was isolated using a rapid mouse tail DNA extraction kit (Thermo Fisher Scientific, USA, 101 BIO T605). PCR results were visualized by gel electrophoresis on 2% agarose gels with ethidium bromide. PCR conditions are shown in Table 2.2.

Table 2.2: PCR conditions for genotyping Cyp11a1 mice.

Step	Temperature (°C)	Time
Initial heat activation	95	2 min
Denaturing	94	30 s
Annealing	60	30 s
Extension	72	30 s
Cycles	Go to Step 2	30 times
Final extension	72	5 min
Hold	4	Forever

2.3 *Ex vivo* cerebellar slice culture

2.3.1 Cerebellar slice culture procedure

Organotypic cerebellar slice cultures were prepared according to established protocols by Stoppini et al. (1991) using brain tissue isolated from postnatal day 7 (P7) C57BL/6 mice[148]. Following decapitation, mice cerebella were removed from the skull and separated from the hindbrain in modified Eagle medium (MEM: Gibco, USA, 11090081) on ice, and cut into 350-µm parasagittal slices using the McIlwain tissue chopper (Ted Pella, Inc., USA, 10810). Slices were separated with fine forceps under a dissection microscope. Three slices were grown on each 30 mm Millicell cell culture insert (MilliporeSigma, USA, PICMORG50) in 1 mL of culture media comprised of 50% basal medium with Earle's salts (Gibco, USA, 21010046), 25% Hanks' buffered salt solution (Invitrogen, USA, 14025050), and 25% Gibco heat-inactivated horse serum (Thermo Fisher Scientific, USA, 26050088), supplemented with 5 mg/ml Gibco glucose (Thermo Fisher Scientific, USA, A2494001), 1% Gibco Penicillin-Streptomycin (Thermo Fisher Scientific, USA, 15140122), and 1% Gibco GlutaMAX Supplement (Thermo Fisher Scientific, USA, 35050061). Slices were given two weeks in culture to myelinate with complete media changes every other day.

2.3.2 Nes treatment of cerebellar slices

Cerebellar slices were prepared as described above. Slices were left to acclimate to culture conditions for two days post-dissection, at which point they were treated with either 20 or 50 µM Nes (MilliporeSigma, USA, SML0550) dissolved in dimethyl sulfoxide (DMSO). Vehicle controls were treated with corresponding concentrations of DMSO. Nes and DMSO were added to fresh media just prior to daily half media changes. Slices were fixed at seven and 14 days post-dissection in 4% paraformaldehyde (PFA).

2.3.3 Staining of cerebellar slices

After fixation, cerebellar slices were gently cut out of the inserts. The slices were then permeabilized with 0.5% Triton X-100, followed by blocking in phosphate buffered saline (PBS) containing 10% normal serum for two to four hours at room temperature (RT). The slices were then incubated with a primary anti-MBP monoclonal antibody (Santa Cruz Biotechnology, USA, sc-271524) diluted 1:200 in PBS buffer containing 0.2% Triton X-100. The slices were washed three times and then incubated with the appropriate FITC-conjugated secondary antibody diluted 1:500 in the same buffer. These steps were all performed overnight at 4ºC. Finally, the sections were mounted in 4',6-diamidino-2-phenylindole (DAPI) containing Vectashield mounting medium (Vector Laboratories, USA, H-1200-10).

2.3.4 Imaging and quantitative analysis

Cerebellar slices were imaged on the Nikon Eclipse 90i Motorized Upright Microscope. All images were taken at the same shutter setting. Green fluorescent protein (GFP) fluorescence intensity was quantified on the ImageJ software, with all raw images adjusted to the same brightness level. Fluorescence intensity measurements were based on lower magnification (10x) images of the cerebellar slices in their entirety; higher magnification images were used for qualitative analysis only.

2.4 *Ex vivo* spinal cord explant culture

2.4.1 Preparation of charcoal-stripped mouse serum

Mouse serum used in spinal cord explant media was subject to charcoal stripping, a process during which prolonged exposure to dextran-coated, activated charcoal facilitates removal of steroid hormones, according to manufacturer's instructions. Briefly, dextran-coated charcoal (DCC) was prepared by incubating Norit A charcoal (MilliporeSigma, USA, C3345) and dextran T-70 (MilliporeSigma, USA, D1390) in 0.25 M sucrose, 1.5 mM $MgCl_2$, and 10 mM HEPES pH 7.4 at final concentrations of 0.25% and 0.0025%, respectively. A volume of the DCC equivalent to that of the serum to be stripped was centrifuged at 500 g for 10 min to pellet the charcoal. The supernatant was decanted and replaced with the same volume of low endotoxin deionized water. The resuspended pellet was then subject to an additional 500 g, 10-minute centrifugation. The washed charcoal pellet was resuspended in the same volume of normal mouse serum (Thermo Fisher Scientific, USA, 10410) for an equivalent of 253 mg DCC per 100 mL normal mouse serum. The mixture was thoroughly mixed by vortexing, and incubated for 12 hours at 4ºC. The stripped serum was then passed through a filter series consisting of a pre-filter, 0.45-μM filter, and 0.2-μm filter, and stored at -20 ºC until use. Charcoal stripping was performed by members in the lab of Dr. Narender Kumar of the Population Council at Rockefeller University.

2.4.2 Spinal cord explant procedure

Litters were obtained from timed pregnancies of B6;129P-*Cyp11a1*$^{tm1(GFP/cre)Pzg}$/J$^{+/-}$ female and B6;129P-*Cyp11a1*$^{tm1(GFP/cre)Pzg}$/J$^{+/-}$ male matings, and embryos were harvested at embryonic day (E)12.5. The day of vaginal plug identification was considered E0.5. Each embryo was assigned a code number for retrograde genotyping via PCR analysis on remaining tissue. Spinal cords were dissected and cut transversely into one- to two-mm fragments for explant culture onto 0.4 *μ*m Millicell cell culture inserts (MilliporeSigma, USA, PICM03050) placed in sterile, flat-bottom, tissue-culture treated six-well cell culture plates (Corning, USA, 3516). Explants were cultured in hormone-free media comprised of DMEM without phenol red (Thermo Fisher Scientific, USA, 21041025), ITS (Thermo Fisher Scientific, USA, 41400045), 2% charcoal-stripped normal mouse serum, and 10 ng/mL PDGF-AA

(PeproTech, USA, 100-13A). This particular media composition was adapted from Vartanian et al., with ITS replacing P4-containing N2 supplement[149]. Half media changes were performed daily to maintain the tissue in culture.

2.4.3 Staining of spinal cord explants

Explants were fixed on hypothetical E17.5 in 4% PFA, 5% sucrose for 20 min at RT. After fixation, explants were gently cut out of the insert. They were then permeabilized with 0.5% Triton X-100, followed by blocking in PBS buffer containing 10% normal serum for two to four hours at RT. Blocked slices were incubated with a primary anti-MBP monoclonal antibody (Santa Cruz Biotechnology, USA, sc-271524) or polyclonal anti-Nkx2.2 antibody (Thermo Fisher Scientific, USA, PA5-78079) diluted 1:200 in PBS buffer containing 0.2% Triton X-100. The slices were washed three times and incubated with the appropriate FITC- (MBP) or Cy3- (Nkx2.2) conjugated secondary antibody diluted 1:500 in the same buffer. These steps were all performed overnight at 4ºC. Finally, the sections were mounted in DAPI-containing Vectashield.

2.4.4 Imaging and quantitative analysis

Fixed and stained spinal cord explants were imaged on the CaliberID ribbon scanning confocal microscope (Caliber Imaging & Diagnostics, Inc., USA) at the Rockefeller University Bio-Imaging Resource Center. Samples were imaged with a 20x/0.8 UplanXApo lens (Olympus,USA), using laser lines of 450 nm, 488 nm, 561 nm, and 640 nm for excitation in the four different channels.

Maximum intensity Z-stack projections of the raw images from both green (MBP) and red (Nkx2.2) channels were generated in Imaris image analysis software, version 9.8.2. To measure the dispersal of cells away from the midline of the explants, fluorescence intensity measurements were made along a series of five parallel lines drawn perpendicular to the midline using Fiji. Briefly, five lines of equal length (1,176 μm) and width (100 μm) were drawn perpendicular to the midline across the length of each explant. Identical sets of lines were applied to the individual explants for the maximum intensity projection images corresponding to both the green and red channels. The fluorescence intensity was measured at regular intervals along the five parallel lines and listed as a set of (x,y) coordinates, with the x coordinate reflecting distance along the line in μm, and the y coordinate reflecting the mean fluorescence intensity at that particular location. These values were saved as an Excel file. A custom R script was written in RStudio to read the Excel file, calculate average fluorescence intensity for all five lines at each point along the line, and plot them as ±SEM. The script was run separately for the MBP and Nkx2.2 channels for each explant. The final line plots depict the fluorescence intensity profiles across the length of the explant, with the solid line representing the mean intensity through the entire Z-stack, and the shaded regions representing the standard error of the mean. Christina Pyrgaki of the Bio-Imaging Resource Center (RRID: SCR_017791) helped with the imaging of the spinal cord explants on the ribbon scanning confocal microscope. Ved Sharma, also from the

Bio-Imaging Resource Center, helped with the quantitative analysis of the explant fluorescence intensity measurements and wrote the R script for the line profile generation.

2.5 Immunohistochemistry on B6:129P-*Cyp11a1*$^{tm1(GFP/cre)Pzg}$/J embryos

2.5.1 Embryo collection and fixation

Litters were obtained from breeding pairs of B6;129P-*Cyp11a1*$^{tm1(GFP/cre)Pzg}$/J$^{+/-}$ females and B6;129P-*Cyp11a1*$^{tm1(GFP/cre)Pzg}$/J$^{+/-}$ males with a 12-hour mating window overnight from 6:00 PM to 6:00 AM. Embryos were harvested at E18.5. The day of vaginal plug identification was designated E0.5.

Each embryo was assigned a code number for retrograde genotyping via PCR analysis on limb tissue. Embryos and corresponding placentae were carefully dissected and weighed. After decapitation using scissors, embryo bodies and heads as well as placentae were fixed in modified Davidson's fixative (Fisher Scientific, USA, 50-292-28) containing 14% denatured ethyl alcohol, 37.5% formalin, and 37-39% glacial acetic acid in deionized water for 48 hours at 4ºC in 50 mL conical tubes to achieve a 10:1 ratio of fixative volume to tissue volume. This fixative was selected based on its optimization for fixation of testis with a capsule similar in thickness to the skin of the E18.5 mouse embryos. Unlike the traditionally used Bouin's fluid (5% acetic acid, 9% formaldehyde, 0.9% picric acid), modified Davidson's fixative is not regulated as a hazardous material, does not spontaneously explode with prolonged storage, and minimizes tissue shrinkage during the fixation process[150]. The tissues were then transferred to new 50 mL conical tubes containing 70% ethanol and shipped to Elizabeth Chlipala of Premier Laboratory in Longmont, Colorado for histological processing.

2.5.2 Histology

For the placenta, one section through the midline of the organ was prepared for hematoxylin and eosin (H&E) staining to assess general architecture.

For each embryo, the head/brain was processed whole to paraffin, after which 5-μm-thick sections were collected at the locations designated 2, 3, 4, and 5 in Figure 2.1, along with hippocampus. The resultant five to eight levels per head/brain per animal were stained with H&E (to demonstrate general organ [brain] architecture) or cresyl violet (to assess specific neuronal populations), or labeled by indirect immunohistochemistry (IHC) to identify the proteins cleaved caspase-3 (for apoptotic cells), class III beta-tubulin (TUJ1, to demonstrate early differentiation stages of neurons), Olig2 (to reveal myelin-producing cells in the CNS), or MBP (to show myelin).

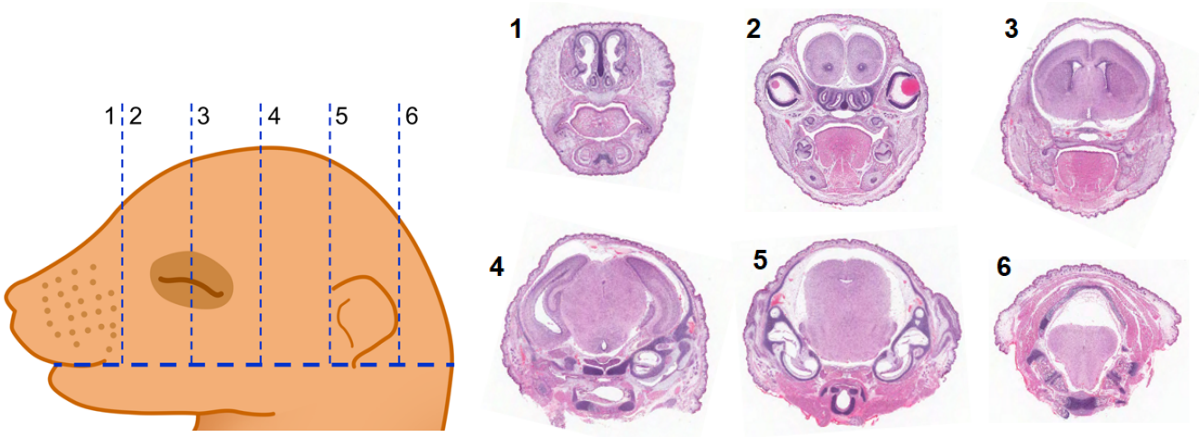

Figure 2.1: E18.5 brain sectioning strategy. Transverse (coronal) brain sections were taken as numerically indicated on the left to produce corresponding tissue sections with region-specific anatomical features shown on the right[151]. Brain is present in levels two through six.

Sagittal slices through the body of each embryo were taken at multiple intervals spaced 100-200 μm apart, resulting in up to ten levels per embryo. The trimming planes were oriented using the umbilicus and tail as external landmarks to ensure that the spinal cord and adrenal gland would be available for evaluation. All levels were stained with H&E, and one spinal cord-containing level was stained for TUJ1, Olig2, and MBP. Transverse spinal cord sections were taken to assess TUJ1, Olig2, and MBP staining. The body of the embryo was grossed into three transverse sections, with the initial sections captured at the last rib, embedded caudal side down. After dividing the remaining portion of the body in half, the middle section was embedded caudal side down, and the lower portion rostral side down. Three levels were collected at 100-μm depths and stained for H&E. One section per body was stained with TUJ1, Olig2, and MBP.

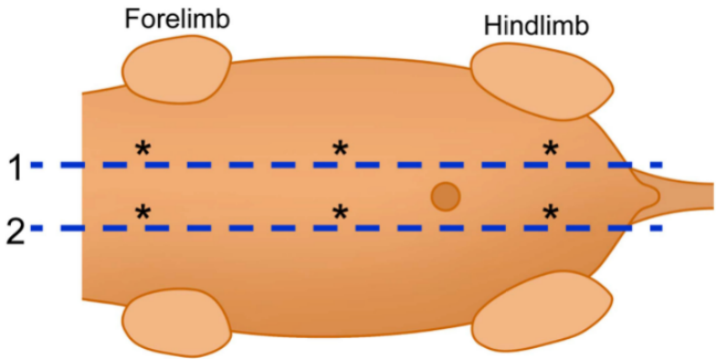

Figure 2.2: E18.5 torso sectioning strategy. Sagittal sections were taken through the torso as numerically indicated for H&E staining[151]. The face denoted by the asterisks was placed down in the cassette. Sectioning through the left part of the torso was done to ensure that structures located only on the left side (e.g. spleen, stomach) would be present for examination.

Samples for IHC were sectioned at 5 μm and mounted onto charged slides. Slides were dried overnight, baked at 60°C for one hour, deparaffinized in xylene, rinsed

in alcohol, rehydrated in water, and equilibrated in wash buffer (Tris buffered saline with 0.05% Tween 20; Dako, K8007). Heat-induced epitope retrieval (HIER) was performed in a Dako PT Link using a 20-minute 95°C program. Tris/EDTA HIER buffer (Dako, #K8004) was used prior to cleaved caspase-3 staining, and Citrate HIER buffer (Agilent, K8005) was used prior to Olig2 and TUJ1. Slides were then cooled and rinsed in wash buffer and the remaining IHC steps were carried out at RT on an Autostainer PlusLink stainer (Dako). Proteolytic-induced epitope retrieval (PIER) using Proteinase K for two minutes (Dako, #S3020) was performed prior to MBP staining. Within the autostainer, serum-free protein block was applied for five minutes (Dako, #X0909).

The following primary antibodies and concentrations were used: rabbit polyclonal-anti beta III tubulin primary antibody (0.16 μg/mL, Sigma, #T2200); rabbit monoclonal [5A1E] anti-cleaved caspase-3 primary antibody (0.27 μg/mL, Cell Signaling, #9664); rabbit polyclonal anti-Olig2 primary antibody (0.67 μg/mL, Millipore #AB9610); and rabbit polyclonal anti-MBP primary antibody (14 μg/mL, Agilent #A0623). All primary antibodies were incubated for 30 minutes at RT. Primary antibodies were detected using EnVision+ anti-Rabbit Labelled Polymer-HRP for 30 minutes (Dako, K4003) and DAB+ Chromogen Solution for five minutes (Dako, K3468). Wash buffer rinses were applied between appropriate reagents. Slides were then manually rinsed in tap water and counterstained for five minutes in a modified Harris hematoxylin (Dako, S3301). The slides were again rinsed in tap water, and wash buffer was used as the hematoxylin bluing reagent. The slides were then dehydrated in absolute alcohol solutions, cleared in xylene, and cover-slipped.

Formalin pigment was observed in some of the samples part way through completing IHC staining. A formalin pigment removal procedure was utilized for slides that were stained for Olig2 and MBP. After IHC staining, prior to counterstaining in hematoxylin, formalin pigment was removed by incubating slides in 70% alcoholic ammonium hydroxide for 30 min. Mark Butters of Premier Laboratory performed the IHC.

2.5.3 Imaging and analysis

All stained slides were scanned at 20x on an Aperio ScanScope AT2. For microscopic evaluation, cell and tissue features were assessed using a conventional bright-field transmitted light microscope (Nikon Eclipse E600) to define potential tissue and cell differences between mutant embryos and WT controls. The assessment was performed by Brad Bolon, an American College of Veterinary Pathologists board-certified experimental pathologist with considerable experience in anatomic analysis of developing mouse embryos and placentae.

The microscopic examination was performed in two stages. The initial phase identified differences and assigned semi-quantitative grades using a tiered scale: within normal limits (grade 0), minimal (grade 1), mild (grade 2), moderate (grade 3), or marked (grade 4) changes. These grades were assigned using an informed approach (i.e., with foreknowledge of the animal genotype). For the second phase, sections of possible target tissues (based on apparent genotype-related differences) were re-

evaluated using a coded (blinded) approach whereby tissues were sorted into groups based on grading criteria developed during the informed analysis. For the study, this phase 2 assessment was performed on the adrenal gland and selected brain sections (specifically those with hypothalamus and pituitary gland [approximately equivalent to level 4 of Figure 2.1)].

CHAPTER 3: Role of P4 in Oligodendrocyte Development

3.1 Confirmation of P4 effects on myelination

3.1.1 Nes is an optimal experimental P4 substitute

Given the abundance of data supporting a role for P4 in remyelination, we sought to determine whether this particular neurosteroid exhibits similar effects during developmental myelination. In terms of experimental P4 treatment, we chose to utilize a synthetic P4 derivative referred to as Nes. While many progestins like Nes are commercially available, they all differ in structure, neurosteroid receptor binding profiles, and biological activity. Nes was deemed the optimal progestin due to its greater impact on myelin repair, as well as higher affinity and specificity for the classical intracellular nPR than P4 itself. As evident in the seven progestins listed in Table 3.1, the binding affinity of Nes to the nuclear glucocorticoid receptor is weaker than that of P4, and is virtually non-existent to the nuclear androgen receptor[152]. These relative binding profiles suggest that Nes is an ideal progestin in terms of ensuring biological activity mediated through nPR. On a similar note, Nes, unlike P4, only undergoes minimal metabolism to 3α- and 5α-tetrahydronestorone. These intermediates have a limited capacity to activate GABA type receptors as the abundant P4 metabolite ALLO does[153]. The physiological conversion of P4 to ALLO occurs within a matter of minutes, thereby complicating the isolation of endogenous P4 in experimental paradigms. Importantly, Nes induces the same neuroprotective and anti-inflammatory effects attributed to P4, as demonstrated in a stroke disease model in mice in which a 0.08 mg/kg dose of Nes intraperitoneally most significantly stimulated neuronal repair[56]. My cerebellar slice culture experiments described below were designed based on this dosage.

Table 3.1: Progestogen binding to nuclear steroid hormone receptors.

Progestogen	nPR IC_{50} (nM)	AR IC_{50} (nM)	GR IC_{50} (nM)
Progesterone	9.01	119.3	6.51
MPA	6.2	4.53	1.42
Nestorone	5.07	No binding	8.71
NET	14.32	18.02	97.84
NETA	38.92	876.9	202.7
Norethynodrel	67.76	196.7	1306
LNG	5.46	2.9	16.73
NGM	482.8	5.02	287.1

3.1.2 Nes enhances MBP expression in cerebellar slices

Due to the paucity of data on the necessity for neurosteroid hormones in neural development, I evaluated the effect of Nes administration to mouse cerebellar slice

cultures on MBP expression during the time period when physiological myelination occurs[106,154]. Briefly, cerebella were dissected from P7 mouse pups, chopped into 350-µm thick slices, and cultured on nylon membrane inserts placed in six-well plates. After 24 hours of acclimating to the culture media, slices were treated with 20 µM or 50 µM Nes, or DMSO vehicle control, for seven or 14 days (Figure 3.1) The nylon membranes were cut out and transferred to 24-well plates for permeabilization in 0.5% Triton-X-100 and blocking in 5% donkey serum. Permeabilized slices were stained with a mouse anti-MBP antibody at 1:100 overnight at 4ºC, followed by an anti-mouse secondary antibody at 1:200 overnight at 4ºC. The nylon membranes were mounted on slides and visualized under a fluorescent microscope.

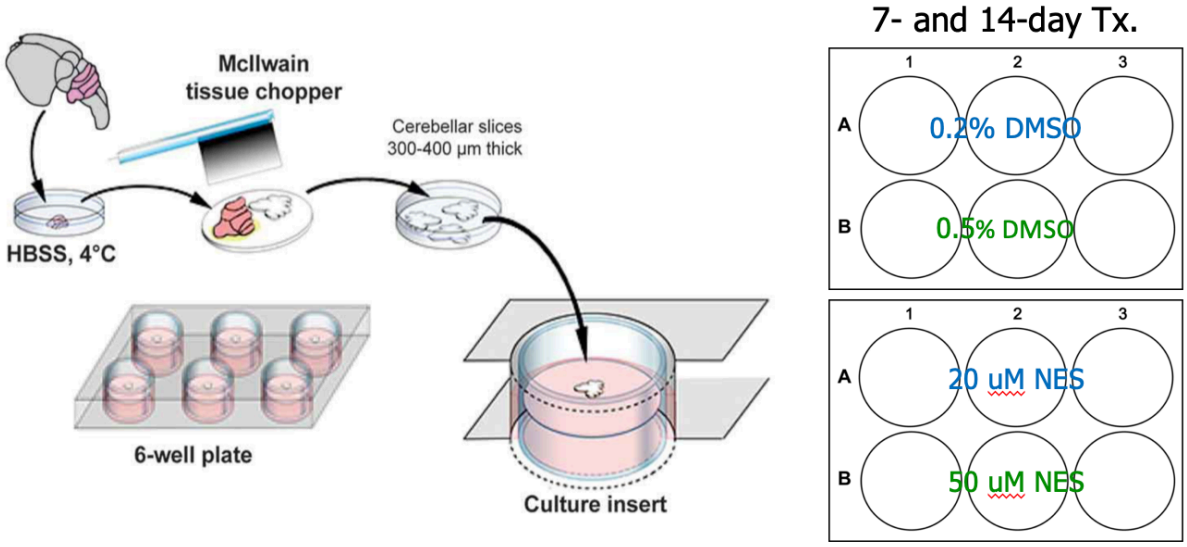

Figure 3.1: Cerebellar slice paradigm to evaluate Nes effects on myelination. 350-micron thick mouse cerebellar slices were dissected from P7 mouse pups and cultured on nylon membrane well inserts placed in six-well plates. Each well contained two to three slices. After Nes or vehicle treatment, the slices were fixed in 4% PFA in the same six-well plates. The nylon membranes were cut out and transferred to 24-well plates for permeabilization in 0.5% Triton-X-100 and blocking in 5% donkey serum. Slices were then stained with a mouse MBP antibody at a concentration of 1:100 overnight at 4ºC followed by an anti-mouse secondary at 1:200 overnight at 4ºC. The nylon membranes were mounted on slides and visualized under a fluorescent microscope.

Nes treatment significantly enhanced myelination as assessed by fluorescent staining intensity of the mature myelin protein, MBP. Representative images from each condition (Fig. 3.2) indicate enhanced MBP expression in Nes-treated as opposed to control-treated slices in nearly all conditions. Quantitative analyses (Fig. 3.2) confirm this trend, with the exception of the 14-day, 50 µM Nes treatment. The most striking effects were seen at the seven-day timepoint, with 20 and 50 µM Nes treatment resulting in 96% and 81% increases in MBP fluorescence intensity, respectively, compared to that in vehicle-treated control slices. This trend was more modest at the 14-day timepoint, with 20 uM Nes treatment leading to a 35% increase in MBP fluorescence intensity. Interestingly, no effect was apparent with 50 uM treatment. This

data suggests P4 is involved in, but not necessarily required for, myelination at an early postnatal age. While my expectation is that the neurosteroid is in fact essential to developmental myelination, such a finding would be novel.

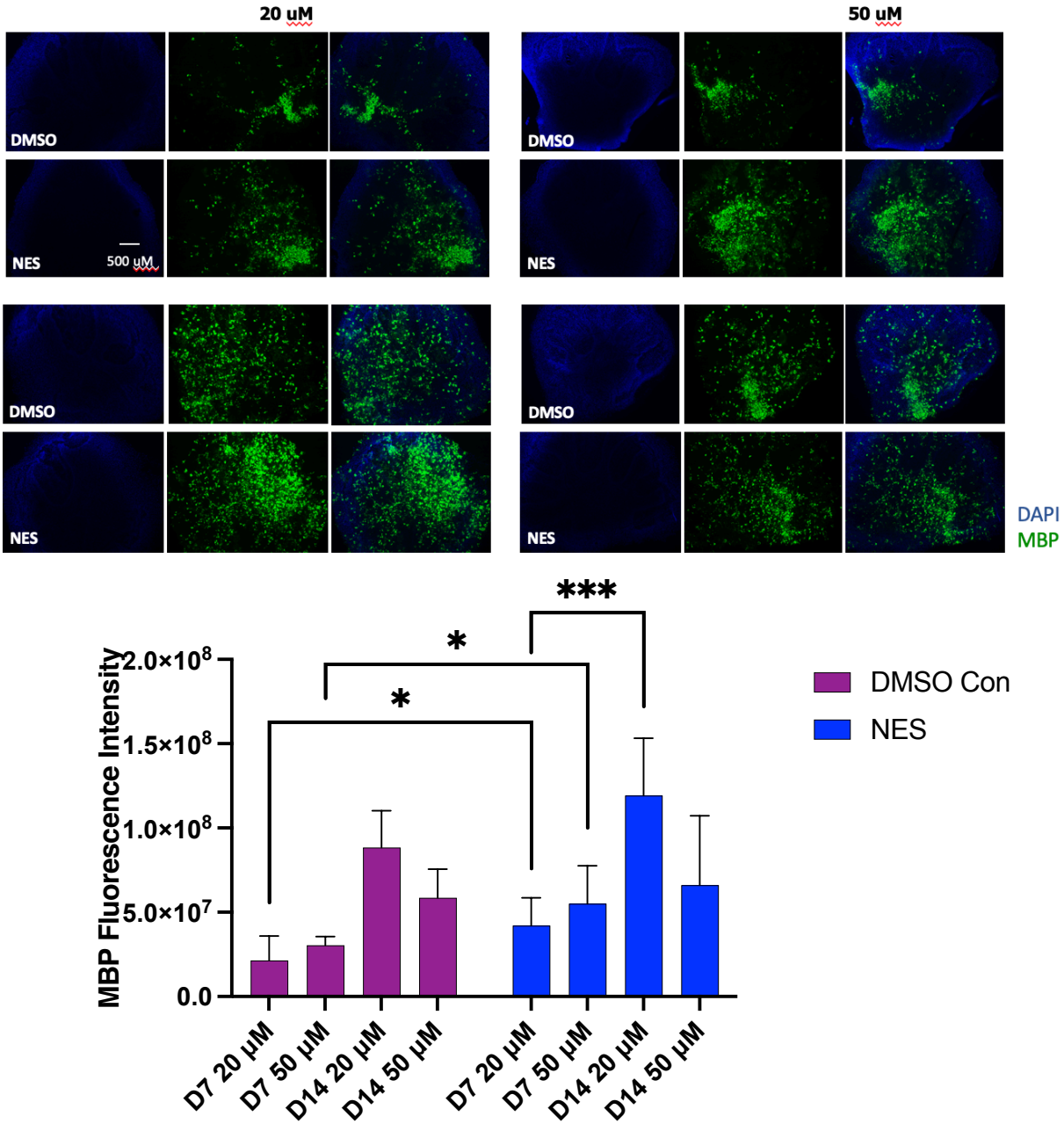

Figure 3.2: Nes-induced MBP expression in developing mouse cerebellar explants. 350-uM thick cerebellar slices were dissected from P7 mouse pups and plated in media containing 20 uM Nes, 50 uM Nes, or DMSO vehicle control for seven or 14 days, and fluorescently stained for DAPI (blue) and MBP (green). Nes stimulated MBP expression at D7 and D14, with the exception of the 50 uM concentration at D14. Quantitative analysis reveals statistically significant increases in MBP expression at D7 with 20 uM and 50 uM Nes treatment compared to DMSO controls, as well as between 20 uM Nes treatment at D7 versus D14. Results expressed as Mean ± STDEV, $p < 0.05$ = *, $p < 0.01$ = **, $p < 0.001$ = *** determined by two-way ANOVA, n = 6 cerebellar slices per condition.

3.1.3 Discussion

The significant increase in MBP expression following one week of treatment with Nes corroborated the little data that is currently available regarding the role of P4 in murine embryonic myelin development[106,154]. However, the reason for the more modest trend in Nes-induced enhancement in MBP expression at the Day 14 timepoint (Figure 3.2) is not yet clear. Presumably, the explanation for this phenomenon depends on the mechanism by which P4 is leading to an increase in MBP-positive cells during early myelination. It is possible that Nes specifically promotes a stage of OPC maturation that has already terminated by the third week of life, corresponding to D14 in the experimental paradigm described here. For instance, the majority of OPCs have already undergone successful differentiation by the peak of myelination which occurs prior to the three weeks post-birth mark[155]. Therefore, if P4 does in fact stimulate OPC differentiation, we would expect the effect of Nes on MBP expression to steadily decline as this fluid process approaches completion.

On a similar note, there is not a distinct difference between MBP expression following administration of 50 uM Nes between D7 and D14 (Figure 3.2). This stagnancy in MBP fluorescence intensity suggests an external factor at play such as oligodendrocyte cell death and/or a threshold of Nes benefits at or near the 50 uM concentration. Consistent with this hypothesis, it is known that CNS development does involve substantial apoptosis of excess OPCs that are not destined to differentiate into myelinating oligodendrocytes. Of note, oligodendrocyte quantities and myelination levels remain relatively constant, even upon introduction of endogenous OPCs into the system[156]. Apoptosis thus seems to be an inevitable aspect of myelin tract formation within the CNS.

Though these preliminary data certainly imply a role for P4 in developmental myelination, inherent limitations of the experimental design warrant further investigation of both the extent to which P4 is required during this window of time, as well as the mechanism of P4-mediated MBP enrichment proposed in the literature and confirmed in these studies. Paramount among these limitations is the lack of mechanistic insight into how the presence of P4 leads to MBP expression in the early postnatal cerebellum. Direct action on OPC differentiation is merely one example of the varied ways in which P4 activity might impact myelin development. Others include effects on OPC proliferation and/or migration, potentially accounted for by a number of candidate signaling cascades associated with neurosteroid hormones. Due to the specificity of Nes for nPR, we conducted follow-up loss of function studies in mice lacking this nuclear receptor. The two manuscripts to date that address Nes effects on developmental myelination rely on cerebellar slice cultures from a mouse strain with a germline loss-of-function mutation at the nPR locus[106,154]. At the time, Dr. John Lydon of Baylor University was the only investigator actively breeding these PRKO mice, and generously offered to contribute animals to my endeavors. He discontinued this line shortly after sending me one male WT and two male Hets. The PRKO mice were successfully acquired from Baylor and quarantined, and ultimately crossed with WT C57BL/6J females from The Jackson Laboratory to produce a full colony.

3.2 Inhibition of nPR during myelination

3.2.1 Establishment of PRKO transgenic mouse line

PRKO mice were created by the insertion of a neomycin resistance gene into exon 1, thereby preventing nPR transcription and inhibiting functional mRNA expression for both nPR isoforms A and B (Figure 3.3)[157]. Members of Dr. Lydon's lab provided primer sequences and a specific PCR protocol for genotyping. The inclusion of three primers yielded a 302-bp amplicon corresponding to the WT nPR allele and a 140-bp amplicon corresponding to the mutant PRKO allele (Figure 3.4). I was able to produce male and female Hets and homozygous KOs. Importantly, homozygous females are sterile, meaning I couldn't generate an entirely homozygous colony for experimental purposes. In the following cerebellar slice experiments, pups were genotyped on P1 or P2 in order to identify the KOs prior to P7 when cerebella are dissected in the slice culture procedure. Homozygous males were continuously bred with heterozygous females to maintain the colony and support related experiments.

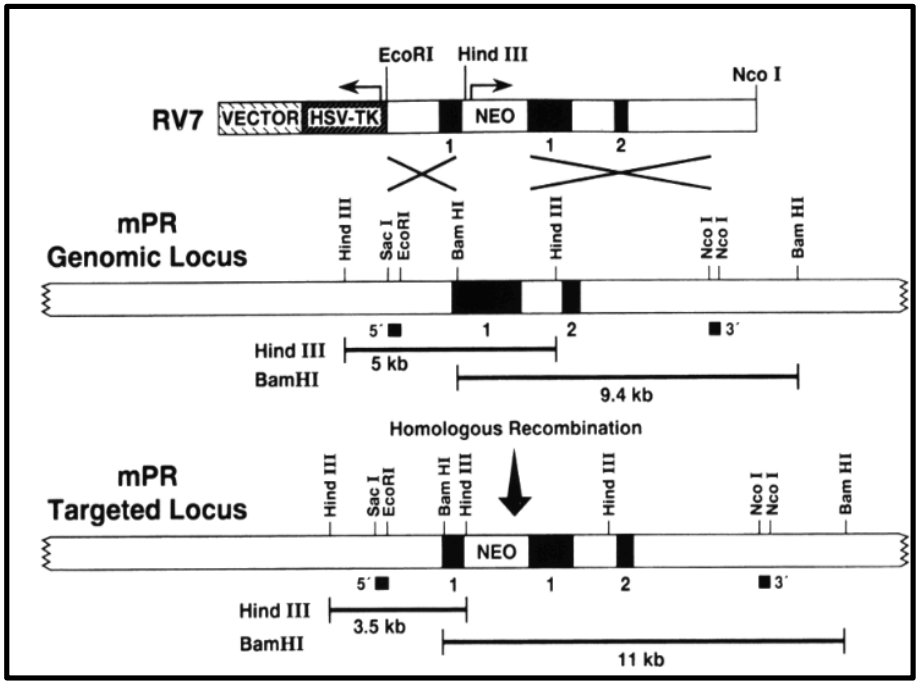

Figure 3.3: Genetic construct of PRKO mice. The targeting vector RV7, used for the positive-negative selection, is shown at the top. The solid boxes represent exon 1 and exon 2. The open boxes that are located 3' to exon 1 and 2 are intronic sequences, whereas the open box 5' to exon 1 represents the 5'-untranslated region. The neo r and the HSV-TK gene are indicated, with arrows showing the direction of transcription. The vector sequence pSP72 is located at the 5' end of RV7. The relevant restriction sites are indicated. After homologous recombination between RV7 and the mPR genomic locus, the predicted structure of the mutated nPR allele is depicted at the bottom. The expected sizes of the various restriction fragments, detected by the 5' and 3' probes, are shown for both the intact and targeted disrupted locus. The 5' and 3' probe fragments are indicated by solid boxes[157]

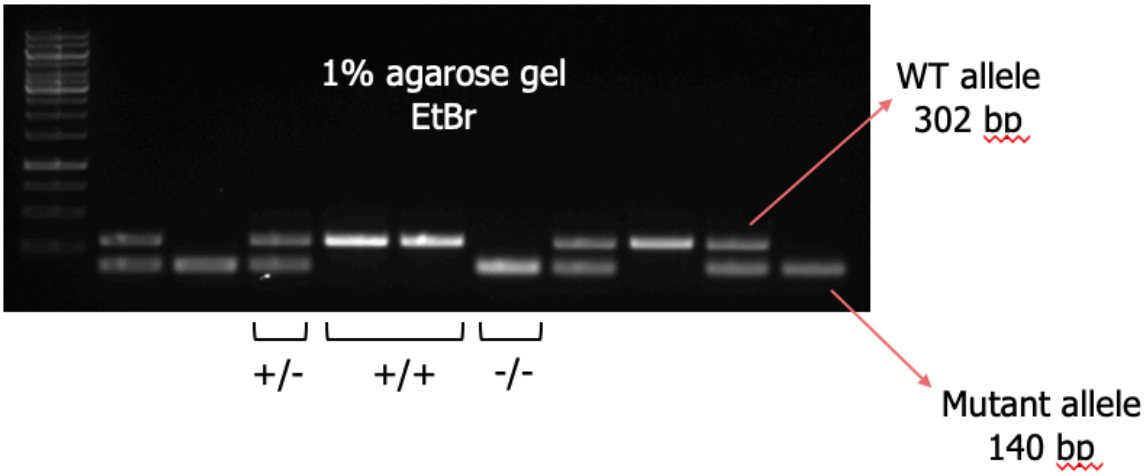

Figure 3.4: Genotyping of PRKO mice. Three primers were combined in the same PCR reaction to generate a 140-bp amplicon corresponding to the PRKO mutation allele and a 302-bp amplicon for the WT allele. Presence of both amplicons indicates a Het.

3.2.2 nPR-mediated effects on myelination

My initial aim was to confirm P4-mediated amplification of MBP staining as suggested in the literature[106]. I employed the same techniques implemented in the previous experiment, in which cerebella were dissected from P7 mouse pups, chopped into 350-µm thick slices, and cultured on nylon membrane inserts placed in six-well plates. The key variable in this experimental paradigm was the mouse genotype. Whereas before I strictly used WT mice to confirm a P4 effect on myelin development in general, I now sought to determine the extent to which nPR regulates myelin development in the PRKO mouse strain. Slices were treated after 24 hours as before with only 20 µM Nes (which was shown to be more effective than the 50 µM concentration, Figure 3.2), or DMSO vehicle control, for seven days (Figure 3.5) The nylon membranes were excised and transferred to 24-well plates for permeabilization in 0.5% Triton-X-100 and blocking in 5% donkey serum. Permeabilized slices were stained with a mouse anti-MBP antibody at 1:100 overnight at 4ºC, followed by an anti-mouse secondary antibody at 1:200 overnight at 4ºC. The nylon membranes were mounted on slides and visualized under a fluorescent microscope.

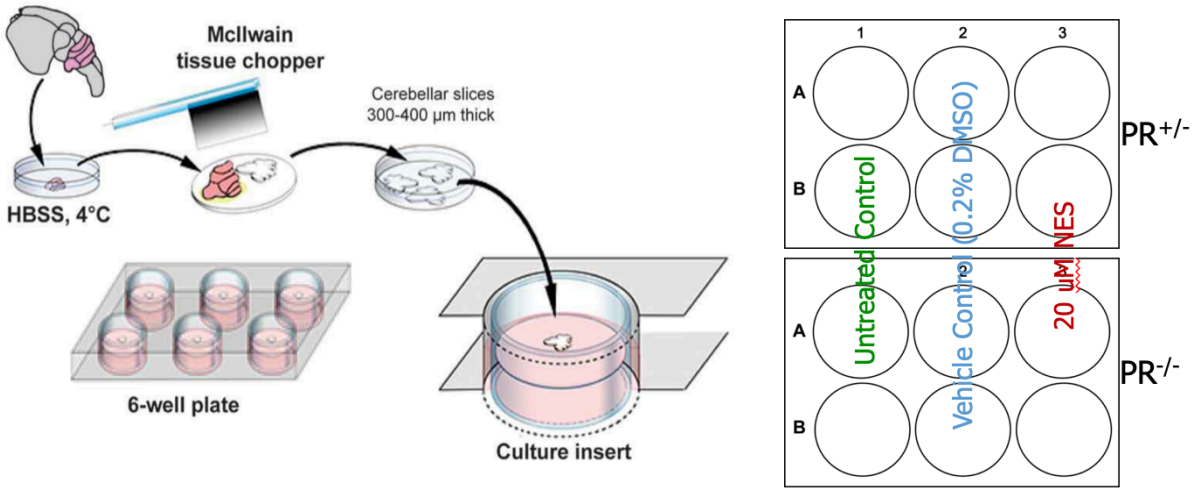

Figure 3.5: Cerebellar slice paradigm to evaluate Nes effects on myelination in PRKO mice. 350-micron thick mouse cerebellar slices were dissected from P7 mouse pups and cultured on nylon membrane well inserts placed in six-well plates. Each well contained two to three slices. After Nes or vehicle treatment, the slices were fixed in 4% PFA in the same six-well plates. The nylon membranes were cut out and transferred to 24-well plates for permeabilization in 0.5% Triton-X-100 and blocking in 5% donkey serum. Slices were then stained with a mouse MBP antibody at a concentration of 1:100 overnight at 4ºC followed by an anti-mouse secondary at 1:200 overnight at 4ºC. The nylon membranes were mounted on slides and visualized under a fluorescent microscope.

As expected, only scarce differences were present between untreated and DMSO controls across both nPR$^{+/-}$ (Het) and nPR$^{-/-}$ (KO) genotypes. Nes treatment did increase MBP expression as compared to the DMSO vehicle control conditions in Hets and KOs by 12.87% and 74.89%, respectively. However, Nes-induced MBP expression was surprisingly 67.3% greater in the KOs than the Hets. In addition to the enhanced fluorescence intensity seen in slices from the nPR$^{-/-}$ mice, the MBP-outlined myelin tracts in this genotype are visibly denser with a much greater extent of branched processes. The majority of the MBP positivity in the KO tissue can be attributed to actively myelinating oligodendrocytes. Most of the MBP-positive cells in the Het tissue, on the other hand, exist in isolation without any evidence of participating in myelination (Figure 3.6). Contradictory to the established notion that P4 stimulates myelin repair in the context of neurodegenerative disease by signaling through nPR, these findings suggest that the mechanism is not as straightforward in developmental myelination[46,53,54,57,92,93,100,101,103-107].

A.

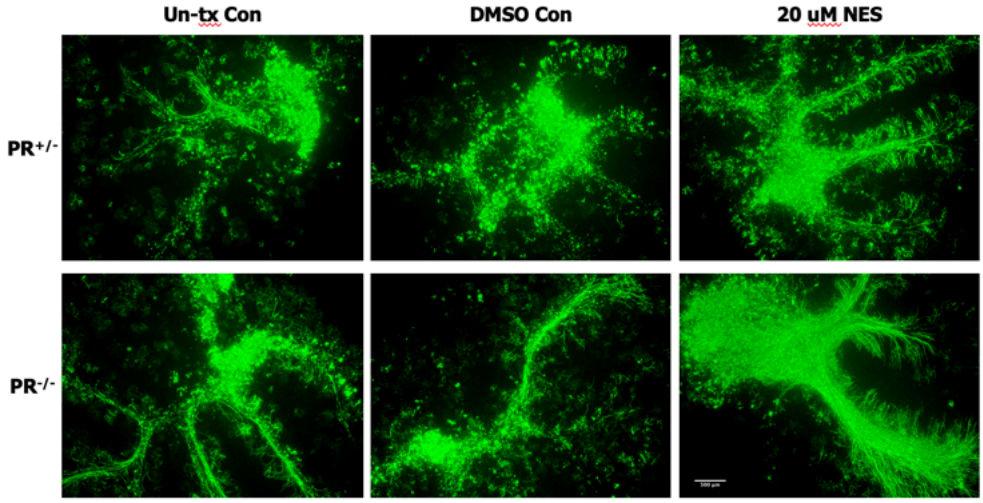
Un-tx Con
DMSO Con
20 uM NES
PR+/-
PR-/-

B.

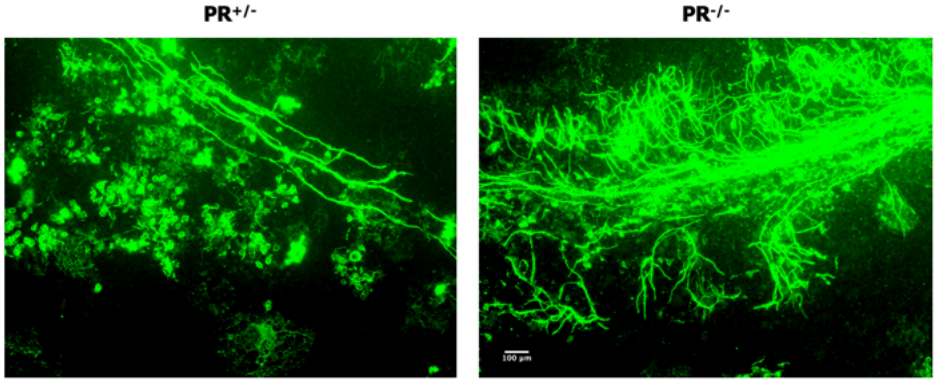
PR+/-
PR-/-

C.

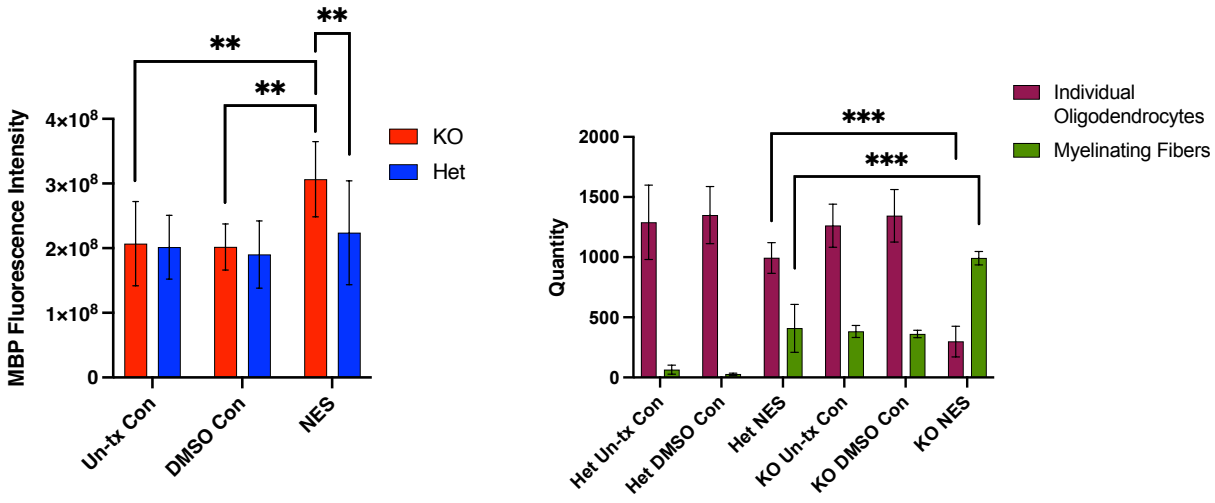
MBP Fluorescence Intensity
4×10^8
3×10^8
2×10^8
1×10^8
0
**
**
**
KO
Het
Un-tx Con
DMSO Con
NES
Quantity
2000
1500
1000
500
0
***
***
Individual Oligodendrocytes
Myelinating Fibers
Het Un-tx Con
Het DMSO Con
Het NES
KO Un-tx Con
KO DMSO Con
KO NES

Figure 3.6: Nes-induced MBP expression in developing cerebellar explants from PRKO mice. 350-uM thick cerebellar slices were dissected from P7 $nPR^{+/-}$ and $nPR^{-/-}$ mouse pups and plated in media containing 20 uM Nes or DMSO vehicle control for seven days, and fluorescently stained for MBP (green). Nes stimulated MBP expression in both phenotypes, although to a greater extent in $nPR^{-/-}$ mice (A). Prominent myelin tracts with numerous processes are visible in the $nPR^{-/-}$ mice as well (B). Quantitative analysis reveals statistically significant increases in Nes-induced MBP expression in the $nPR^{-/-}$ as compared to the $nPR^{+/-}$ mice (C). Results expressed as Mean ± STDEV, $p < 0.05$ = *, $p < 0.01$ = **, $p < 0.001$ = *** determined by two-way ANOVA with Tukey's honestly significant difference post-hoc testing, n = 6 cerebellar slices per condition.

3.2.3 Discussion

The expedited myelin development in the PRKO mice as compared to the Hets was rather surprising. Not only did Nes increase MBP fluorescence intensity in the KOs, but distinctly altered myelin architecture as well. The enlarged images in Figure 3.6, B show small clusters of MBP-positive cells dispersed throughout the Het cerebellum adjacent to several myelinated tracts (left), as opposed to abundant processes extending from a dense bundle of overlapping myelin tracts illuminating the PRKO cerebellum (right). We would have expected a drastic decrease in MBP expression in the PRKO mice under the assumption that Nes is signaling through nPR to impact myelin development. The data, however, challenge this hypothesis, as the PRKO mice feature a more robust and mature myelin phenotype than their Het counterparts in response to 20 uM Nes.

One plausible scenario involves compensatory action by redundant pathways initiated by P4, or Nes in this case. Myelination is such a vital neurological process that it is reasonable to suspect multiple pathways have evolved to ensure that it proceeds normally. Perhaps Nes has the capacity to activate other receptors in the absence of nPR that in turn upregulate MBP expression during myelin development. Alternatively, P4 signaling through nPR could exert dual effects on myelination. For example, it is conceivable that P4 could inhibit OPC maturation and differentiation, but stimulate OPC proliferation. This explanation is compatible with the MBP-positive cell clusters without extensive myelination seen in the Hets in the presence of nPR, contrasted with the heavily myelinated tracts seen in the PRKO mice lacking nPR.

Gender is another factor that was not accounted for here but must be taken into consideration for analytical purposes. Males and females are known to differ drastically in quantities of hormones like P4, as well as overall myelin content and structure[158]. Cerghet et al. implemented immunocytochemistry and in situ hybridization to demonstrate that oligodendrocyte density is 20-40% greater in the young and adult male versus female corpus callosum, fornix, and spinal cord. MBP expression, the quantitative metric used in my cerebellar slice paradigm, can be up to 160% greater in the male brain as assessed by Western blot. Interestingly, oligodendrocyte and therefore myelin turnover is much more rapid in the female rodent brain, with rampant glial generation and apoptosis[159]. The consequences of such sexually dimorphic oligodendrocyte content and lifespan in the CNS are not fully comprehended.

Because the pups used in these experiments were not segregated by sex, we cannot rule out a potential role for gender in the novel data. On one hand, the heavily myelinated and branched tracts featured in the KO cerebella may be attributed to a greater number of females assigned to that cohort, with correspondingly higher levels of P4. Regardless of sex, P4 in the KOs must still be acting, at minimum, through a non-nPR-mediated pathway. On the other hand, or perhaps in parallel, P4 may activate different signaling pathways according to sex. Still, the logical conclusion remains that the molecular mechanism of P4-induced myelination phenotypes extends beyond the traditional nPR.

Based on the sheer complexity of P4 signaling, additional receptors are likely responsive to Nes. González-Orozco et al. maintain nPR is responsible for embryonic oligodendrogenesis and early postnatal OPC proliferation and differentiation, questioning only the isoform of nPR involved[51]. Yet my data from Nes-treated cerebellar slices from PRKO mice suggests nPR may not even be necessary at all for P4 to influence early myelin development in terms of speed and robustness.

3.3 Complexities of CNS P4 signaling

3.3.1 P4 exerts CNS effects via numerous distinct receptors

In my ultimate aim to deduce the signaling pathway underlying P4-mediated myelin regeneration, the receptor(s) involved in this pathway must be identified. However, there are at least 11 confirmed functional P4 receptors including the traditional nPR for which Nes is a potent agonist, along with multiple membrane-associated progesterone receptors (MAPRs) and 7-transmembrane domain receptors (Figure 3.7)[160]. nPR, the most thoroughly studied of the P4 receptors by far, exists in alpha and beta isoforms, the former of which is simply a truncated version of the latter. The beta form has been identified in the cytoplasm in addition to the nucleus[28]. The seven-transmembrane class 2 progestin and adipoQ receptor (TMPR) family proteins Paqr5, Paqr6, Paqr7, Paqr8, and Paqr9 have also been linked to P4 signaling in the CNS, as have MAPRs progesterone receptor membrane components 1 and 2 (Pgrmc1 and Pgrmc2), neudesin neurotrophic factor (Nenf), and neuferricin (Cyb5d2)[110,161]. The MAPRs, also referred to as b5-like heme-/steroid-binding protein family members, are proposed to regulate iron transport within the CNS. Pgrmc1 and Pgrmc2 shuttle iron from the mitochondria to the nucleus[162]. Iron, in turn, is a critical co-factor in lipid (i.e. myelin) biosynthesis, and facilitates oxidative metabolism in oligodendrocytes[163]. Nenf and Cyb5d2 both exert neurotrophic effects via binding to iron[164].

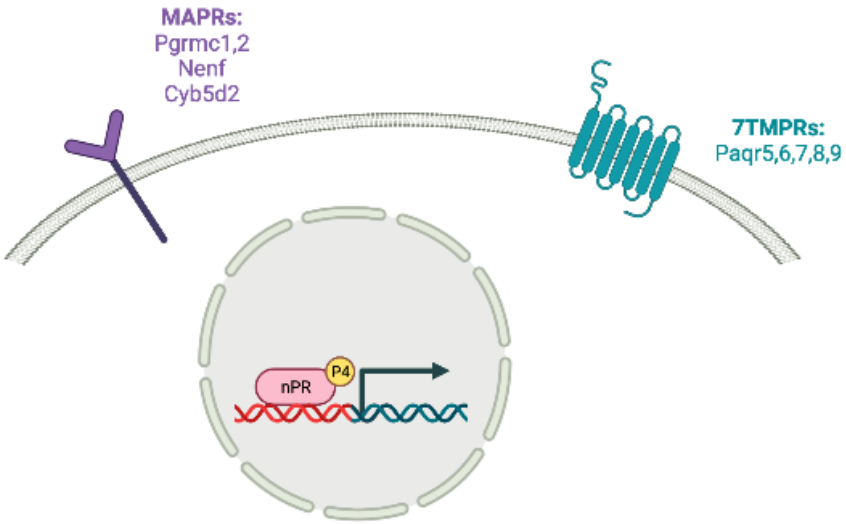

Figure 3.7: Cellar localization of numerous P4 receptors. There are currently 11 P4 receptors with documented CNS expression. The classical nuclear receptor, here denoted nPR, exists in two discrete isoforms. Structurally, nPR-alpha is a truncated version of nPR-beta. Spatially, nPR-alpha is strictly localized to the nucleus, while nPR-beta can be found in the cytoplasm as well. Five of the TMPR proteins, PAQR5, 6, 7, 8, and 9, as well as b5-like heme-/steroid-binding protein family members PGRMC1, PGRMC2, neudesin, and neuferricin have also been shown to mediate P4 signaling.

Curious as to which of these numerous P4 receptors are actually expressed in the CNS, I consulted the Barres Brain Atlas database of differential gene expression in the brain available online. To create this resource, neurons, astrocytes, microglia, endothelial cells, pericytes, and oligodendrocytes at successive stages of maturation were purified from mouse cortex and subject to RNA-Seq to generate a high-resolution transcriptome database of over 22,000 genes. In my semi-quantitative extrapolation of the graphical data provided on the Barres Brain Atlas website, I found that RNA coding for all 11 of the P4 receptors described above is present to varying degrees in at least one stage of oligodendrocyte development (Table 3.2)[165].

Table 3.2: Smmary of Barres Brain Atlas RNA-Seq data of P4 receptor expression in oligodendrocytes.

	nPR	Pgrmc1	Pgrmc2	Paqr5	Paqr6	Paqr7	Paqr8	Paqr9	Nenf	Cyb5d2
OPCs	+	++	+++	+	+	+	+	++	+++	++
Newly Formed OLs	+	+	++	+	+	+	++	+	++	+++
Myelinating OLs	+	+	+	+	+	+	++	+	++	+++

+ = low expression, ++ = moderate expression, and +++ = high expression of RNA in human brain.

To conduct an independent validation of the Barres Brain Atlas data, I performed an analysis to quantify translated RNAs associated with each individual P4 receptor in

murine oligodendrocytes in collaboration with Eric Schmidt of the Heintz lab. Such data is generated through translating ribosome affinity purification using the bacteria artificial chromosome (bacTRAP), an elegant method developed in the Greengard and Heintz labs to isolate translated RNAs in specific cell populations within the brain. Briefly, expression of an eGFP-tagged L10 ribosomal transgene in whole animals labels polysomes that can be immunoprecipitated with an anti-eGFP antibody, and analyzed via RNA-Seq to generate translational profiles from discrete cell types[166]. Cmtm5, CNP, and Olig2 are the three currently available oligodendrocyte-specific bacTRAP mouse lines. Due to logistical issues of low expression and male sterility in the Cmtm5 and CNP lines, respectively, I chose to focus on the Olig2 line in an effort to gain clarity on which P4 receptor(s) should be the focus of my subsequent studies (Figure 3.8).

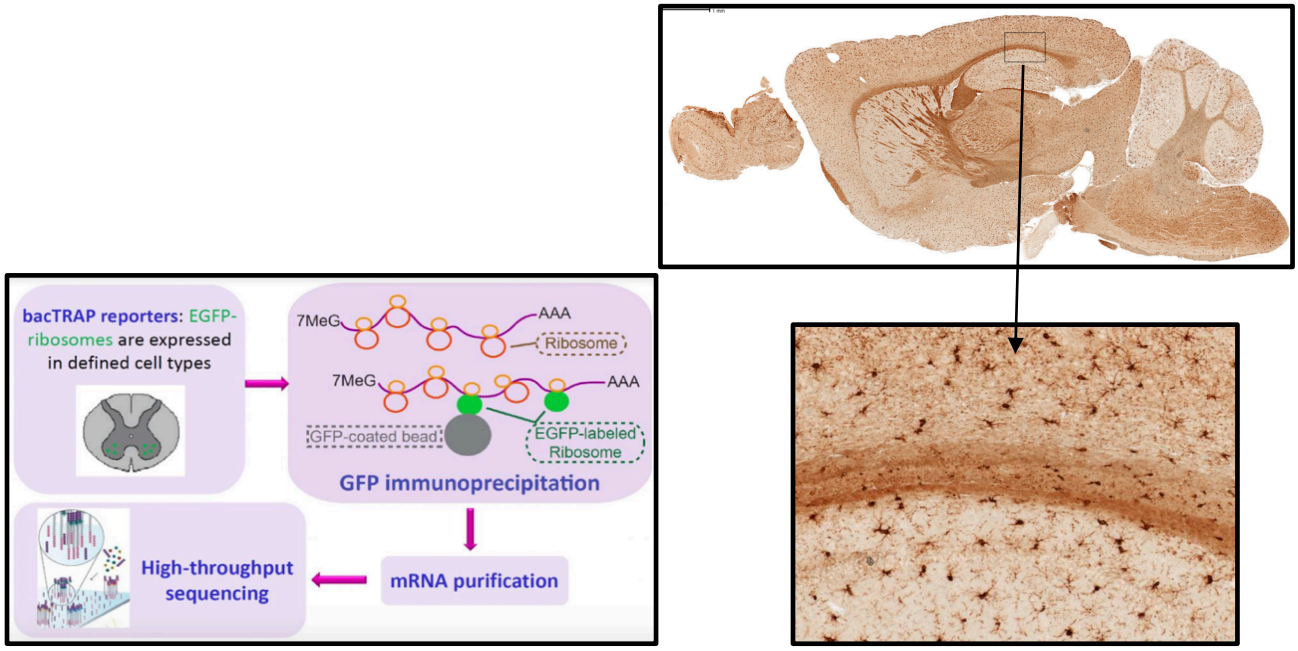

Figure 3.8: bacTRAP technique. The bacTRAP method relies on the immunoprecipitation of labeled polysomes for subsequent RNA-Seq analysis. This sagittal section from the Olig2 oligodendrocyte-specific bacTRAP mouse line illustrates Olig2 expression by OPCs and mature oligodendrocyte processes, both of which contain clusters of ribosomes. The magnified section is an enlargement of the heavily myelinated corpus callosum, in which interfascicular compact white matter is linearly organized[167].

Previous assessments of microarray data from the Olig2 bacTRAP line highlight the presence of both P4 receptors and additional genes relevant to P4 synthesis and metabolism in oligodendrocytes. Multiple P4 receptors including Paqr8, Cyb5d2, and Nenf are enriched in oligodendrocytes as compared to whole brain with fold changes greater than 1.5 (Figure 3.9). Interestingly, Paqr8 is linked to neurite outgrowth and ERK phosphorylation, which has been implicated in the regulation of new myelin production as well as myelin sheath thickness relative to axonal diameter during remyelination[28,113,114,168-170]. The heme-binding proteins Nenf and Cyb5d2 are abundant in oligodendrocytes, where iron delivery is crucial to myelination. Injury and/or stress

likely impacts receptor expression, as upregulated Paqr7 has been detected in oligodendrocytes following TBI[171]. In addition to receptors, enzymes necessary for P4 synthesis and metabolism including diazepam binding inhibitor (Dbi), 5α-reductase (Srd5a1 and Srd5a3), 3β-hydroxysteroid dehydrogenase (Hsd3b7), and cytochrome P450 (Cyp11a1) are significantly enriched in oligodendrocytes compared to whole brain. Srd5a1, Srd5a3, and Hsd3b7 are constitutively expressed in the human brain throughout life[49,55,59,130,172,173]. This high concentration of P4-related genes in oligodendrocytes is encouraging in the sense that myelin-producing cells are also equipped with the machinery to produce and sustain P4 levels (Figure 3.9, Table 3.3).

The Barres Brain Atlas confirms enrichment of many genes implicated in P4 synthesis and signaling in oligodendrocytes as compared to other neural cell types. Expression of the P4 receptor progestin and adipoQ receptor 8 (Paqr8) is restricted to the nervous system and greatly elevated in oligodendrocytes, with a 70.673-fold change in newly formed oligodendrocytes versus microglia, and 6.669- and 65.977-fold changes in myelinating oligodendrocytes versus neurons and microglia, respectively. Additional genes involved in P4 synthesis from cholesterol are highly enriched in OPCs as opposed to more mature forms of oligodendrocytes. Cyp4f15, Cyp1b1, Hsd11b1, and Tspo2 are expressed 41.54-, 29.295-, 23.401-, and 11.587-fold, respectively, in OPCs as opposed to newly formed and/or myelinating oligodendrocytes. Cyp4f15, Cyp1b1, and Hsd11b1 encode enzymes required in the production of certain lipids such as myelin in the CNS, and Tspo2 protein products mediate cholesterol targeting and trafficking that facilitates myelin production. While this expression data is certainly compelling, expression levels do not necessarily correspond to the magnitude of the associated cellular impact. Hence, the P4 receptors that fluctuate significantly in expression during different developmental stages are of particular interest.

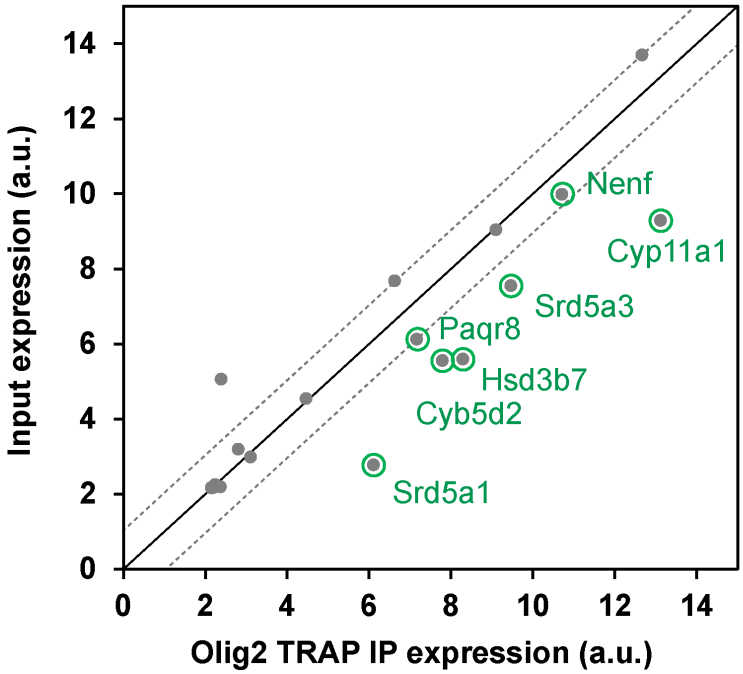

Figure 3.9: P4 receptor-related genes enriched in oligodendrocytes vs whole brain. This scatter plot is derived from microarray data on Olig2-bacTRAP mice. The x-axis reflects gene expression in oligodendrocytes, and the input expression on the y-axis represents whole brain. The dotted lines indicate 2-fold changes in gene expression. The genes highlighted in green with a minimum of 1.5-fold greater expression in oligodendrocytes alone than whole brain are crucial to proper P4 synthesis and functional signaling.

Table 3.3: P4-related genes enriched in oligodendrocytes vs whole brain.

Gene	Protein	Function	logFC	Adj. P Value
Paqr8	PAQR8	P4 Receptor	1.055056	0.207838
Nenf	Neudesin	P4 Receptor	0.72844	0.286415
Cyb5d2	Neuferricin	P4 Receptor	2.248932	0.001114
Cyp11a1	p450scc	P4 Synthesis	3.838916	0.001652
Srd5a1	5α-reductase 1	P4 Metabolism	3.345268	0.000831
Srd5a3	5α-reductase 3	P4 Metabolism	1.916009	0.003233
Hsd3b7	3β-HSD	P4 Metabolism	2.711691	0.007422

Included here are P4 receptors and other associated genes enriched in oligodendrocytes vs whole brain, with fold changes of greater than 1.5, or logFC > 0.585. Adjusted p values are also included, and those <0.05 highlighted in green have the highest confidence of enrichment.

3.3.2 Discussion

One previously alluded to and pivotal aspect of P4 signaling is its rapid metabolism. Despite its short half-life in blood on the order of minutes, P4-induced effects in tissues persist after the hormone has been cleared from serum. These data suggest that P4 metabolites may be at least partially responsible for such effects. In fact, many contributors to the P4 literature concede they cannot experimentally differentiate between P4 and one of its metabolites, ALLO, due to an inability to physiologically isolate one from the other. Among the neuroprotective properties commonly attributed to ALLO are attenuated BBB dysfunction and coagulopathy following ischemic events, decreased neuroinflammation in disease states, and regenerative potential in AD and MS (Figure 3.10)[94,174-176].

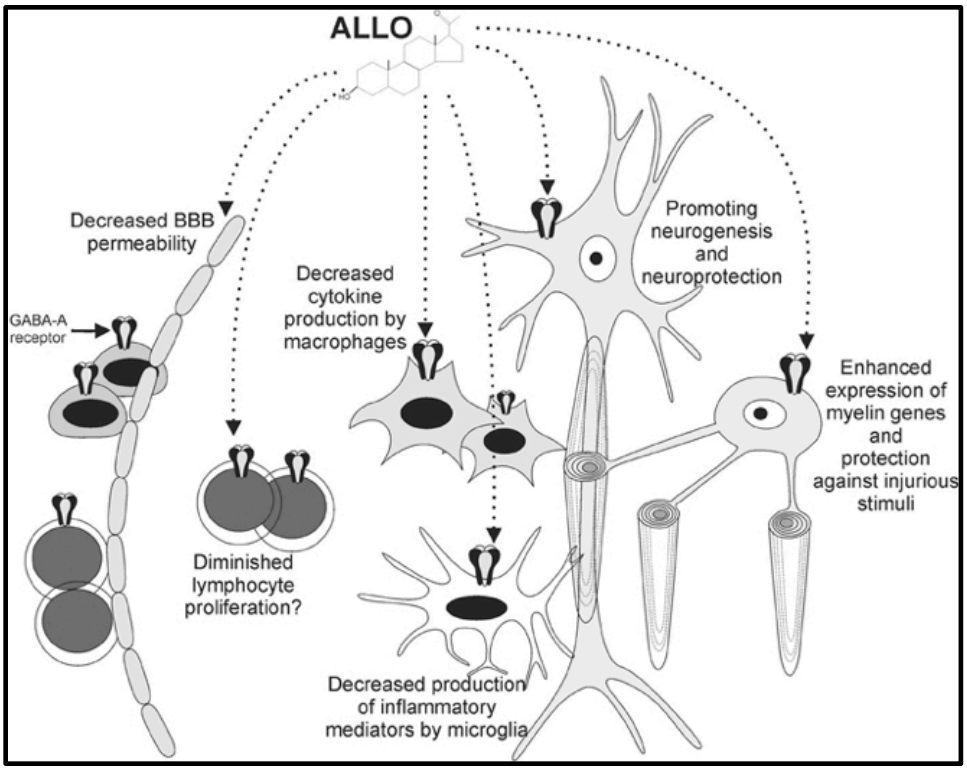

Figure 3.10: ALLO actions in the CNS. ALLO in particular has received much attention in the literature for its neuroprotective properties including upregulation of myelin genes, decreased inflammation and microglial activation, promotion of neurogenesis, and decreased BBB permeability[94].

While OPCs generate large quantities of the immediate P4 precursor, Preg, astrocytes are the primary P4 producers in the CNS (Figure 3.11)[55,57,58,127]. The unique autocrine and paracrine signaling of P4 and its metabolites, namely ALLO, emphasize a profound obstacle to determining the necessity for P4 in CNS development: widespread endogenous generation of P4 throughout life from the adrenal glands, gonads, and CNS itself via neurons and glial cells. Due to pervasive production of neurosteroids and their capacity to infiltrate the BBB when dissociated from albumin, prior studies merely speculate as to mechanisms of P4 activity on myelin development and pathology.

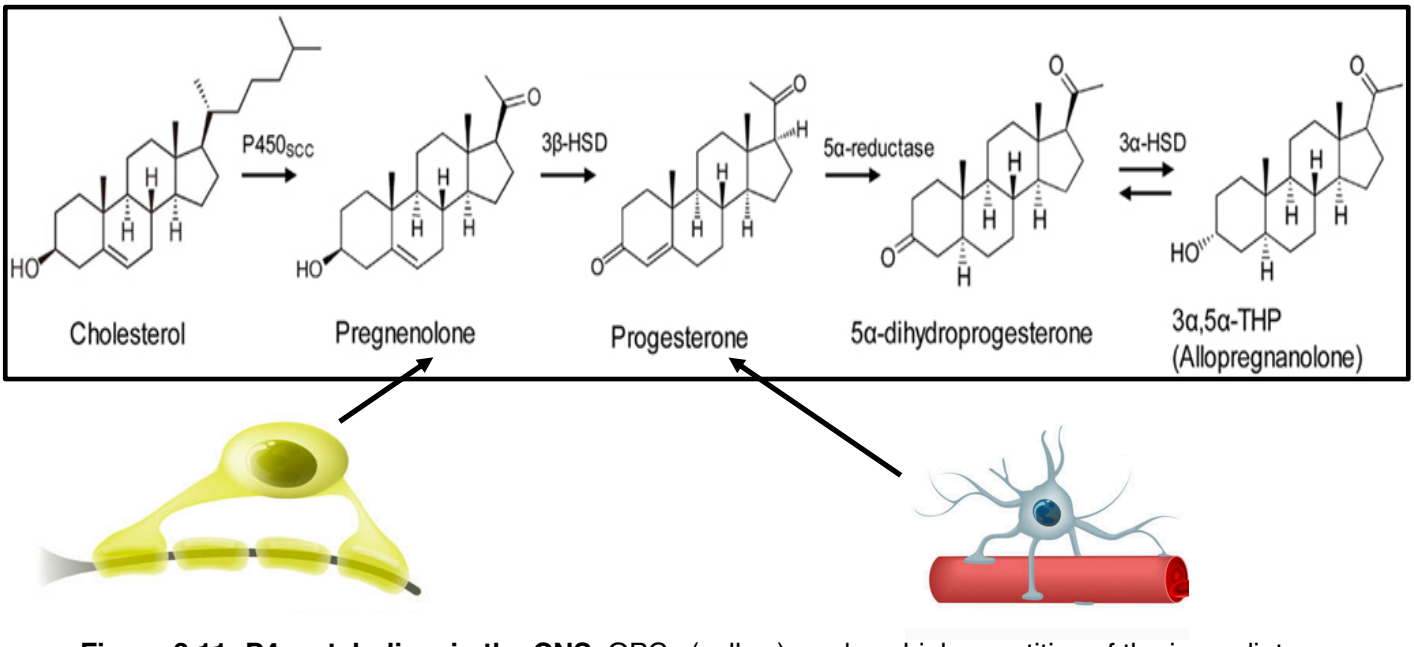

Figure 3.11: P4 metabolism in the CNS. OPCs (yellow) produce high quantities of the immediate P4 precursor, Preg, while astrocytes (blue) are the primary producers of P4. Peripherally, P4 is typically bound to albumin, leaving little free P4 in the blood. However, free P4 easily crosses the BBB via transmembrane diffusion[177].

These limitations prompted me to shift my experimental paradigm to one entirely devoid of any P4, whether it be endogenous or exogenous. I considered this a more rigorous strategy to determine whether or not the hormone is required for myelination. Thorough research of the neurosteroid synthesis pathway aided my evaluation of candidate enzymes to inhibit in my hypothetical P4-free mouse. I chose p450scc, encoded by the CYP11A1 gene, as it initiates hormone synthesis by converting cholesterol into Preg, the immediate precursor to P4[178]. Mice lacking functional p450scc are unable to produce any neurosteroids at all, and not surprisingly, die shortly after birth. According to the literature, they can be rescued with a daily injection of a steroid cocktail consisting of dexamethasone 21-phosphate, prednisolone, and fludrocortisone acetate for about one postnatal week; yet I was unable to reproduce this rescue procedure[179]. The Jackson Laboratory has a cryopreserved Cyp11a1-GFP-Cre strain in which a GFP-Cre cassette (GC) was inserted into the *Cyp11a1* locus (JAX stock #010988). This Cyp11a1-GC strain, traditionally utilized in the context of genitourinary and mammary development, can be manipulated to produce a Cyp11a1 KO mouse[180]. There are no records indicating any relevant CNS phenotypes have been evaluated. I ordered and cryo-recovered this strain with the intent to perform a comprehensive analysis of the CNS architecture.

CHAPTER 4: Implementation of a Neurosteroid-free Model System

4.1 Characterization of Cyp11a1 KO mouse

4.1.1 Establishment of Cyp11a1-GC transgenic mouse line

PRKO mice were created by the insertion of a targeting vector containing a GFP-Cre cassette (GC) and FRT site-flanked kanamycin and neomycin resistance cassette into the first coding exon of the endogenous Cyp11a1 gene immediately following the ATG translation initiation codon (Figure 4.1)[180]. This entire construct essentially serves as one large insertional mutation, thereby allowing the generation of Cyp11a1-null homozygotes.

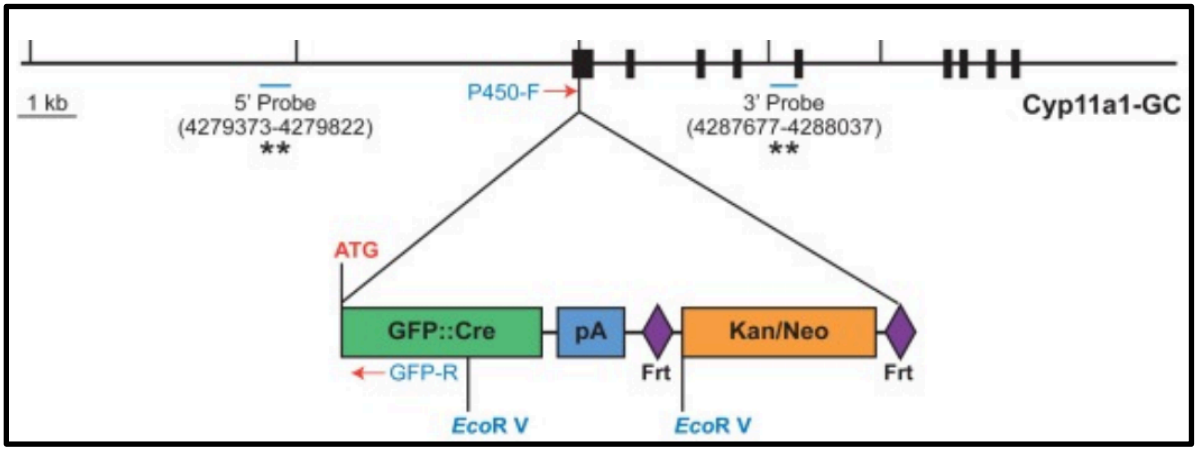

Figure 4.1: Genetic construct of Cyp11a-GC mice. A 7.9 kb genomic fragment of *Cyp11a1* (containing the first four exons) was gap repaired by homologous recombination onto pDTA.4B from a BAC clone obtained from Sanger Institute. A targeting vector containing a GFP-Cre cassette (GC) and FRT site flanked Kanamycin/neomycin selection cassette was used to disrupt the exon containing the ATG translation start-site. Following electroporation, correctly targeted embryonic stem cells were injected into recipient blastocysts. The resulting chimeric animals were crossed to C57BL/6 mice[180].

Members of Dr. Bon-chu Chung's lab at the Institute of Molecular Biology, Academia Sinica in Taiwan provided primer sequences and a specific PCR protocol for genotyping. The inclusion of three primers yielded a 368-bp amplicon corresponding to the WT allele and a 296-bp amplicon corresponding to the mutant allele (Figure 4.2).

Seven Het and one WT mouse of the B6;129P-*Cyp11a1*$^{tm1(GFP/cre)Pzg}$/J strain (Stock No. 010988) were cryorecovered and transferred from the Jackson Laboratory to Weill Cornell Medicine. Due to early postnatal death of homozygous KOs, Het males and females were crossed to generate WT, Het, and homozygous KO offspring.

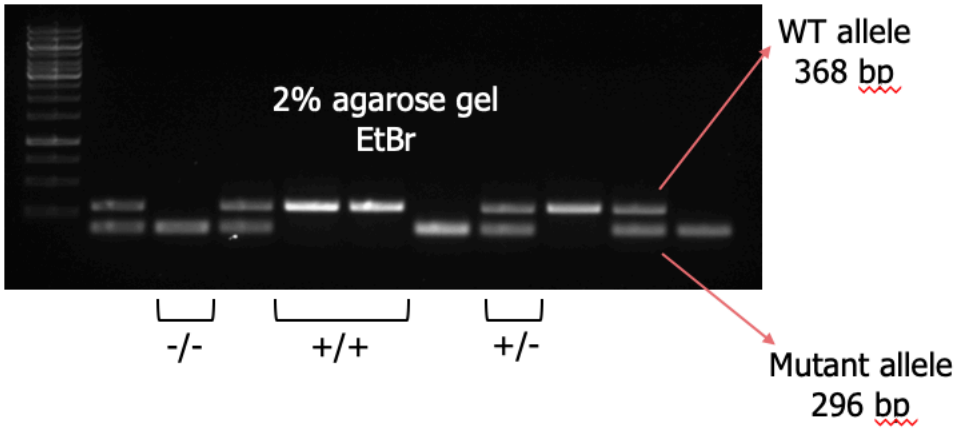

Figure 4.2: Genotyping of Cyp11a1-GC mice. Three primers were combined in the same PCR reaction to generate a 296-bp amplicon corresponding to the mutant allele and a 368-bp amplicon for the WT allele. Presence of both amplicons indicates a Het.

4.1.2 Documented physiological abnormalities

Four Cyp11a1-deficinet mouse models in addition to the B6;129P-*Cyp11a1*$^{tm1(GFP/cre)Pzg}$/J strain I'm using here have undergone primarily adrenal and reproductive characterization. Table 4.1 lists the nomenclature for each of these strains, along with the nature of the mutations and institutional sources. Despite the abundance of abnormalities associated with such mutations, it is immediately apparent that no methodical evaluation of the nervous system has been attempted in any of the transgenic strains. The few CNS-relevant phenotypes that have been identified were not directly derived from targeted analyses of the CNS, highlighting the need for clarification of the roles for neurosteroids like P4 in brain and spinal cord development and physiology. Table 4.2 provides a comprehensive overview of confirmed phenotypes attributed to Cyp11a1 deficiency categorized at the functional level. Check marks indicate the phenotype has been confirmed in the respective strain. Dashes indicate the phenotype was specifically evaluated but not observed. Blank cells indicate the specific phenotype was not addressed. Phenotypes highlighted in red are relevant, either directly or indirectly, to the CNS.

Table 4.1: Existing Cyp11a1-deficient mouse models.

Strain Name	Allele Type	Mutation	Mutation Details	Source
Cyp11a1$^{tm1(GFP/cre)Pzg}$	Targeted (recombinase)	Insertion	Targeting vector containing GFP-Cre cassette and FRT site-flanked kanamycin and neomycin resistance cassette inserted into first coding exon of endogenous gene immediately following ATG translation initiation codon	Pumin Zang, Baylor College of Medicine
Cyp11a1^{tm1Bcc} / Cyp11a1$^{E1\text{-}neo}$	Targeted (Null/KO)	Insertion	Exon 1 disrupted by insertion of floxed neomycin selection cassette; absence of protein in homozygous mutant mice confirmed by WB of adrenal and testis extracts*	Bon-chu Chung; Institute of Molecular Biology, Academia Sinica
Cyp11a1$^{tm1.1Bcc}$ / Cyp11a1$^{E1\text{-}loxP}$	Targeted (Null/KO)	Insertion, intragenic deletion	Floxed neo cassette replaced part of Exon 1; cre-mediated recombination removed neo cassette; absence of protein expression in E18.5 adrenal tissue confirmed by WB*	Bon-chu Chung; Institute of Molecular Biology, Academia Sinica
Cyp11a1^{tm2Bcc} / Cyp11a1^{L}	Targeted	Insertion, nucleotide substitutions	Proximal SF-binding site in Intron 1 replaced with one in which genetic sequence was altered from TAGCCTTGA to TAGaaTTGA; floxed neo cassette with 3' loxP site inserted in Intron 1 but removed by germ-line, cre-mediated recombination; protein expression reduced 7-fold in adrenal and testis but unaffected in placenta and ovary*	Bon-chu Chung; Institute of Molecular Biology, Academia Sinica
Cyp11a1$^{tm1b(EUCOMM)Hmgu}$	Targeted (Null/KO, reporter)	Insertion, intragenic deletion	Cre-mediated excision of parental CYP11a1 allele resulted in removal of promoter-driven neomycin selection cassette and critical exon(s), leaving behind inserted lacZ reporter sequence	Helmholtz Zentrum Muenchen GmbH, part of EUCOMM consortium

*Note that these sources only probed for p450scc protein expression in endocrine and reproductive glands, and not the CNS[133,180-185].

Table 4.2: Abnormal phenotypes in Cyp11a1-deficient mouse strains.

Functional Category	Phenotype	Strain 1	Strain 2	Strain 3	Strain 4	Strain 5
Adrenal	Abnormal adrenal gland physiology	✓	✓		✓	
	Abnormal adrenal gland morpholgy	✓	✓	✓	✓	
	Abnormal adrenal cortex morphology		✓		✓	
	Abnormal adrenocortical cell morhology			✓		
	Absent adrenal chromaffin cells			✓		
	Abnormal zona fasciculate morphology				✓	
	Abnormal zona glomerulosa morphology				✓	
	Enlarged adrenal glands		–		✓	
	Small adrenal glands		✓		–	
	Enlarged adrenocortical cells		✓			
	Excessive lipid (cholesterol) accumulation		✓	✓	✓	
	Altered adrenal circadian rhythms		✓			
Genital	Reproductive system abnormalities	✓	✓			
	Absent bulbourethral gland		✓		–	
	Absent prostate gland		✓		–	
	Abnormal seminiferous tubule morphology		✓			
	Small testes		✓			
	Ectopic CYP21 expression in testes		✓			
	Abnormal spermatogenesis		✓		–	
	Absent scrotum		✓		–	
	Abnormal epididymis epithelium morphology		✓			
	Absent coagulating gland		✓		–	
	Abset ampulla		✓		–	
	Abnormal vas deferens morphology		✓			
	Secondary male to female sex reversal		✓		–	
Hormone Levels	Increased circulating adrenocorticotropin		✓	✓	✓	
	Decreased adrenaline			✓		
	Decreased noradrenaline			✓		
	Abnormal corticosterone		✓	✓	✓	
	Decreased circulating aldosterone		✓			
Electrolyte Levels	Abnormal circulating sodium		✓			
	Abnormal circulating potassium		✓			
	Increased urinary sodium		✓			
Growth	Placental defects				–	✓
	Postnatal growth retardation		✓		–	
	Muscular atrophy		✓		–	
Neonatal Lethality	Complete penetrance	✓		✓	–	
	Incomplete penetrance	–	✓		✓	
Liver	Dilated sinusoidal spaces					✓
	Dilated bile duct					✓
Eye	Abnormal optic cup morphology	✓				✓
	Retrolental blood					✓
Behavioral	Decreased food intake		✓			
	Hypoactivity		✓			
Cellular	Abnormal mitochondrion morphology			✓	✓	
Cardiovascular	Hemopericardium					✓
Immune	Decreased T cell apoptosis under stress				✓	
PNS	Thin hypoglossal nerve					✓

Nervous system phenotypes listed in red in Table 4.2 include absent adrenal chromaffin cells, abnormal optic cup morphology, and retrolental bleeding. Chromaffin cells innervating the adrenal gland and sympathetic nervous system are responsible for the body's involuntary catecholamine response to different types of stressors, colloquially known as the "fight or flight" response. Fear- or stress-induced input from splanchnic nerves promotes adrenal chromaffin cells to secrete hormones such as epinephrine (adrenaline), norepinephrine (noradrenaline), dopamine, enkephalin, and enkephalin-containing peptides, amongst others, into the bloodstream[186]. Without functional adrenal chromaffin cells, Cyp11a1-deficient mice are particularly vulnerable to various environmental and physiological stressors. The phenotypes most directly related to the CNS involve ocular defects. As altered optic disc morphology is visible to the naked eye as early as E12.5 based on my dissection experience, it is not surprising that mice lacking sufficient p450scc protein exhibit delayed optic cup development[185]. Retrolental or retinal bleeding is most commonly a result of premature birth, in which case retinal blood vessels fail to grow properly, if at all, into the back of the eye. These fragile vessels are prone to leakiness, leading to bleeding that can precede retinal detachment and even blindness[187].

Abnormal mitochondrial structure, though not in and of itself a CNS phenotype, may be applicable throughout the entire body at the cellular level. According to previous studies of enteroendocrine cell-resident mitochondria, Cyp11a1 deficiency interferes with the cell's inherent steroidogenic capacity by reducing the number of cristae, thus eliminating critical opportunities for cholesterol conversion at the mitochondrial membrane. Decreased and at times completely absent cristae are evident as early as E9.5 in the placenta and E18.5 in the adrenal gland in mice, demonstrating the autocrine nature by which p450scc is both required to generate normal cristae, and subsequently dependent on maximally efficient mitochondria to facilitate expeditious steroidogenesis[133]. Similar adrenal mitochondrial malformations were noted in a mouse strain with a mild mutation in the *Cyp11a1* promoter that evades neonatal lethality as late as postnatal 18 weeks[184]. Again, these studies have failed to incorporate neural mitochondria thus far, reiterating the dearth of experimental efforts centered on the presumably wide-ranging consequences of CNS cells deprived of steroidogenic capability.

4.1.3 Discussion

Despite the current lack of data on neurosteroid contributions to CNS development, the various phenotypic abnormalities identified above offer compelling insights into the vast potential for discovery in this nascent field. The established presence of neurosteroid hormones throughout life is remarkably apparent as early as neural crest formation. Major vertebrate neural crest derivatives are diverse, including PNS cells, endocrine and paraendocrine cells, pigment cells, facial cartilage and bone, and connective tissue. As illustrated in Figure 4.3, these derivatives occupy transient regions of the neural crest before migrating to fulfill their destined cell fates upon neural tube closure. These regions are defined by the classes of cells and tissue they

propagate. The cranial or cephalic region yields the bone and cartilage of the face and neck, bones of the middle ear and jaw, cranial neurons, facial glia and connective tissue, thymic cells, odontoblasts of tooth primordia, and epidermal pigment cells. Parasympathetic ganglia of the gut can be traced to the vagal and sacral regions. Somites one through three comprise cardiac neural crest cells necessary to divide the aorta and pulmonary artery. The epinephrine-producing chromaffin cells that fail to populate the adrenal medulla in Cyp11a1-deificent mice are typically born within the most expansive neural crest region, the trunk. Somites contained within the boundaries of the trunk neural crest give rise to sympathetic neurons, a subset of which (18 through 24) generate the medulla portion of the adrenal gland[188].

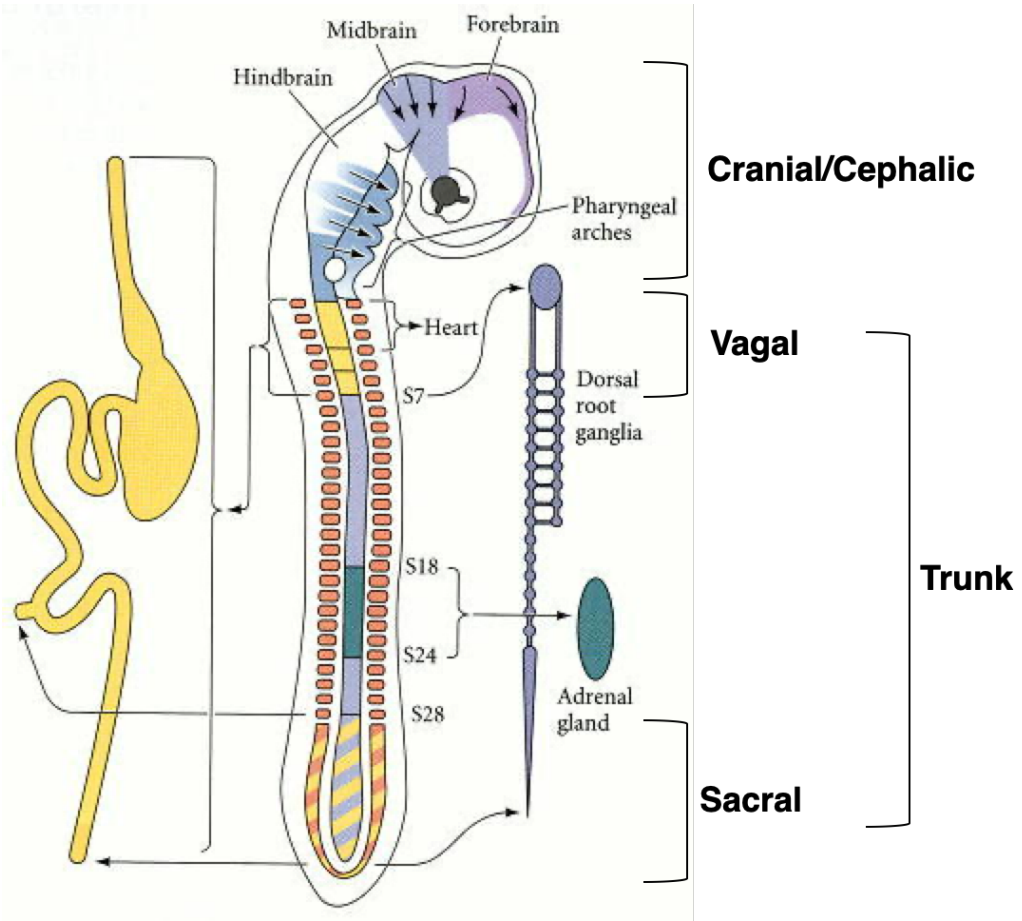

Figure 4.3: Vertebrate neural crest fate map. Vertebrate neural crest derivatives are confined to the distinct regions delineated by numerical somites. Of particular interest with respect to Cyp11a1 deficiency are the adrenal chromaffin cells, which arise from somites 18 through 24 within the trunk region.

Ventrolateral migration of trunk neural crest cells driven by extracellular matrix (ECM) components among other migratory cues allows for final differentiation[189]. This process is highly glucocorticoid-dependent at multiple defining points along the pathway to adrenomedullary specification (Figure 4.4). First, glucocorticoids are required to inhibit factors that, in the presence of fibroblast growth factor 2 (FGF2) and nerve growth factor (NGF), would otherwise promote differentiation into sympathetic neurons.

Cells that evade neuronal specification then further rely on glucocorticoids to activate enzymes associated with their newfound adrenomedullary fate[190]. The capacity for catecholamine synthesis is attributed to two glucocorticoid-induced enzymes in particular. Interestingly, tyrosine hydroxylase (TH), indicative of proper trunk cell migration into the medulla, is expressed at normal levels in the Cyp11a1-deficient adrenal gland. However, expression of phenylethanolamine-N-methyltransferase (PMNT), the enzyme that enables catecholamine synthesis and thus serves as a classical marker for adrenergic chromaffin cells, is not detectable in the absence of Cyp11a1[133]. This suggests that in Cyp11a1-deficient mice, maternal glucocorticoids delivered via the placenta are sufficient to generate adrenal chromaffin precursor cells. Maturation into fully functional chromaffin cells capable of catecholamine synthesis, however, must demand additional sources of endogenous embryonic glucocorticoids.

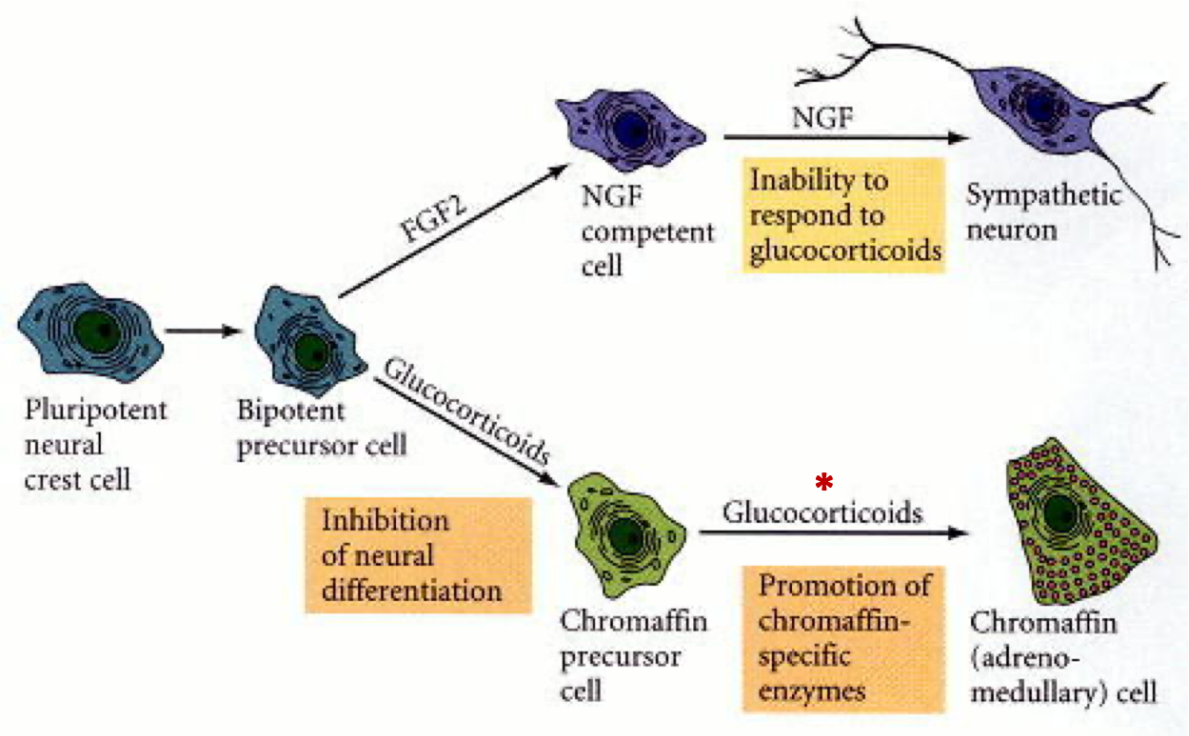

Figure 4.4: Adrenal chromaffin cell differentiation. The red asterisk indicates the point at which a presumed lack of adequate glucocorticoids prevents PMNT expression in Cyp11a1 mutant mice, rendering chromaffin precursor cells unable to produce catecholamines critical to the stress response such as epinephrine.

In terms of the CNS proper, the retinal and mitochondrial defects ascribed to Cyp11a1-deificient mouse strains draw striking parallels to morphological patterns characteristic of demyelinating diseases like MS. Mitochondrial alterations have been documented in oligodendrocytes, peripheral blood mononuclear cells (PBMCs), and peripheral lymphocytes from MS patients. De Rasmo et al. found a high incidence of PBMC optic atrophy 1 (OPA1) deregulation in the MS cases. This protein is vital to mitochondrial health, mediating cellular bioenergetics, cristae architecture, and release

of pro-apoptotic factors when necessary[191]. The abnormal cristae phenotype associated with MS mirrors that of the Cyp11a1-deficient adrenal gland, suggesting similar issues with general steroidogenesis. Oligodendrocytes are particularly vulnerable to mitochondrial dysfunction due to the exceptionally high energy expended producing myelin as well as releasing lactate to drive neuronal action potentials. The brain milieu of chronic inflammation and demyelination leads to redistribution of ion channels populating the Nodes of Ranvier. Consequent disturbances to the propagation of the electrochemical gradient along the neuron increase ATP consumption, thereby forcing compensatory mechanisms in the effected mitochondria. As such, increased oligodendroglial mitochondria with a swollen appearance and altered cell morphology often accumulate in the context of MS. A vicious cycle of oxidative stress and ongoing inflammation perpetuate further mitochondrial damage, until the energy imbalance is so great that action potentials are not maintained[192]. The ensuing buildup of sodium in the cytoplasm forces calcium transfer into the cell which in turn activates an apoptotic response. The resulting and often irreversible neuronal death and Wallerian degeneration both contribute to MS pathology.

As the leading cause of cell death in neurodegenerative conditions, mitochondrial dysfunction is certainly a worthy therapeutic target[193]. The defective cristae in the Cyp11a1-deficient mice emphasize the vitality of steroidogenesis to maintaining mitochondrial architecture and dynamics. Such defects, if present in the MS-afflicted CNS, would only exacerbate the already debilitating cascade of energy depletion in oligodendrocyte metabolism and the inevitable neurodegeneration that follows. Again, a thorough assessment of the embryonic rodent CNS in the absence of p450scc protein is necessary to determine whether or not neurosteroid deficiency can elicit mitochondrial damage in future myelinating oligodendrocytes.

4.2 Anatomical analysis of Cyp11a1-GC transgenic mouse

4.2.1 Gross embryonic physical assessment

To this end, E18.5 Cyp11a1-GC transgenic mouse embryos were subject to retrospective genotyping and gross physical assessment. Traits including size, weight, and overall morphology were evaluated. Counter to my initial expectations, the absence of significant trends in size precluded the ability to predict genotype by the naked eye alone. Similarly, the slight variation in weights of the entire embryos and their respective placentae and brains was a universal characteristic of the litter at large that was not strictly correlated with genotype (Figure 4.5, A). One trend that did become apparent over the course of multiple embryonic dissections with respect to general anatomy was abnormal optic disc morphology (Figure 4.5, B), consistent with previous reports summarized in Table 4.2[180-182,185]. This defect was initially visible at E12.5.

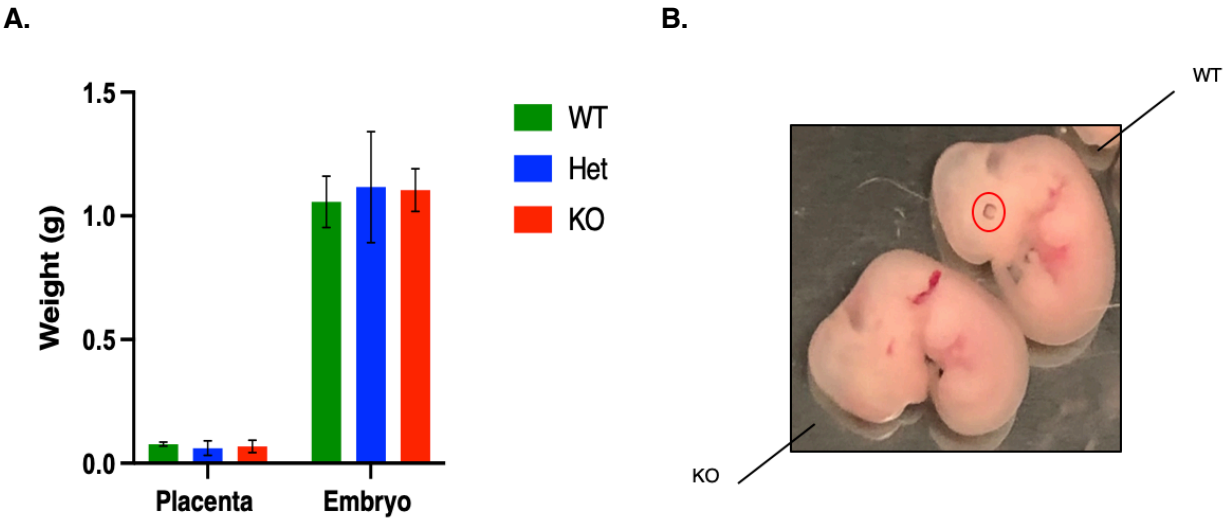

Figure 4.5: Summary of morphological comparisons across embryonic B6;129P-*Cyp11a1*$^{tm1(GFP/cre)Pzg}$/J genotypes. No significant weight differences exist at E18.5 (A). Results expressed as Mean ± STDEV, n = 12 embryos per genotype. However, Cyp11a1-deficient embryos as young as E12.5 appear to lack proper optic discs (B). The normally developing optic disc circled in red in the WT embryo is not present in the KO embryo.

4.2.2 Phenotypes associated with perinatal lethality

H&E staining of the E18.5 Cyp11a1-GC transgenic embryos revealed several factors contributing to the perinatal lethality seen in the homozygous KO mouse. The most prominent defects in the KO animals are adrenal gland abnormalities previously described in the literature[133,180,183,184]. The three magnifications provided in Figure 4.6 of the adrenal glands of WT compared to KO mice depict both broad architectural as well as cellular damage. In contrast to the WT adrenal glands featuring discrete corticomedullary regions, the disorganized KO adrenal glands lack such anatomical boundaries. Cortical cells in these animals show rampant signs of degeneration including cytoplasmic granularity. The high magnification image of the KO tissue in Figure 4.6 exemplifies the progressive cellular degeneration initiated by irreversible condensation of nuclear chromatin, or pyknosis, preceding necrotic or apoptotic cascades. These pyknotic cells inevitably undergo subsequent karyorrhexis, or destructive nuclear fragmentation, leaving condensed chromatin dispersed randomly throughout the cytoplasm. Karyorrhexis events manifest as variably sized, round, clear, and colorless cytoplasmic holes as labeled in Figure 4.6. Cell shrinkage alongside cytoplasmic hypereosinophilia are further hallmarks of the adrenal insufficiency attributed to the KO mice with grave functional consequences. Under normal conditions, the adrenal gland secretes abundant glucocorticoids which in turn inhibit white blood cell proliferation and survival. Inadequate adrenal glucocorticoid stores yield unusually high numbers of eosinophils with the potential to harm surrounding tissue. Staining for TUJ1, the primary neuron-specific component of microtubules, labels the compact bundles of chromaffin cells inhabiting the WT adrenal tissue. Their counterparts in the KO tissue, however, are markedly fewer in number and more dispersed throughout the

entirety of the adrenal gland (Figure 4.6). As stated above, the absence of chromaffin cells is one of the few neural phenotypes previously identified in Cyp11a1-deficient mice. While these cells are present to some extent according to the immunohistochemistry (IHC) images in Figure 4.6, the loss of medulla-specific localization likely inhibits their functionality of releasing the neurohormones epinephrine and norepinephrine into the bloodstream[186].

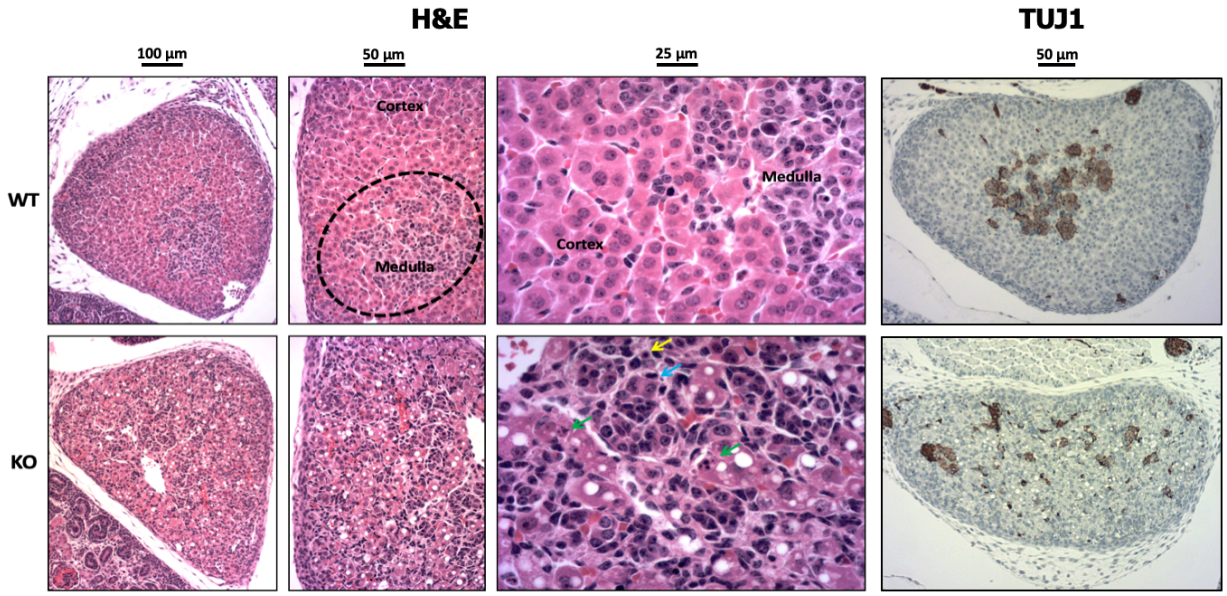

Figure 4.6: Embryonic adrenal gland abnormalities in homozygous KO E18.5 B6;129P-*Cyp11a1*$^{tm1(GFP/cre)Pzg}$/J mice. This H&E analysis of the adrenal gland not only indicates indistinct boundaries defining the cortex and medulla in the KO, but rampant cell death of cortical cells as well. Arrows in bottom right provide examples of the pyknosis (yellow), cytoplasmic vacuolation (blue), and karyorrhexis (green) associated apoptotic and/or necrotic cascades.

While the aforementioned adrenal defects are perhaps the defining phenotype of the Cyp11a1-GC homozygous KO embryo, liver abnormalities are also likely to play a role in perinatal lethality. The top horizontal panel of Figure 4.7 illustrates significantly decreased cytoplasmic vacuolation of hepatocytes originating from KO as compared to WT animals. This observation suggests hindered organ metabolism in the liver of KO mice in which hepatocytes are unable to properly absorb glycogen. Alternatively or additionally, hepatocytes' failure to meet the liver's metabolic needs may inhibit an effective stress response at the cellular level. This novel cytoplasmic vacuolation phenotype is distinct from previously documented dilated sinusoidal spaces. Dynamic microvascular hepatic structures serve as the capillaries and venules of the liver. The swelling cited in the literature points to decreased blood cell production, as the liver is a major site of extramedullary hematopoiesis during development[185]. Sinusoidal dilation might also emerge following hepatocyte atrophy in some cases, though this has not been confirmed.

The H&E staining revealed yet another, likely more acute cause of perinatal death in KO animals. Incredibly robust lung abnormalities in bronchial expansion

suggest marked difficulty with inspiration immediately following birth. The bottom horizontal panel of Figure 4.7 illustrates the great extent to which airway expansion is restricted in the lungs of KO mice. This novel finding, though yet to be reported, adds respiratory inhibition to the slew of physiological stressors certain to prevent perinatal survival. One proposed mechanism that might impair proper airway expansion involves a failure to generate and mobilize sufficient surfactant molecules in the absence of endogenous glucocorticoids. Typically, these molecules reduce surface tension via interposition between water molecules, thereby effectively creating alveolar space requisite for normal respiration. The ensuing molecular events entail a carefully orchestrated sequence among pulmonary-resident steroid hormones and their related receptors and metabolic enzymes. Specifically, expression of p450scc, the enzyme produced from the CYP11A1 gene, promotes the release of abundant glucocorticoids at E15. The resultant activation of their respective glucocorticoid receptors around E16 allows for the conversion of fetal lung glycogen to surfactant by E17[194]. The surfactant surge is crucial for airway expansion to begin at this developmental stage. By E18.5, prominent bronchial expansion should be visible, as seen in the H&E staining of the WT, but not KO, mouse lung (Figure 4.7). Notably, all enzymes necessary for glucocorticoid synthesis are expressed in pulmonary tissue at E15 just prior to the glucocorticoid surge, including StAR, 3ß-hydroxysteroid dehydrogenase, 21-hydroxylase, and 11ß-hydroxylase[195]. The presence of all of these enzymes simultaneously supports the glucocorticoid-driven model of surfactant-induced airway expansion during normal lung development.

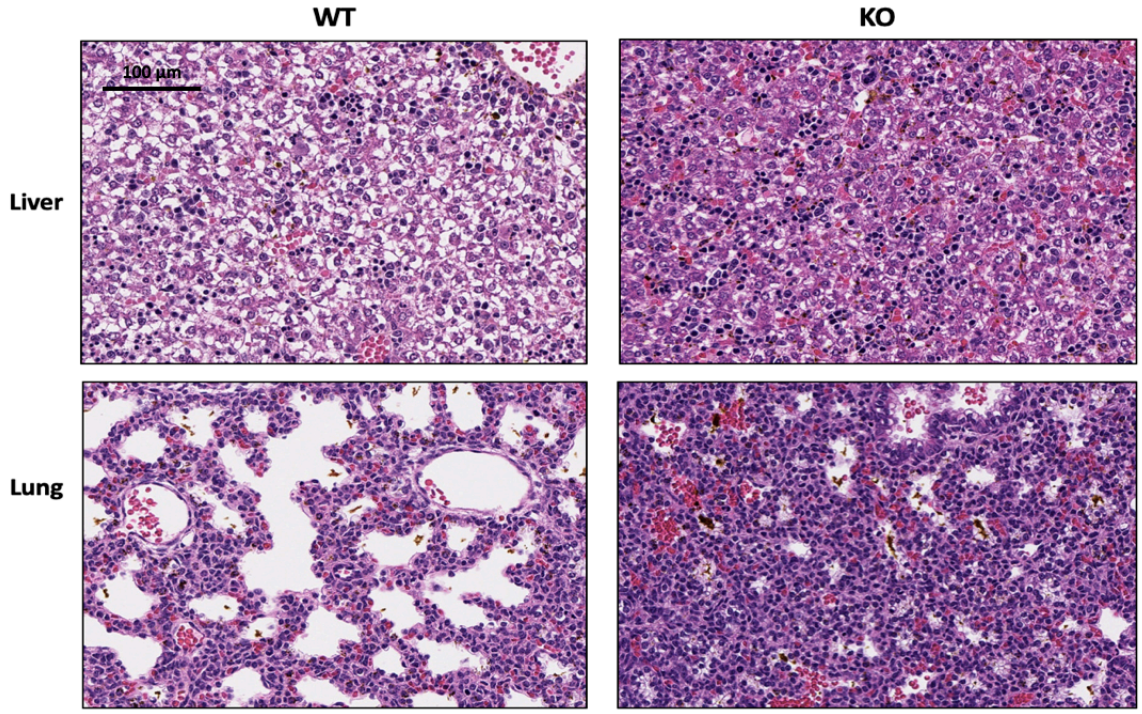

Figure 4.7: Embryonic liver and lung abnormalities in homozygous KO E18.5 B6;129P-*Cyp11a1*$^{tm1(GFP/cre)Pzg}$/J mice. H&E analysis of the liver suggests that KO animals experience altered organ metabolism due to the markedly decreased cytoplasmic vacuolation of hepatocytes compared to their WT counterparts (top panel). H&E staining additionally offers novel insight into a pulmonary phenotype in the KOs of highly inadequate airway expansion (bottom panel). The ensuing respiratory issues likely contribute to the robust neonatal lethality in these animals.

4.2.3 Brain histological analysis

A comprehensive histological analysis of the WT and Cyp11a1-null brains unexpectedly yielded no significant anatomical differences between the two genotypes. The similar H&E profiles eliminate the suspicion of anatomical abnormalities in the KO brain. The cresyl violet and TUJ1 staining do not provide any indication of atypical neural architecture in the KO brain. Finally, the lack of differences in cleaved caspase-3 staining suggest developmental apoptotic patterns in the brain at large have not gone awry in the KO brain either by E18.5 (Figure 4.8).

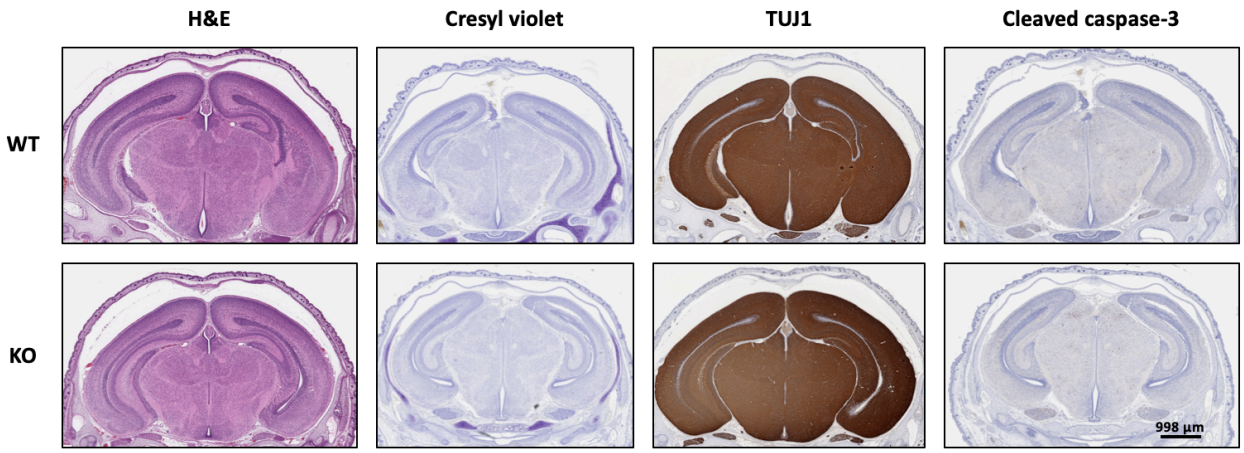

Figure 4.8: Brain anatomy in homozygous KO E18.5 B6;129P-*Cyp11a1*$^{tm1(GFP/cre)Pzg}$/J mice. No significant differences are observed distinguishing WT from Cyp11a1 KO E 18.5 brain tissue by H&E, cresyl violet, TUJ1, or cleaved caspase-3 staining.

4.2.4 Spinal cord histological analysis

Much like the brain, the spinal cord is anatomically comparable between WT and Cyp11a1 KO E18.5 brain tissue according to H&E in addition to TUJ1 staining (Figure 4.9). The virtually identical spatial localization of cells and neurons in both genotypes implies the absence of endogenous neurosteroid production does not drastically compromise anatomical brain development, at least up to E18.5.

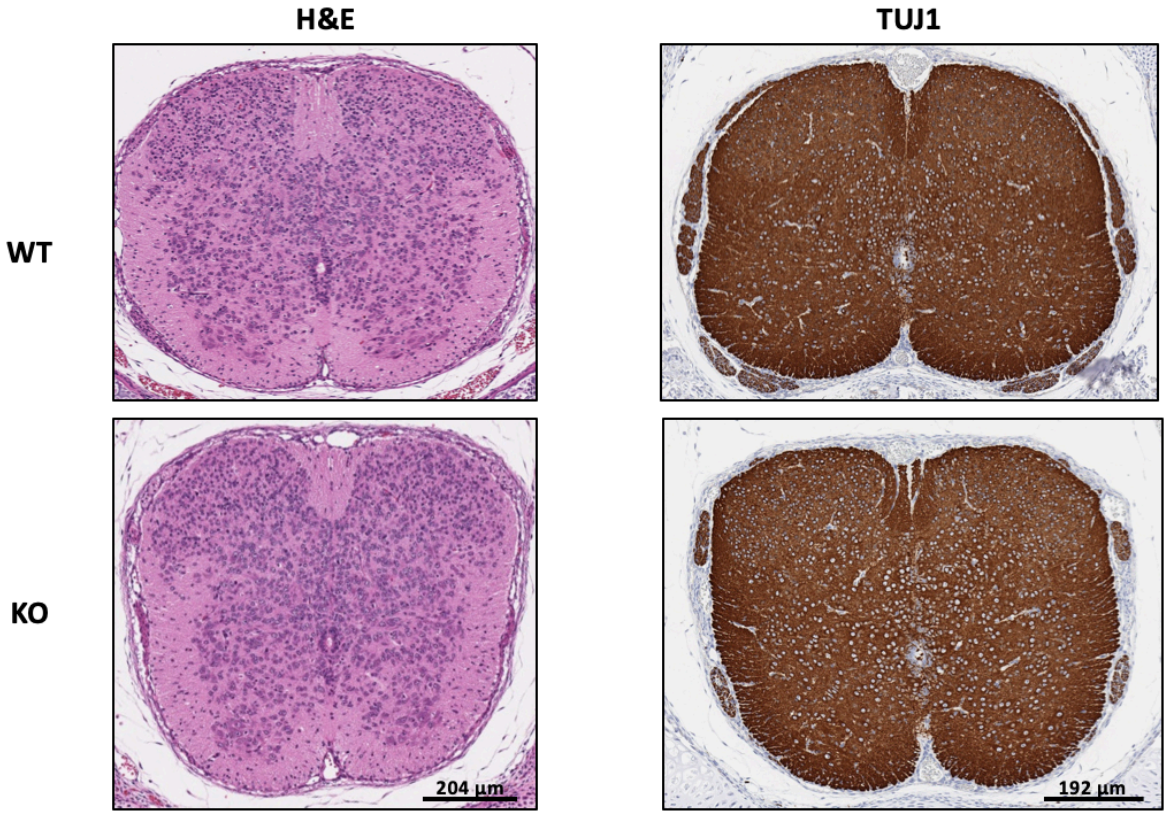

Figure 4.9: Spinal cord anatomy in homozygous KO E18.5 B6;129P-*Cyp11a1*$^{tm1(GFP/cre)Pzg}$/J mice. No significant differences are observed distinguishing WT from Cyp11a1 KO E 18.5 spinal cord tissue by H&E or TUJ1 staining.

4.2.5 CNS oligodendrocyte immunohistochemistry

Despite the absence of any glaring structural brain abnormalities, it is conceivable that oligodendrocyte biology might vary based on the extent of local neurosteroid synthesis. However, no differences in oligodendrocyte frequency or spatial organization emerge from nuclear Olig2 or MBP plasma membrane staining (Figure 4.10).

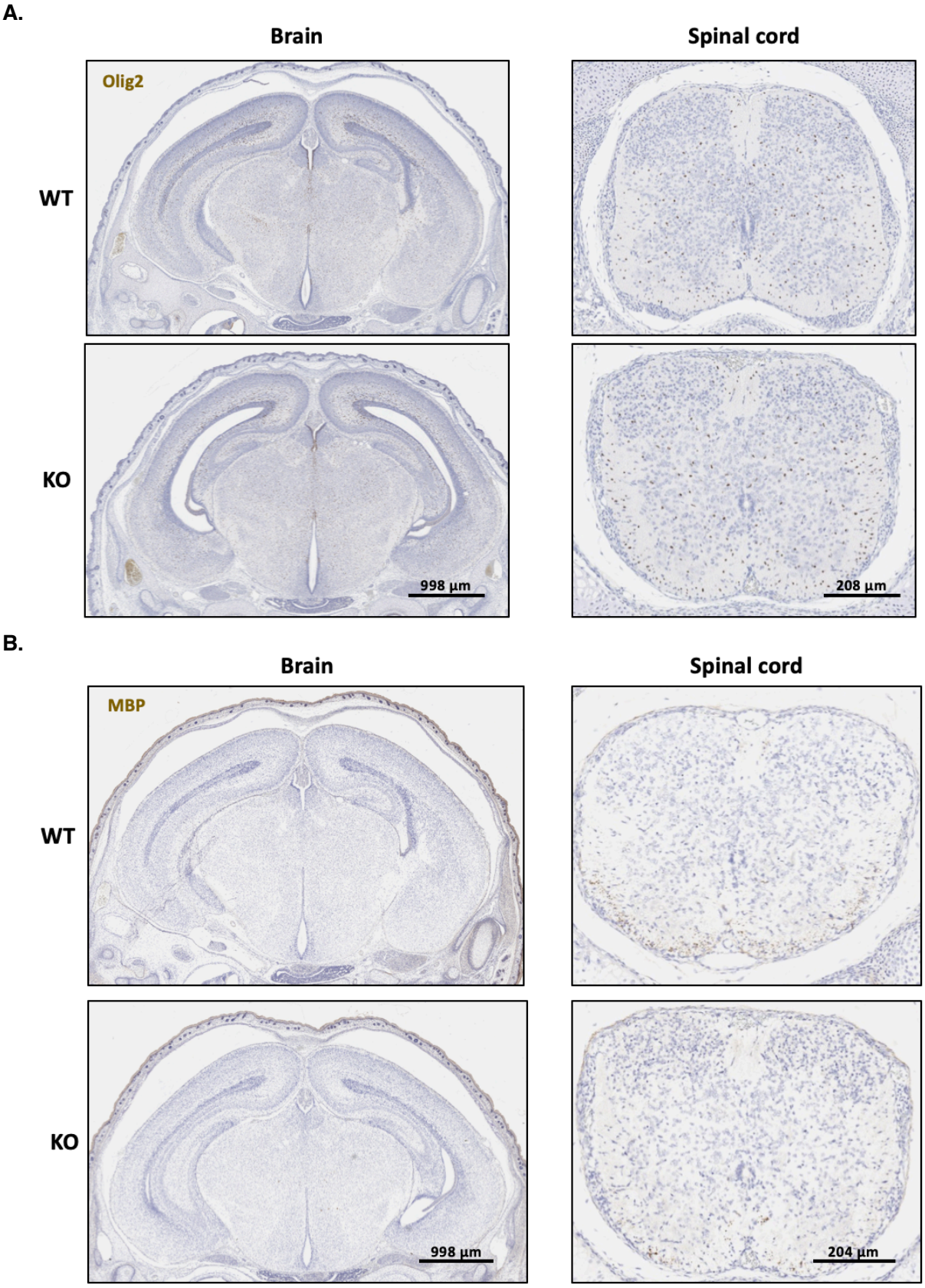
A.
Brain
Spinal cord
Olig2
WT
KO
998 µm
208 µm
B.
Brain
Spinal cord
MBP
WT
KO
998 µm
204 µm

Figure 4.10: Oligodendrocyte immunohistochemistry in homozygous KO E18.5 B6;129P-*Cyp11a1*$^{tm1(GFP/cre)Pzg}$/J mice. Coronal brain sections taken from E18.5 CYP11A1 KO mice were histologically stained for oligodendrocyte markers Olig2 and MBP. Positive staining is indicated in brown. No significant localization or quantitative differences are observed distinguishing WT from Cyp11a1 KO E18.5 CNS tissue by Olig2 (A) or MBP (B) staining.

4.2.6 Discussion

The novel histological analysis of the homozygous B6;129P-*Cyp11a1*$^{tm1(GFP/cre)Pzg}$/J mouse CNS described in detail above holds various implications for the roles of neurosteroid hormones in prenatal brain and spinal cord development. Although the images do not support anatomical, neural, or oligodendroglial phenotypes in the late embryonic Cyp11a1-null CNS, the perinatal lethality of the homozygous mutants indicates endogenous neurosteroid production is in fact requisite for survival. Prenatal exposure to maternal neurosteroids via the placenta must compensate for the inability of the KOs to synthesize their own. As soon as the pups are isolated from that rich source of neurosteroids upon birth, their suddenly steroid-deprived bodies are unable to sustain life. Given the de novo production of neurosteroids in glial cells, the fact that the brain and spinal cord develop normally without the enzymatic activity of p450scc is quite remarkable. Histological analyses on pups obtained in the minutes to hours between birth and death might be enlightening in terms of discerning the timeline of CNS and peripheral changes due to denied access to maternal neurosteroid pools.

The traditional oligodendrocyte markers Olig2 and MBP rely on spatial and temporal patterning to promote distinct waves of OPC induction and eventually support OPC maturation into myelinating cells. Olig2 appears around E9 in mice to initiate the beginning stages of oligodendrocyte specification. By E13, ventral Olig2 expression delineates the origin of OPC generation and subsequent migration[196]. The spinal cord images in Figure 4.10, A reflect diffuse migration of Olig2-positive OPCs throughout the WT and KO explants alike. Early localization of brain Olig 2 to the ventricular zone (VZ) and subventricular zone (SVZ) suggests its involvement in the fate specification of neural progenitor cells into oligodendrocytes as opposed to motor neurons[197].

Shortly before birth around E18.5, the timepoint at which I collected tissue for this work, OPCs populating the spinal cord begin to express MBP. Notably, these oligodendrocytes undergo maturation and ensheath their first axons within the ventral and dorsal funiculi. Further migration out of the funiculi and into surrounding white and gray matter increases postnatally[198,199]. Consistent with this established route of oligodendrocyte genesis and proliferation, both WT and KO spinal cord explants depicted in Figure 4.10, B feature MBP-positive cells lining the ventral rim of the tissue. MBP expression in the brain, however, is typically evident prior to the initiation of spinal cord myelination, as early as E14 for some embryonic-specific MBP isoforms[200].

While the WT versus KO B6;129P-*Cyp11a1*$^{tm1(GFP/cre)Pzg}$/J CNS tissue was not distinguishable by histology, I sought to determine whether or not the same was true of oligodendrocyte functionality. I intended to conduct cerebellar slice experiments mirroring those performed with Nes in WT and PRKO mice to evaluate OPC generation, proliferation, migration, and maturation in steroid-free embryos separated from maternal neurosteroids at E12.5. My hypothesis that the Cyp11a1 KO mice would fail to undergo proper developmental myelination was predicated on the knowledge of ample Preg and P4 synthesis in CNS-resident glial cells, as well as the prominent impacts of Nes described in the previous chapter on both MBP expression and the wrapping capacity of cerebellar oligodendrocytes.

CHAPTER 5: *Ex vivo* effects of Neurosteroid-free Environment on Oligodendrocyte Development in Prenatal Mouse Spinal Cord

5.1 Establishment of experimental paradigm to interrogate oligodendrocyte development in Cyp11a1 KO mouse

5.1.1 Strategies to circumvent perinatal lethality

Theoretically, the cerebellar slice culture system previously implemented to study Nes effects on oligodendroglial developmental would have been an ideal strategy to repeat in a completely steroid-free environment. However, the perinatal lethality of the Cyp11a1 KO mice posed what proved to be an insurmountable obstacle to the cerebellar slice paradigm, which requires brain tissue from P7 pups. According to the Chung lab where this transgenic strain originated, daily administration of a steroid cocktail was sufficient to rescue the pups for approximately one week. This life-saving combination of glucocorticoids and mineralocorticoids consisted of dexamethasone 21-phosphate (glucocorticoid) at 4 μg/mL, prednisone 21-hemisuccinate (glucocorticoid) at 4 μg/mL, and fludrocortisone acetate (glucocorticoid and mineralocorticoid) at 10 μg/mL[179]. In my hands, subcutaneously injecting this solution into the pups was not feasible in sesame oil, the recommended solvent. The fragile pups required the use of a needle with the smallest circumference possible, which did not permit the viscous steroid cocktail solution to flow freely. My attempts to overcome this impediment by relying on oils of varying consistencies including corn oil and olive oil proved futile. Water was the only solvent that I was able to successfully and reliably administer to the newborn pups through a needle of appropriate size. Unfortunately, the logistics of being physically present at the time of birth were too cumbersome, and the majority of the KO pups had already perished by the time I reached the new litter.

As an alternative to injecting the pups, I sought to dissolve the steroid cocktail in the pregnant female's drinking water. This was not an efficient long-term solution, as the steroids eventually come out of solution in water alone. Additionally, I had no way of controlling dosage, a key factor in ensuring the steroids produced only their intended effects. Finally, I resorted to injecting females with the steroid cocktail beginning late in their pregnancies and in the days following birth. My hope was that the steroids would then transfer to the pups via breastmilk. This method would also eliminate the need for me to access the KO pups within the first (and last) few minutes of their lives. Ultimately, none of these approaches achieved the objective of rescuing the Cyp11a1 KO pups to facilitate cerebellar dissections at P7. I therefore turned to a new experimental paradigm focused on prenatal oligodendrocyte development.

5.1.2 Ex vivo *spinal cord explant system*

With the shift to the *ex vivo* spinal cord explant system, I no longer had to take such painstaking efforts to prolong the short lives of the Cyp11a1 KO pups.

Oligodendrocytes within such explants undergo spatial and temporal development under cell culture conditions analogous to that seen in the CNS *in vivo*[149]. This physiological relevance enhanced the validity of the data, thus providing a functional accompaniment to the previously described histological imaging. Briefly, E12.5 embryos were dissected from Cyp11a1 female Hets, spinal cords isolated and cut into approximately 1-mm segments, and explants cultured in hormone-free media until putative E17.5. The culture media composition was adapted from Vartanian et al., 1999, and prepared with no phenol red due to its reported estrogenic activity[149,201]. Extraneous embryonic tissue was used for retrospective genotyping once the explants were all in culture.

Much like the cerebellar slice culture system, this spinal cord explant paradigm allowed for the elimination of maternally derived steroids during a pivotal period of early oligodendrocyte development from the ventral ventricular zone (VVZ). The Het by Het breeding scheme necessitated by the perinatal lethality of the KO animals ensured the ability for each individual litter to contain representatives from all three WT, Het, and KO genotypes. Of course, this wasn't always the case, but comparisons across genotypes from the same litter were made whenever possible. The spinal cord explant protocol also comes with several inevitable disadvantages, namely difficulty in removing the delicate cord completely intact and the need to sever the cords by hand as opposed to in a mechanical tissue chopper such as that used in the cerebellar slice experiments. That being said, the tissue, whether initially intact or not, was subject to blunt cutting with a scalpel, and proved rather resilient in culture after enduring such aggressive manipulation. With respect to maintaining consistent explant length, I learned over time the optimal size to maximize the probability of adherence and survival in culture. Excessively thick explants tended to lift off the plate and die, while the thinnest explants were highly susceptible to breakage and other means of damage throughout the fixation and staining processes. Taking care to generate explants as uniform in size as manageable also reduced the likelihood of ascribing legitimacy to apparent phenotypes directly resulting from variations in tissue thickness.

5.1.3 Optimization of tissue culture protocol

The tissue culture protocol for the spinal cord explants required a fair amount of troubleshooting as well. Traditionally, explants are positioned in plates coated in Matrigel matrix with a high concentration of ECM proteins and various growth factors[202]. However, these matrices also contain indiscriminate amounts of hormones that could presumably negate the intentional deprivation of placental steroid hormones. Numerous trials using coverslips coated in individual as well as different combinations of ECM proteins failed to reach a desirable adherence rate, severely limiting the data accumulated from any given experiment. Embedding the explants in a thicker collagen gel matrix directly in glass-bottom plates compatible with confocal microscopes was not a viable option either. The gel did not always solidify adequately to hold the explants in place, often leading to tissue death. Additionally, fluorescent labeling of any tissue that did survive required unreasonably high concentrations of antibody, and was therefore

not sustainable to accommodate multiple experiments over an extended period of time. Ultimately, implementing the same nylon membranes utilized in the cerebellar slice culture procedure produced the highest proportion of viable tissue sufficiently durable to withstand the fixation, staining, and imaging steps.

5.1.4 Discussion

Applying the spinal cord explant experimental paradigm to the Cyp11a1 mice retained all of the benefits of the cerebellar slice system, particularly interrupting the flow of maternal steroid hormones to the growing embryos, thereby creating a truly neurosteroid-free environment in the KO animals. Upon resolving several logistical obstacles to tissue handling and maintenance, I carefully considered oligodendrocyte-related proteins that might be the most informative during the E12.5 to E17.5 window of development. The oligodendrocyte transcription factor Nkx2.2 and the mature myelin protein MBP qualified as prime candidates. Nkx2.2 is associated with oligodendrocyte differentiation from neural progenitor cells (NPCs). The highly conserved transcription factor is believed to favor differentiation over proliferation by repressing downstream genes in tandem with corepressors and/or epigenetic factors[203]. MBP expression right around E18.5 coincides with oligodendrocyte maturation into myelinating cells. Though the rate of oligodendrocyte maturation certainly increases substantially over the course of the first two to four postnatal weeks, MBP expression is observed prior to birth[198]. I opted to stain the spinal cord explants for these two proteins in part to complement my previous Nes work showing marked differences in MBP expression in developing cerebellar slices from PRKO mice. I also reasoned that the addition of a protein like Nkx2.2 involved in even earlier stages of oligodendrocyte differentiation might provide valuable insight into the developmental timepoint at which steroid hormones like P4, among others, begin to exert their myelin-related effects. These findings would simultaneously help to clarify the role of neurosteroid hormones at large in CNS development, and perhaps indicate molecular mechanisms responsible for myelin repair in disease contexts during which newly generated oligodendrocytes are more amenable to remyelination than existing oligodendrocytes that survive the insult[204].

5.2: Phenotypic analysis of spinal cord oligodendrocyte development in Cyp11a1 KO mouse

5.2.1 Confocal image analysis of spinal cord explants

Confocal microscopy on the spinal cord explant tissue fluorescently labeled with Nkx2.2 and MBP was conducted on a CaliberID ribbon scanning confocal microscope. Both Nkx2.2 and MBP exhibited diffuse expression patterns throughout each individual explant. The Cyp11a1 KO tissue was remarkable in that the MBP staining appeared highly concentrated along the midline of each explant, almost as if a wave of MBP-positive cells was paralyzed and prevented from migrating (Figure 5.1). This robust phenotype was visible in all of the KO (n = 7), and none of the WT (n = 9) spinal cord explants (Figure 5.2).

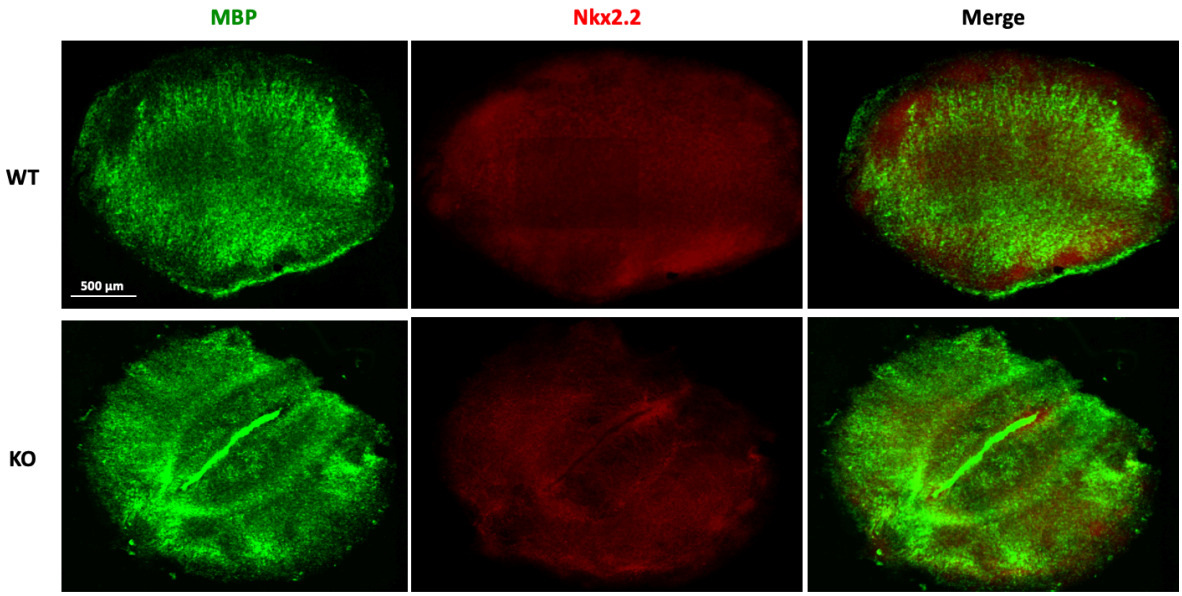

Figure 5.1: Cyp11a1 spinal cord explant confocal imaging. Spinal cord explants slices were dissected from E12.5 Cyp11a1 WT and KO mouse embryos and cultured in the absence of neurosteroid hormones. Spinal cord explants from Het (not shown) all appeared similar to those from WT embryos. Tissue was fixed at hypothetical E17.5 and fluorescently stained for MBP (green) and Nkx2.2 (red). Dense clusters of MBP-positive cells along the midline are visible in the KO explant.

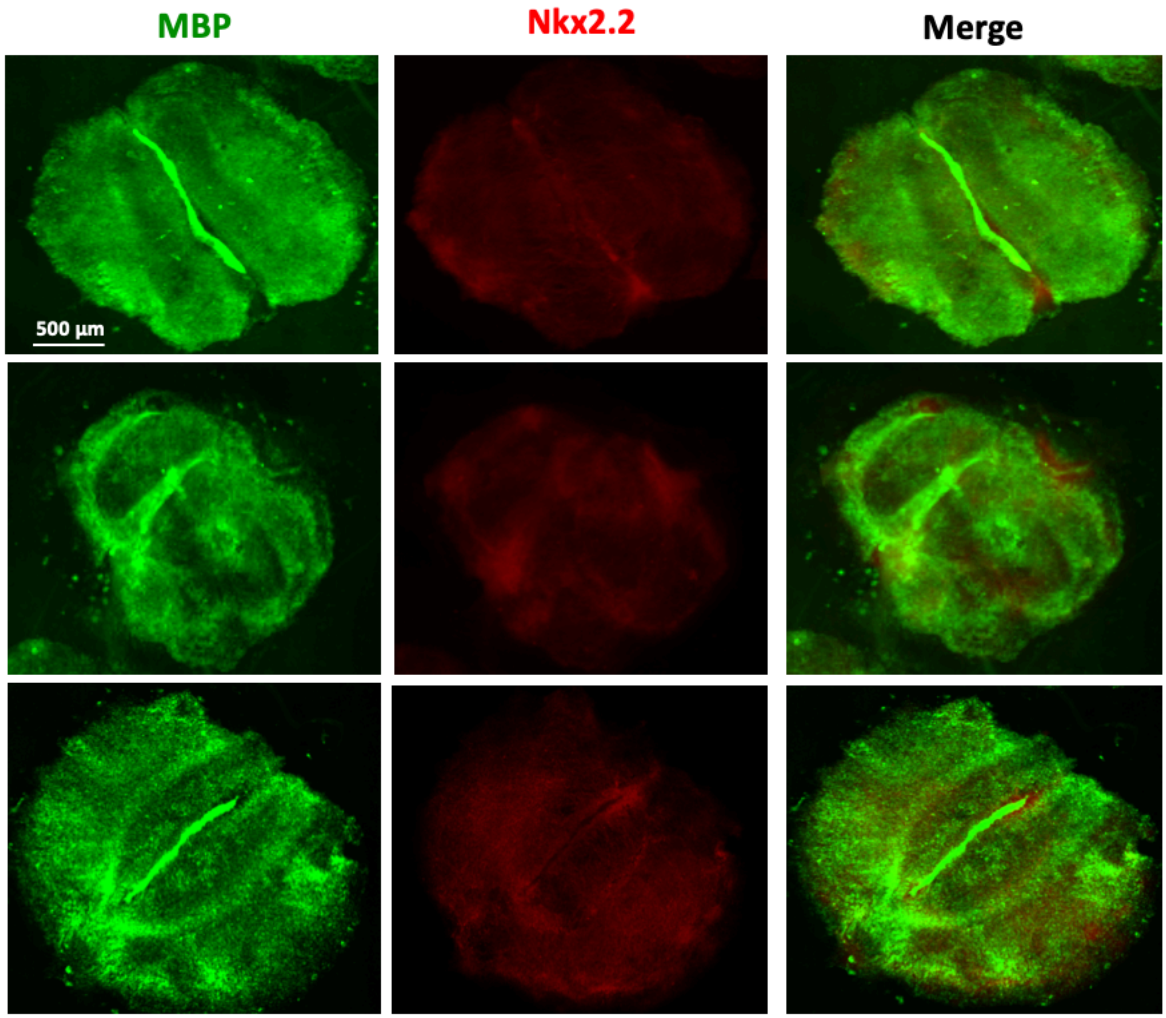

Figure 5.2: Cyp11a1 KO spinal cord explant confocal imaging. Seen here is MBP (green) and Nkx2.2 (red) staining as described in Figure 5.1 for three individual KO explants. The abnormal phenotype featuring densely concentrated MBP-positive cells along the midline is visible in all three explants.

The MBP fluorescence intensity was slightly elevated in the KO tissue as well, implying there was no shortage of OPC production in the absence of neurosteroid hormones. In terms of Nkx2.2, the fluorescence intensity was significantly higher in WT than KO tissue (Figure 5.3), but the striking bundles of immobile cells as seen with the MBP staining were not present.

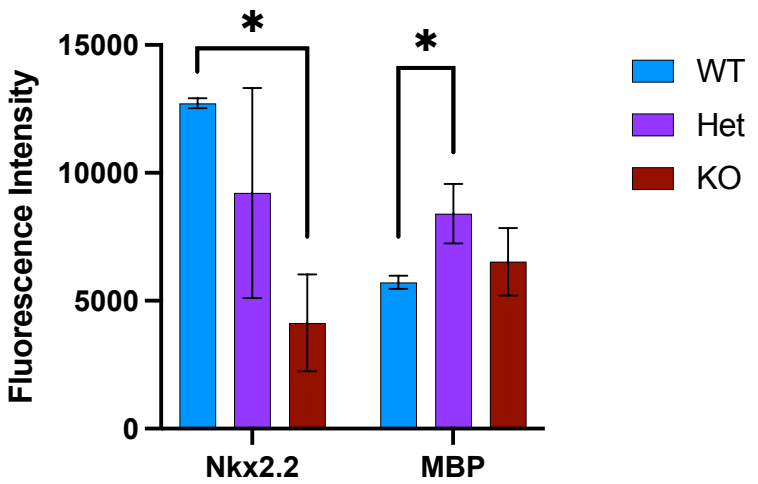

Figure 5.3: Nkx2.2 and MBP fluorescence intensity in Cyp11a1 spinal cord explants. Quantification of mean fluorescence intensity of Nkx2.2 and MBP staining in Cyp11a1 WT, Het, and KO spinal cord explants. Nkx2.2 expression levels were significantly higher in WT versus KO tissue, while MBP expression levels were lowest in WT tissue, significantly higher in Het tissue, and somewhat elevated in KO tissue. Results expressed as Mean ± STDEV, $p < 0.05$ = *, $p < 0.01$ = **, $p < 0.001$ = *** determined by two-way ANOVA with Tukey's honestly significant difference post-hoc testing, n = 4-6 spinal cord explants per condition.

5.2.2 Development of line plot quantitative analysis method

In light of the unique phenotype identified in the Cyp11a1 KO spinal cord tissue, I attempted to quantify the data in a way that would accurately reflect the dense population of MBP-positive cells along the midline of the tissue. Mean fluorescence intensity alone, while informative, fails to capture the striking localization pattern seen here. Aiming to portray the fluorescence intensities at defined intervals across the length of the explant, I collaborated with Ved Sharma of the Rockefeller University Bio-Imaging Resource Center. We were able to conceive of a strategy to plot these discrete fluorescence intensities and depict them in a visually intuitive manner. Briefly, raw confocal images were processed in Imaris software into Z-stack projections, which were opened in Fiji and normalized to account for variations in tissue size. Five lines of equal length were drawn perpendicular to the midline across the length of each explant, and Fiji then generated graphical data points reflecting fluorescence intensities at regular intervals along the five parallel lines. Figure 5.4 illustrates this initial processing of the confocal images.

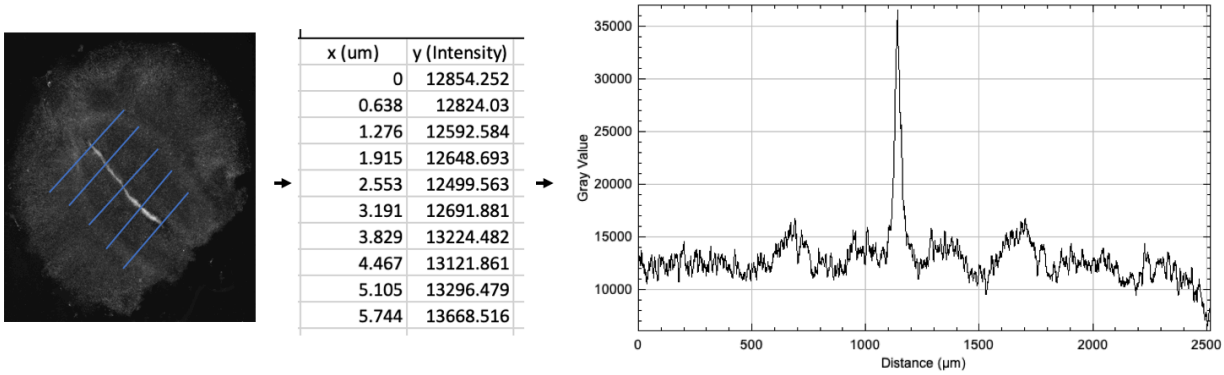

Figure 5.4: Schematic of line plot analysis strategy. Briefly, confocal images of fixed and stained spinal cord explants were converted to Z-stack projections from both green (MBP) and red (Nkx2.2) channels using the Imaris microscopy image analysis software. Line plots were constructed in Fiji based on the normalized Z-stack projections. For quantification of fluorescence intensities at defined points throughout the entire explant, five lines of equal length were drawn perpendicular to the midline across the length of each explant. Fluorescence intensities taken at regular intervals along the five parallel lines were quantified and listed as a set of (x,y) coordinates, with the x coordinate reflecting distance along the line in μm, and the y coordinate reflecting the mean fluorescence intensity at that particular location throughout the depth of the Z-stack.

Ved Sharma composed an algorithm using the RStudio software that automatically read a spreadsheet of all of the data points compiled in Fiji, and generated the elegant line plots displayed in Figure 5.5. The solid lines in these plots convey the mean fluorescence intensities through the Z-stack projection at specific points along the explant, with the surrounding shaded regions representing the standard error of the mean. The distinct peaks in the center of the MBP KO plots (Figure 5.5, B) coincide with the intensely concentrated MBP-positive cells down the midline. A similar yet much subtler trend is seen in the Nkx2.2 KO explants (Figure 5.5, A). The bar graph in Figure 5.6 quantifies the fold change in peak fluorescence intensity over basal fluorescence intensity values for each line plot shown in Figure 5.5. For the KO explants, this maximum value corresponds to the area of the most densely concentrated population of MBP-positive cells at the midline. Again, modest deviations from the basal fluorescence intensity are associated with Nkx2.2 in all genotypes, while those deviations are much more pronounced for the KO MBP tissue.

A.

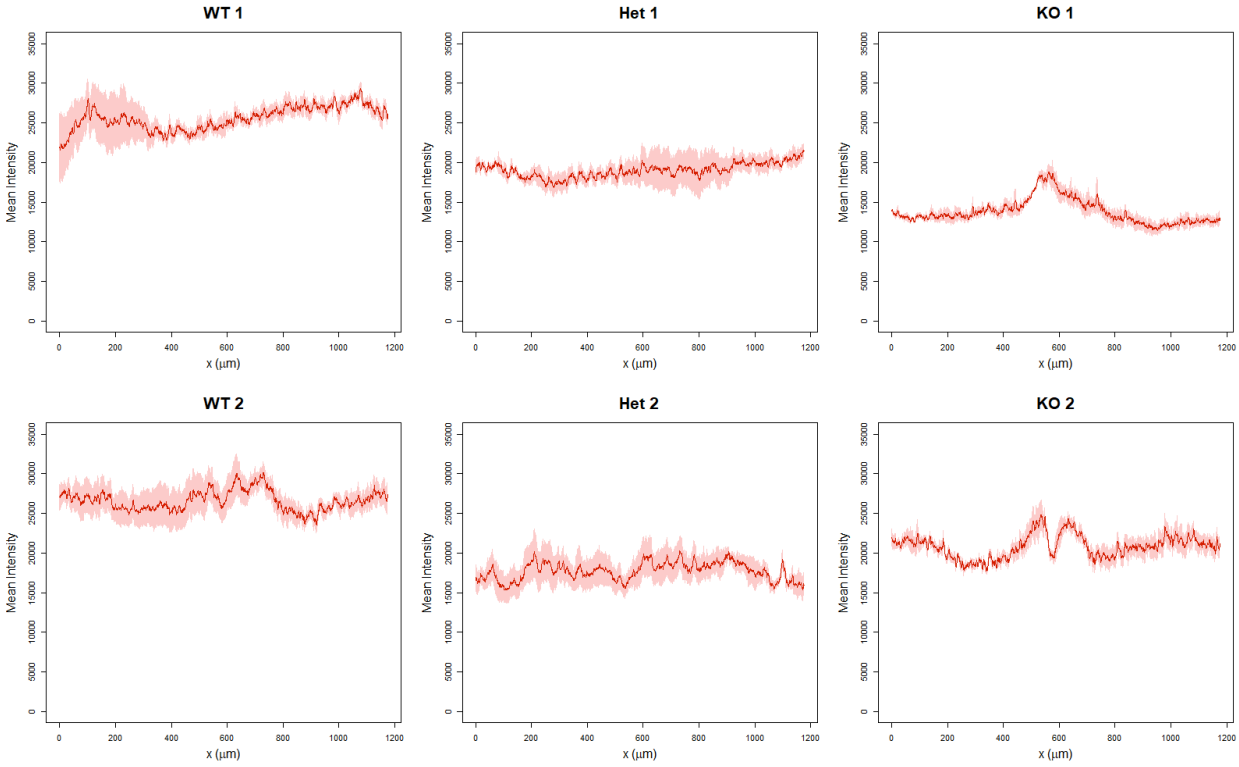
WT 1
Het 1
KO 1
WT 2
Het 2
KO 2
Mean Intensity
x (µm)

B.

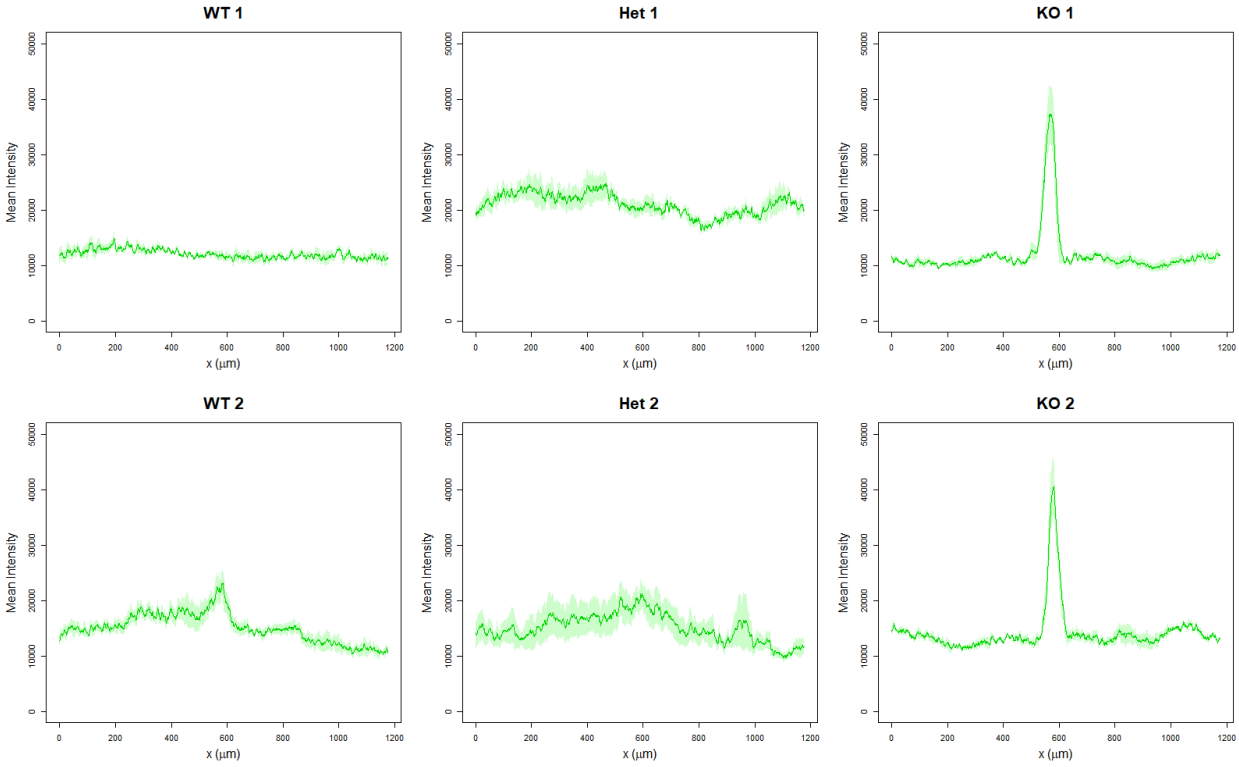
WT 1
Het 1
KO 1
WT 2
Het 2
KO 2
Mean Intensity
x (µm)

Figure 5.5: Line plot analyses of Nkx2.2 and MBP fluorescence intensity in Cyp11a1 spinal cord explants. Line plot summaries corresponding to each individual explant were produced by an algorithm created in RStudio by Ved Sharma of the Bio-Imaging Resource Center. The algorithm was programmed to read the (x,y) coordinates generated through the Fiji analysis described in Figure 5.4 from an Excel file, and convert them into the final line plots shown here for Nkx2.2 (A) and MBP (B) staining. The final line plots depict the fluorescence intensity profiles across the length of the explant, with the solid line representing the mean intensity through the entire Z-stack, and the shaded regions representing the standard error of the mean.

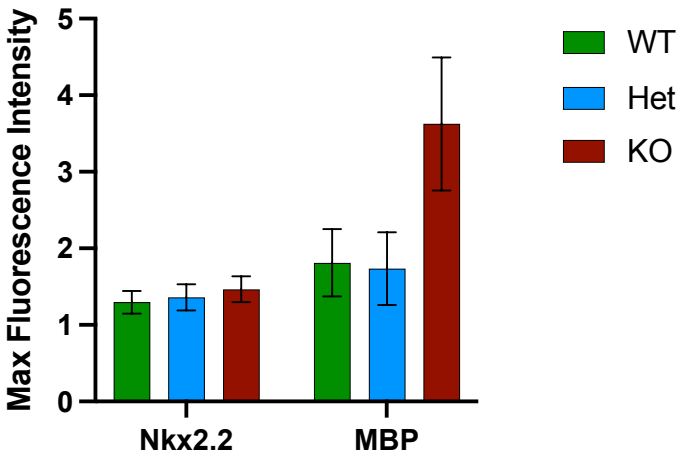

Figure 5.6: Nkx2.2 and MBP spinal cord explant maximum fluorescence intensity comparisons across Cyp11a1 genotypes. Plotted in this bar graph are the ratios of the fluorescence intensity peaks to the basal fluorescence intensity corresponding to each explant from Figure 5.5. Basal fluorescence intensity values were approximated based on a line of best fit spanning the range of fluorescence intensities in the entire line plot, excluding the maximum peak. The normalized max fluorescence intensity values shown here thus account for variations in basal fluorescence intensities among the individual tissues. Results are expressed as the mean max fluorescence intensity values with SD for the two spinal cord explants shown in Figure 5.5 where n = 2 mice per genotype.

5.2.3 Discussion

Myelin development in the spinal cord is classified by two distinct waves of oligodendrocyte production. The ventral wave begins around E12.5 in mice, leaving highly proliferative OPCs scattered throughout the spinal cord in both gray and white matter by E15 prior to expressing MBP shortly before birth[198]. This coincides chronologically with the even distribution of MBP-positive cells in the WT spinal cord explants, in which these ventrally-derived OPCs migrated normally in culture over the course of five days (Figure 5.1). The second wave of dorsal oligodendrocyte production accounts for just 20% of spinal cord OPCs, which lack the migratory and proliferative capacity of OPCs associated with the ventral wave[199]. Differentiation into oligodendrocytes expressing mature myelin proteins including MBP occurs in the ventral and dorsal funiculi, marking the onset of active axon ensheathment. The rate of differentiation and ensuing myelination increases postnatally for up to eight months, peaking around one month[205].

With respect to this physiological timeline of typical myelin development, the Cyp11a1 KO explants do not appear to numerically hinder oligodendrocyte generation by the E17.5 fixation point, as evidenced by the broadly distributed MBP-positive cells characterizing both the WT and KO tissue (Figure 5.1). If anything, the MBP mean fluorescence intensity quantification (Figure 5.3) suggests that the absence of neurosteroid hormones in the KO explants leads to an overproduction of oligodendrocytes. If this is in fact the case, excess oligodendrocytes might then fail to

migrate radially from the ventral and dorsal funiculi, instead accumulating along the midline of the spinal cord along the rostral/caudal axis.

The underlying reasons for this potential overproduction defect, not to mention its functional consequences, are not clear from these experiments alone. Multiple factors in isolation or in parallel could contribute to this unique phenotype, including, but not limited to, insufficient space to accommodate all of the oligodendrocytes, diminished migratory and/or proliferative cues, and indirect effects on overall spinal cord anatomy that interfere with migration and/or proliferation. The notoriously high energetic demand of oligodendrocytes and the myelin sheaths they form is yet another factor that would almost certainly induce further perinatal cellular stress[192]. It is even conceivable that reactive oxygen species and other toxic byproducts of the biological stress response might play a role, along with the adrenal, hepatic, and pulmonary abnormalities previously characterized, in the postnatal lethality of Cyp11a1 KO pups.

CHAPTER 6: Concluding Remarks

6.1 Summary of conclusions

With our continually evolving understanding of the molecular mechanisms underpinning demyelinating diseases like MS, increasing evidence for crosstalk between the CNS and the endocrine system cannot be discounted. The highly reproducible impact of neurosteroid hormones including P4 on remyelination begs the question of their role(s) in early myelin development. The work described here provides novel insights into the intricacies of CNS-derived P4 signaling, along with potential kinetic and regulatory functions in sustaining normal oligodendrocyte development in the embryonic spinal cord. An increased emphasis on the influence of neuroendocrine factors on myelin development, maintenance, and regeneration in pathological contexts will undoubtedly hold myriad implications for oligodendroglial biology and improved treatments for demyelinating disorders.

In **Chapter 3**, the cerebellar slice culture system was implemented in P7 WT mice to interrogate the effects of P4 on developmental myelination. In accordance with the current literature concerning neurosteroid-induced remyelination, culturing the cerebellar slices in 20 μM Nes, a synthetic P4 derivative, resulted in a significant increase in expression of the mature myelin protein MBP. However, contrary to what has been published with regards to the molecular mechanisms responsible for P4-driven myelin repair, the elevated MBP expression in the cerebellar slices is not solely attributable to the classical nPR. Repeating the cerebellar slice experiments with Nes treatment in a PRKO mouse strain in which the KO has no functional nPR revealed expedited myelination in the KO animals after one week in culture. This advanced myelin maturation was evidenced by greater quantities of myelinated fibers at the expense of individual oligodendrocytes lacking processes making physical contact with axons. The accelerated myelination effect due to Nes was therefore magnified in the absence of nPR, indicating involvement of other P4 receptor candidates, of which 11 have been identified.

The existence of numerous P4 receptors is the first major caveat I encountered to studying neurosteroid hormones like P4 in isolation. Since all 11 P4 receptors are expressed, albeit at varying levels, in oligodendrocytes in all stages of maturation, I would have needed to probe each individual receptor in order to delineate those participating in developmental myelination. The extremely short half-life of P4 must also be considered, given its propensity to introduce the possibility of confounding P4 activity with that of its metabolites, namely ALLO. Multiple receptors and rapid metabolism, coupled with the fact that CNS-resident cells, primarily astrocytes, serve as endogenous sources of P4, deterred me from pursuing the PRKO mouse model further. Alternatively, I sought to continue studying developmental myelination in a completely steroid-free environment to eliminate the any neurosteroid hormone interference in the data.

In **Chapter 4**, the establishment of a transgenic mouse colony lacking the CYP11A1 gene encoding the p450scc enzyme enabled me to prevent all endogenous

steroid production in the KO genotype. This enzyme is responsible for the initial conversion of cholesterol to Preg, the immediate precursor to P4 and the first step in all neurosteroid hormone synthesis. Notably, the CNS had never been evaluated in the Cyp11a1 KO mouse prior to these studies. To this end, a thorough histological analysis was performed in E18.5 embryos in an effort to characterize all phenotypes associated with steroid hormone deprivation, with a focus on oligodendrocyte development. Although neither embryo nor placenta weight was predictive of genotype, the majority of the KO animals did not have visible optic discs as the WT animals did. H&E chemical staining, on the other hand, not only provided confirmation of the previously described adrenal defects in steroid-deprived tissue, but revealed novel phenotypes in the liver and lung as well. The disorganization and rampant cellular degeneration in the adrenal gland, decreased cellular vacuolation in the liver, and failed bronchial expansion in the lungs all likely ensure the perinatal lethality seen in Cyp11a1 KO mice. These adrenal, hepatic, and pulmonary abnormalities inhibit proper secretion of regulatory hormones, cellular metabolism, and respiration, respectively.

In stark contrast to the glaring peripheral abnormalities, no major differences in CNS anatomy were observed among the WT, Het, and KO genotypes. Paraffin-embedded brain sections were subject to H&E staining for basic structure, cresyl violet and TUJ1 staining for neural anatomy, and cleaved caspase-3 for cell death patterns. Transverse spinal cord sections were also subject to H&E and TUJ1 staining. Perhaps more surprising than the normal CNS anatomy in the Cyp11a1 KO mice was the seemingly normal distribution of oligodendrocytes as assessed by Olig2 and MBP IHC. Despite these unremarkable histological findings, I still suspected the Cyp11a1of KO mice might suffer functional repercussions of steroid hormone-starved oligodendrocytes.

In **Chapter 5**, the cerebellar slice method was replaced with a spinal cord explant procedure due to postnatal lethality in Cyp11a1 KO mice. Spinal cords were dissected from E12.5 embryos, cultured in specially formulated steroid-free media until physiological E17.5, and fixed and fluorescently labeled with antibodies to the oligodendrocyte transcription factor Nkx2.2 and the mature myelin protein MBP. WT, Het, and KO spinal cord tissue featured broadly distributed Nkx2.2- and MBP-positive cells. In addition to this diffuse expression, a brightly labeled bundle of MBP-positive cells ran along the midline of each KO explant. Fluorescence intensity measurements alone did not fully encompass the scope of the phenotype at hand; I therefore collaborated with the Bio-Imaging Resource Center to generate line plots of Nkx2.2 and MBP fluorescence intensities across the length of the explants. The algorithm-based line plot representations convey dramatic peaks of MBP positivity found along the midlines of KO spinal cord tissue. Further experiments are warranted to determine if this robust phenotype is related to oligodendrocyte overproduction and/or migratory or proliferative errors.

6.2 Implications for oligodendroglial development

The complex process of developmental myelination entails constant crosstalk among glial cells and the surrounding extracellular environment. OPCs, by necessity due to their ventricular origin, migrate rapidly and extensively, often through dense tissue, to populate the CNS[206]. Successful myelination requires a carefully orchestrated collaboration of long-range guidance cues, mediators of cellular motility, and factors that inhibit further migration once OPCs reach their final destinations. Semaphorin and netrin proteins are the most thoroughly studied long-range OPC guidance cues that facilitate ventral to dorsal migration. Potent chemorepellents include netrin-1, some semaphorins, Bmp4, Bmp7, Tgfß1, and Reelin, while CNTF in concert with several other semaphorins acts as strong chemoattractants[207]. OPCs are simultaneously under the influence of an array of ECM proteins. Laminin, fibronectin, and vitronectin encourage, whereas collagen prevents, migration, and tenascin-C is thought to regulate migration speed by interfering with OPC motility[208]. Recently conducted live imaging of OPC migration in developing brain slices brings to light the notion that the vasculature serves as a substrate for OPC migration. Expansive interactions between migrating OPCs and blood vessels are observed, with the former moving in crawling and jumping motions along the latter. Wnt-mediated OPC-blood vessel contact in turn stimulates migration at the expense of differentiation[209]. Wnt in parallel with chemokines CXCL1 and CXCL12 enables the cessation of migration to trigger differentiation when appropriate. Byproducts of the cholesterol biosynthetic pathway such as isoprenoids play pivotal roles in this transition phase. The spinal cord MBP phenotype I have identified in mice unable to metabolize cholesterol may therefore result from dysregulated migration cues that leave MBP-positive cells susceptible to premature differentiation prior to the completion of migration. Cholesterol itself, presumably produced in normal quantities in the Cyp11a1 KO mouse, is sufficient to activate myelin gene expression, which would account for the MBP positivity in OPCs with migratory defects[210].

Yet another possible explanation for the seemingly paradoxical phenotype of increased MBP fluorescence intensity in the Cyp11a1 KO spinal cord explants is an overproduction of OPCs. Ventrally- and dorsally-derived OPCs comprise two distinct migratory waves in the spinal cord. Under physiological conditions, these waves generate an excess of OPCs with access to limited survival factors, not to mention space[211]. This tendency towards overproduction is not restricted to the spinal cord. In the developing optic nerve, nearly half of all oligodendrocytes die as a direct result of competition for survival signals such as platelet-derived growth factor (PDGF) and insulin-like growth factor (IGF). Adding PDGF to the developing optic nerve in culture has been shown to drastically decrease OPC and oligodendrocyte death by 90%[212]. Abnormally high PDGF and/or IGF levels in the Cyp11a1 KO spinal cord explants may contribute to the observed MBP phenotype. The optic nerve findings described above indicate that while OPC overproduction is the norm, unanimous OPC survival is not. Performing cleaved-caspase 3 staining on the Cyp11a1 WT and KO spinal cord as was done in the brain could expose any differences in cell death frequency.

In addition to molecular survival factors, OPCs rely heavily on astrocytes and axons for sustenance. Premyelinating oligodendrocytes respond primarily to astrocyte-derived signals until day three post-differentiation, at which point axonal signals are the dominant mediators of oligodendrocyte fate. One such axonal signal, neuregulin (NRG), may be responsible for the coupling of myelinating oligodendrocyte number to total axonal surface area[213]. According to this model, PDGF receptors are immediately eliminated from newly differentiated oligodendrocytes. Without sensitivity to former survival factors like PDGF, the oligodendrocytes must reach an axon in need of myelination within a matter of days to avoid death[214]. A mutually beneficial relationship is born in which bare axons need oligodendrocytes for myelination and the oligodendrocytes depend on axonal cues for survival. This elegant example of biological synergy ensures neuronal and oligodendroglial preservation without imposing superfluous energy demands due to a chronic overabundance of OPCs. Maintaining the Cyp11a1 spinal cords a few days longer in culture could prove very informative in terms of neurosteroid effects on axon-glia communication. The endurance of the MBP phenotype over time might imply an important role for neurosteroids in matching oligodendrocyte quantity to axonal need.

6.3 Implications for demyelinating diseases

As the primary lipid component of myelin, cholesterol is a critical component in both developmental and pathological contexts. The spinal cord explant experiments provide confirmation that the mere presence of cholesterol is not sufficient for proper myelination. On a similar note, abnormal cholesterol synthesis and recycling have been repeatedly observed in the MS CNS[215]. Demyelination essentially leads to an accumulation of myelin debris, largely comprised of cholesterol, in the brain and spinal cord. Neurodegenerative diseases often compromise the BBB, allowing this cholesterol debris from damaged myelin to cross into the periphery. Ensuing low cholesterol levels in the CNS present further obstacles to remyelination, especially on oligodendrocytes to maximize Preg and P4 production, respectively. The extracellular environment of acute lesions is much more amenable to cholesterol metabolism than that of chronic lesions, the latter of which teem with foamy phagocytes that have lost their lipid recycling capabilities[216]. Significant cholesterol and subsequent neurosteroid loss from the CNS therefore partially account for the steady decrease in spontaneous remyelination seen as MS progresses and cholesterol synthesis becomes more and more restricted. This notion is supported by the finding that dietary supplementation of cholesterol to chronically ill MS patients stimulates the production of growth factors linked to oligodendrocyte proliferation and differentiation requisite to remyelination[217]. On the contrary, inhibiting cholesterol synthesis either pharmacologically or genetically as in the Cyp11a1 mouse, undermines myelin repair in animal models of cuprizone-induced demyelination[218].

Despite the clear need for continuous cholesterol processing in remyelination, several compounds that directly inhibit enzymes relevant to the cholesterol synthesis pathway actually promote OPC differentiation. The widely agreed upon assumption is

that steroid precursors known as sterols are responsible for this perplexing effect, mirroring the apparent neuroprotective capacity of P4 intermediates like ALLO. Multiple pro-myelinating small molecules identified in high throughput chemical screens mediate myelin formation by inhibition of enzymes within the cholesterol biosynthesis pathway, as opposed to signaling through their canonical receptors. The subsequent aggregation of 8,9-unsaturated sterols has been shown to promote OPC differentiation into mature oligodendrocytes[219]. The presence of these sterols, if sufficient to induce OPC differentiation, might partially account for the increased MBP expression in the PRKO cerebellar slices and/or the spinal cord MBP phenotype in which placental neurosteroids were no longer available. The ability to stimulate OPC differentiation into myelinating oligodendrocytes through pharmacological modulation of CNS cholesterol synthesis could introduce a new class of therapeutic targets for demyelinating diseases like MS. The importance of generating new oligodendrocytes from pre-existing OPC stem cell populations cannot be overstated. Studies in zebrafish suggest that oligodendrocytes that survive demyelinating insults often direct new myelin formation to neuronal cell bodies rather than axons, recapitulating a common pathological feature of MS. On the contrary, oligodendrocytes generated from OPCs following demyelination produce greater quantities of myelin properly targeted to damaged myelin sheaths[204]. Based on this data, prompt and complete clearance of myelin debris along with expedited production of new oligodendrocytes, perhaps via regulation of cholesterol synthesis, should be prioritized in MS drug development efforts.

6.4 Future directions

The novel findings addressed here regarding the relevance of neurosteroid synthesis to myelinogenesis lend themselves to ample future research opportunities. The observation that P4 stimulates MBP expression in developing cerebellar slices independently of nPR leaves the question of the molecular mechanism underpinning this phenomenon unanswered. Ongoing efforts to characterize this mechanism might hone in on each of the 11 P4 receptors using genetic and experimental techniques. Ideally, a KO strain corresponding to each receptor would be generated, and cerebellar slices from these strains evaluated for MBP expression. Subsequent RNA-Seq experiments might shed light on the signaling pathways activated, either directly or indirectly, by different P4 receptors. One possible rationale for the diminished myelination seen in the PRKO Het as compared to the KO cerebellar slices is inhibition of differentiation due to premature vascular detachment of OPCs. Abnormal Wnt signaling, for example, can exert this effect, leading to clusters of OPCs adjacent to blood vessels. Further exploration of the relationship of the OPC clusters to the surrounding vasculature could help determine whether or not this is the case in the Nes-treated Het PRKO cerebellar slices. Perhaps Nes signaling through an alternative P4 receptor in the absence of nPR modulates Wnt signaling in a manner that actually enhances OPC differentiation. The complex interactions between P4, nascent OPCs, and the vasculature is worthy of additional research, as MS lesions often feature OPCs clustered around a central vein[209]. The quiescent OPCs then block additional OPC

migration to the demyelinated portion of the axon while simultaneously compromising the associated vessels[220].

The surprising results of the PRKO experiments conducted here may initially appear to contradict claims in the literature that P4 promotes remyelination through nPR. However, it is my belief that the increased MBP expression and enhanced myelination in the KO compared to the Het cerebellar slices simply emphasizes the acute need to distinguish between myelinogenesis and remyelination. Investigations into potential MS therapeutics have been largely predicated on the idea that remyelination recapitulates developmental myelination despite growing evidence to the contrary. Multiple factors including glial scarring, buildup of myelin and other cellular debris, and chronic inflammation in cases of progressive MS likely serve as blockades to the processes underlying myelinogenesis under physiological conditions early in life. Parsing out the molecular differences in oligodendrocyte development versus remyelination necessitated by injury or disease will prove critical to improving current treatment modalities for MS and other related disorders. Defining the role(s) of neurosteroid hormones, from synthesis to signaling, in myelin development versus myelin regeneration is a pivotal component of this urgent endeavor.

The P4-specific impact on oligodendrocytes in development and disease is merely one example of the broader neuroendocrine scope of myelin formation and regeneration. The spinal cord explant MBP midline phenotype in Cyp11a1 KO mice typifies the pertinence of cholesterol biosynthesis and metabolism within the CNS. One time- and labor-intensive yet equally informative experiment would involve reintroducing single neurosteroids one by one to the cultured explants to establish which hormones are responsible for particular aspects of oligodendrocyte development during early myelination. My prediction is one neurosteroid hormone in isolation would be inadequate to entirely rescue the midline phenotype, simply given the wide-ranging intricacies of the neurosteroid synthesis pathway from cholesterol.

Regardless of the hormones needed to reverse the spinal cord phenotype, determining the source of the elevated oligodendroglial density along the midline of explants devoid of neurosteroids remains a critical task. Future experiments discriminating between proliferation, migration, and overproduction defects are needed to advance the field's limited understanding of oligodendrocyte maturation from NPCs. One such experiment to assess the involvement of cell proliferation in the spinal cord explant phenotype is to include staining with a marker such as BrdU or Ki67. Since these stains are best suited for cell suspensions or monolayers, they might not fully penetrate the thick spinal cord explants. Applying these stains to dissociated oligodendrocyte cultures, though less physiologically relevant than intact spinal cord tissue, could serve as a starting point. Even the dissociated cultures have their drawbacks, namely the rapid loss of OPC-specific markers from differentiated oligodendrocytes. Whereas BrdU incorporation among OPCs is therefore not representative of their proliferation rate, the relative quantities of OPCs versus oligodendrocytes are much more accurate proliferative indicators[213]. Simply staining for Olig2 along with MBP to determine the absolute numbers of OPCs and oligodendrocytes in the explants is therefore superior to BrdU or Ki67 markers as a

method to establish a proliferation defect underlying the spinal cord phenotype. Follow-up experiments would ideally address the postnatal consequences of excessive oligodendrocyte production. Presumably, the oligodendrocytes that seem to be stuck in the midline of the spinal cord explants will fail to contact a bare axon and die within a matter of days. Depending on how efficiently astrocytes and microglia can clear the debris, the midline phenotype might in fact disappear by the time of birth. These temporal aspects of oligodendrocyte development also raise the question of a similar phenotype in the embryonic and/or early postnatal brain lacking neurosteroid hormones.

Abundantly clear endocrine involvement in neurodegenerative disease reiterates the as of yet enigmatic sexual dimorphism corresponding with MS diagnosis and severity. Differential hormone production accompanied by distinct molecular and cellular responses to those hormones in males and females demands further investigation, especially in women who have been historically underrepresented in biomedical research. Clarifying the gender-specific roles of individual neurosteroid hormones in
oligodendrocyte maturation during physiological and pathological conditions will impel the field in the direction of personalized medicine. At the very minimum, the general understanding of oligodendrocyte development and remyelination as uniform processes is a vastly oversimplified one. The concept of sexual dimorphism as it pertains to both basic and translational neurobiology must guide future efforts to pharmacologically disrupt, and optimally prevent, MS progression in all of those afflicted.

REFERENCES

1 Corpéchot, C., Robel, P., Axelson, M., Sjövall, J. & Baulieu, E. E. Characterization and measurement of dehydroepiandrosterone sulfate in rat brain. *Proc Natl Acad Sci U S A* **78**, 4704-4707, doi:10.1073/pnas.78.8.4704 (1981).

2 Baulieu, E. E. Neurosteroids: a novel function of the brain. *Psychoneuroendocrinology* **23**, 963-987, doi:10.1016/s0306-4530(98)00071-7 (1998).

3 Corpéchot, C. *et al.* Pregnenolone and its sulfate ester in the rat brain. *Brain Res* **270**, 119-125, doi:10.1016/0006-8993(83)90797-7 (1983).

4 Lacroix, C. *et al.* Simultaneous radioimmunoassay of progesterone, androst-4-enedione, pregnenolone, dehydroepiandrosterone and 17-hydroxyprogesterone in specific regions of human brain. *J Steroid Biochem* **28**, 317-325, doi:10.1016/0022-4731(87)91025-9 (1987).

5 Robel, P. & Baulieu, E. E. Neuro-steroids: 3?-hydroxy-?(5)-derivatives in the rodent brain. *Neurochem Int* **7**, 953-958, doi:10.1016/0197-0186(85)90143-3 (1985).

6 Lloyd-Evans, E. & Waller-Evans, H. Biosynthesis and signalling functions of central and peripheral nervous system neurosteroids in health and disease. *Essays Biochem* **64**, 591-606, doi:10.1042/EBC20200043 (2020).

7 Thomas, P. & Pang, Y. Membrane progesterone receptors: evidence for neuroprotective, neurosteroid signaling and neuroendocrine functions in neuronal cells. *Neuroendocrinology* **96**, 162-171, doi:10.1159/000339822 (2012).

8 Leicaj, M. L. *et al.* Changes in neurosteroidogenesis during demyelination and remyelination in cuprizone-treated mice. *J Neuroendocrinol* **30**, e12649, doi:10.1111/jne.12649 (2018).

9 Usui, M., Yamazaki, T., Kominami, S. & Tsutsui, K. Avian neurosteroids. II. Localization of a cytochrome P450scc-like substance in the quail brain. *Brain Res* **678**, 10-20, doi:10.1016/0006-8993(95)00117-9 (1995).

10 Guennoun, R., Fiddes, R. J., Gouézou, M., Lombès, M. & Baulieu, E. E. A key enzyme in the biosynthesis of neurosteroids, 3 beta-hydroxysteroid dehydrogenase/delta 5-delta 4-isomerase (3 beta-HSD), is expressed in rat brain. *Brain Res Mol Brain Res* **30**, 287-300, doi:10.1016/0169-328x(95)00016-l (1995).

11 Diotel, N. *et al.* Steroid Transport, Local Synthesis, and Signaling within the Brain: Roles in Neurogenesis, Neuroprotection, and Sexual Behaviors. *Front Neurosci* **12**, 84, doi:10.3389/fnins.2018.00084 (2018).

12 Tsutsui, K. & Yamazaki, T. Avian neurosteroids. I. Pregnenolone biosynthesis in the quail brain. *Brain Res* **678**, 1-9, doi:10.1016/0006-8993(95)00116-8 (1995).

13 Mensah-Nyagan, A. G. *et al.* Immunocytochemical localization and biological activity of 3 beta-hydroxysteroid dehydrogenase in the central nervous system of the frog. *J Neurosci* **14**, 7306-7318 (1994).

14 Sakamoto, H., Ukena, K. & Tsutsui, K. Activity and localization of 3beta-hydroxysteroid dehydrogenase/ Delta5-Delta4-isomerase in the zebrafish central nervous system. *J Comp Neurol* **439**, 291-305, doi:10.1002/cne.1351 (2001).

15 Baulieu, E. & Schumacher, M. Progesterone as a neuroactive neurosteroid, with special reference to the effect of progesterone on myelination. *Steroids* **65**, 605-612, doi:10.1016/s0039-128x(00)00173-2 (2000).

16 Grube, M., Hagen, P. & Jedlitschky, G. Neurosteroid Transport in the Brain: Role of ABC and SLC Transporters. *Front Pharmacol* **9**, 354, doi:10.3389/fphar.2018.00354 (2018).

17 Platt, F. M. *et al.* Disorders of cholesterol metabolism and their unanticipated convergent mechanisms of disease. *Annu Rev Genomics Hum Genet* **15**, 173-194, doi:10.1146/annurev-genom-091212-153412 (2014).

18 Miller, W. L. & Bose, H. S. Early steps in steroidogenesis: intracellular cholesterol trafficking. *J Lipid Res* **52**, 2111-2135, doi:10.1194/jlr.R016675 (2011).

19 Omura, T. Mitochondrial P450s. *Chem Biol Interact* **163**, 86-93, doi:10.1016/j.cbi.2006.06.008 (2006).

20 Thomas, J. L., Frieden, C., Nash, W. E. & Strickler, R. C. An NADH-induced conformational change that mediates the sequential 3 beta-hydroxysteroid dehydrogenase/isomerase activities is supported by affinity labeling and the time-dependent activation of isomerase. *J Biol Chem* **270**, 21003-21008, doi:10.1074/jbc.270.36.21003 (1995).

21 Banati, R. B. *et al.* Positron emission tomography and functional characterization of a complete PBR/TSPO knockout. *Nat Commun* **5**, 5452, doi:10.1038/ncomms6452 (2014).

22 Simard, J. *et al.* Molecular biology of the 3beta-hydroxysteroid dehydrogenase/delta5-delta4 isomerase gene family. *Endocr Rev* **26**, 525-582, doi:10.1210/er.2002-0050 (2005).

23 Penning, T. M., Jin, Y., Steckelbroeck, S., Lanisnik Rizner, T. & Lewis, M. Structure-function of human 3 alpha-hydroxysteroid dehydrogenases: genes and proteins. *Mol Cell Endocrinol* **215**, 63-72, doi:10.1016/j.mce.2003.11.006 (2004).

24 Haggstrom, M. & Richfield, D. (WikiJournal of Medicine, 2014).

25 Melcangi, R. C., Celotti, F., Castano, P. & Martini, L. Intracellular signalling systems controlling the 5 alpha-reductase in glial cell cultures. *Brain Res* **585**, 411-415, doi:10.1016/0006-8993(92)91247-c (1992).

26 Morita, K., Arimochi, H. & Tsuruo, Y. Adrenergic activation of steroid 5alpha-reductase gene expression in rat C6 glioma cells: involvement of cyclic amp/protein kinase A-mediated signaling pathway. *J Mol Neurosci* **22**, 205-212, doi:10.1385/JMN:22:3:205 (2004).

27 Dhandapani, K. M., Mahesh, V. B. & Brann, D. W. Astrocytes and brain function: implications for reproduction. *Exp Biol Med (Maywood)* **228**, 253-260, doi:10.1177/153537020322800303 (2003).

28 Brinton, R. D. *et al.* Progesterone receptors: form and function in brain. *Front Neuroendocrinol* **29**, 313-339, doi:10.1016/j.yfrne.2008.02.001 (2008).

29 Auger, C. J. & De Vries, G. J. Progestin receptor immunoreactivity within steroid-responsive vasopressin-immunoreactive cells in the male and female rat brain. *J Neuroendocrinol* **14**, 561-567, doi:10.1046/j.1365-2826.2002.00809.x (2002).

30 Singh, M. Ovarian hormones elicit phosphorylation of Akt and extracellular-signal regulated kinase in explants of the cerebral cortex. *Endocrine* **14**, 407-415, doi:10.1385/ENDO:14:3:407 (2001).

31 Singer, C. A., Figueroa-Masot, X. A., Batchelor, R. H. & Dorsa, D. M. The mitogen-activated protein kinase pathway mediates estrogen neuroprotection after glutamate toxicity in primary cortical neurons. *J Neurosci* **19**, 2455-2463 (1999).

32 Edwards, H. E., Epps, T., Carlen, P. L. & J MacLusky, N. Progestin receptors mediate progesterone suppression of epileptiform activity in tetanized hippocampal slices in vitro. *Neuroscience* **101**, 895-906, doi:10.1016/s0306-4522(00)00439-5 (2000).

33 Nilsen, J. & Brinton, R. D. Impact of progestins on estrogen-induced neuroprotection: synergy by progesterone and 19-norprogesterone and antagonism by medroxyprogesterone acetate. *Endocrinology* **143**, 205-212, doi:10.1210/endo.143.1.8582 (2002).

34 N-Wihlbäck, A. C., Sundström-Poromaa, I. & Bäckström, T. Action by and sensitivity to neuroactive steroids in menstrual cycle related CNS disorders. *Psychopharmacology (Berl)* **186**, 388-401, doi:10.1007/s00213-005-0185-2 (2006).

35 Bäckström, T. *et al.* Mood, sexuality, hormones, and the menstrual cycle. II. Hormone levels and their relationship to the premenstrual syndrome. *Psychosom Med* **45**, 503-507, doi:10.1097/00006842-198312000-00004 (1983).

36 Sundström, I. *et al.* Patients with premenstrual syndrome have a different sensitivity to a neuroactive steroid during the menstrual cycle compared to control subjects. *Neuroendocrinology* **67**, 126-138, doi:10.1159/000054307 (1998).

37 Mitchell, E. A., Herd, M. B., Gunn, B. G., Lambert, J. J. & Belelli, D. Neurosteroid modulation of GABAA receptors: molecular determinants and significance in health and disease. *Neurochem Int* **52**, 588-595, doi:10.1016/j.neuint.2007.10.007 (2008).

38 Johansson, I. M., Birzniece, V., Lindblad, C., Olsson, T. & Bäckström, T. Allopregnanolone inhibits learning in the Morris water maze. *Brain Res* **934**, 125-131, doi:10.1016/s0006-8993(02)02414-9 (2002).

39 van Wingen, G. *et al.* How progesterone impairs memory for biologically salient stimuli in healthy young women. *J Neurosci* **27**, 11416-11423, doi:10.1523/JNEUROSCI.1715-07.2007 (2007).

40 Silvers, J. M., Tokunaga, S., Berry, R. B., White, A. M. & Matthews, D. B. Impairments in spatial learning and memory: ethanol, allopregnanolone, and the hippocampus. *Brain Res Brain Res Rev* **43**, 275-284, doi:10.1016/j.brainresrev.2003.09.002 (2003).

41 Gould, E., Woolley, C. S., Frankfurt, M. & McEwen, B. S. Gonadal steroids regulate dendritic spine density in hippocampal pyramidal cells in adulthood. *J Neurosci* **10**, 1286-1291 (1990).

42 Wilson, M. A. GABA physiology: modulation by benzodiazepines and hormones. *Crit Rev Neurobiol* **10**, 1-37, doi:10.1615/critrevneurobiol.v10.i1.10 (1996).

43 Mahley, R. W. & Rall, S. C. Apolipoprotein E: far more than a lipid transport protein. *Annu Rev Genomics Hum Genet* **1**, 507-537, doi:10.1146/annurev.genom.1.1.507 (2000).

44 Duan, H., Gu, D. & Mazzone, T. Sterols and inhibitors of sterol transport modulate the degradation and secretion of macrophage ApoE: requirement for

the C-terminal domain. *Biochim Biophys Acta* **1484**, 142-150, doi:10.1016/s1388-1981(00)00005-6 (2000).

45 Martini, L., Magnaghi, V. & Melcangi, R. C. Actions of progesterone and its 5alpha-reduced metabolites on the major proteins of the myelin of the peripheral nervous system. *Steroids* **68**, 825-829, doi:10.1016/s0039-128x(03)00134-x (2003).

46 Magnaghi, V. *et al.* Sex-dimorphic effects of progesterone and its reduced metabolites on gene expression of myelin proteins by rat Schwann cells. *J Peripher Nerv Syst* **11**, 111-118, doi:10.1111/j.1085-9489.2006.00075.x (2006).

47 Stewart, F. *et al.* Identification of the horse epidermal growth factor (EGF) coding sequence and its use in monitoring EGF gene expression in the endometrium of the pregnant mare. *J Mol Endocrinol* **12**, 341-350, doi:10.1677/jme.0.0120341 (1994).

48 Begliuomini, S. *et al.* Influence of endogenous and exogenous sex hormones on plasma brain-derived neurotrophic factor. *Hum Reprod* **22**, 995-1002, doi:10.1093/humrep/del479 (2007).

49 Guennoun, R. *et al.* Progesterone and allopregnanolone in the central nervous system: response to injury and implication for neuroprotection. *J Steroid Biochem Mol Biol* **146**, 48-61, doi:10.1016/j.jsbmb.2014.09.001 (2015).

50 Wang, J. M., Liu, L., Irwin, R. W., Chen, S. & Brinton, R. D. Regenerative potential of allopregnanolone. *Brain Res Rev* **57**, 398-409, doi:10.1016/j.brainresrev.2007.08.010 (2008).

51 González-Orozco, J. C. & Camacho-Arroyo, I. Progesterone Actions During Central Nervous System Development. *Front Neurosci* **13**, 503, doi:10.3389/fnins.2019.00503 (2019).

52 De Nicola, A. F. *et al.* Progesterone neuroprotection in traumatic CNS injury and motoneuron degeneration. *Front Neuroendocrinol* **30**, 173-187, doi:10.1016/j.yfrne.2009.03.001 (2009).

53 Labombarda, F. *et al.* Progesterone attenuates astro- and microgliosis and enhances oligodendrocyte differentiation following spinal cord injury. *Exp Neurol* **231**, 135-146, doi:10.1016/j.expneurol.2011.06.001 (2011).

54 Hussain, R. *et al.* Progesterone and Nestorone facilitate axon remyelination: a role for progesterone receptors. *Endocrinology* **152**, 3820-3831, doi:10.1210/en.2011-1219 (2011).

55 Cabeza, M., Heuze, Y., Sánchez, A., Garrido, M. & Bratoeff, E. Recent advances in structure of progestins and their binding to progesterone receptors. *J Enzyme Inhib Med Chem* **30**, 152-159, doi:10.3109/14756366.2014.895719 (2015).

56 Liu, A. *et al.* Progesterone receptors: a key for neuroprotection in experimental stroke. *Endocrinology* **153**, 3747-3757, doi:10.1210/en.2012-1138 (2012).

57 Yu, H. J. *et al.* Progesterone attenuates neurological behavioral deficits of experimental autoimmune encephalomyelitis through remyelination with nucleus-sublocalized Olig1 protein. *Neurosci Lett* **476**, 42-45, doi:10.1016/j.neulet.2010.03.079 (2010).

58 Giatti, S. *et al.* Neuroprotective effects of progesterone in chronic experimental autoimmune encephalomyelitis. *J Neuroendocrinol* **24**, 851-861, doi:10.1111/j.1365-2826.2012.02284.x (2012).

59 Tuem, K. B. & Atey, T. M. Neuroactive Steroids: Receptor Interactions and Responses. *Front Neurol* **8**, 442, doi:10.3389/fneur.2017.00442 (2017).

60 Theis, V. & Theiss, C. Progesterone Effects in the Nervous System. *Anat Rec (Hoboken)* **302**, 1276-1286, doi:10.1002/ar.24121 (2019).

61 Ben-Ari, Y. Limbic seizure and brain damage produced by kainic acid: mechanisms and relevance to human temporal lobe epilepsy. *Neuroscience* **14**, 375-403, doi:10.1016/0306-4522(85)90299-4 (1985).

62 Turski, L., Ikonomidou, C., Turski, W. A., Bortolotto, Z. A. & Cavalheiro, E. A. Review: cholinergic mechanisms and epileptogenesis. The seizures induced by pilocarpine: a novel experimental model of intractable epilepsy. *Synapse* **3**, 154-171, doi:10.1002/syn.890030207 (1989).

63 Jung, M. E., Lal, H. & Gatch, M. B. The discriminative stimulus effects of pentylenetetrazol as a model of anxiety: recent developments. *Neurosci Biobehav Rev* **26**, 429-439, doi:10.1016/s0149-7634(02)00010-6 (2002).

64 Rhodes, M. E. & Frye, C. A. Actions at GABA(A) receptors in the hippocampus may mediate some antiseizure effects of progestins. *Epilepsy Behav* **6**, 320-327, doi:10.1016/j.yebeh.2005.02.006 (2005).

65 Ciriza, I., Azcoitia, I. & Garcia-Segura, L. M. Reduced progesterone metabolites protect rat hippocampal neurones from kainic acid excitotoxicity in vivo. *J Neuroendocrinol* **16**, 58-63, doi:10.1111/j.1365-2826.2004.01121.x (2004).

66 Lephart, E. D. & Husmann, D. A. Altered brain and pituitary androgen metabolism by prenatal, perinatal or pre- and postnatal finasteride, flutamide or

dihydrotestosterone treatment in juvenile male rats. *Prog Neuropsychopharmacol Biol Psychiatry* **17**, 991-1003, doi:10.1016/0278-5846(93)90026-o (1993).

67 Simpkins, J. W. & Dykens, J. A. Mitochondrial mechanisms of estrogen neuroprotection. *Brain Res Rev* **57**, 421-430, doi:10.1016/j.brainresrev.2007.04.007 (2008).

68 Robertson, C. L. *et al.* Physiologic progesterone reduces mitochondrial dysfunction and hippocampal cell loss after traumatic brain injury in female rats. *Exp Neurol* **197**, 235-243, doi:10.1016/j.expneurol.2005.09.014 (2006).

69 Gibson, C. L., Constantin, D., Prior, M. J., Bath, P. M. & Murphy, S. P. Progesterone suppresses the inflammatory response and nitric oxide synthase-2 expression following cerebral ischemia. *Exp Neurol* **193**, 522-530, doi:10.1016/j.expneurol.2005.01.009 (2005).

70 Roof, R. L., Hoffman, S. W. & Stein, D. G. Progesterone protects against lipid peroxidation following traumatic brain injury in rats. *Mol Chem Neuropathol* **31**, 1-11, doi:10.1007/BF02815156 (1997).

71 Grossman, K. J., Goss, C. W. & Stein, D. G. Effects of progesterone on the inflammatory response to brain injury in the rat. *Brain Res* **1008**, 29-39, doi:10.1016/j.brainres.2004.02.022 (2004).

72 Azcoitia, I. *et al.* Progesterone and its derivatives dihydroprogesterone and tetrahydroprogesterone reduce myelin fiber morphological abnormalities and myelin fiber loss in the sciatic nerve of aged rats. *Neurobiol Aging* **24**, 853-860, doi:10.1016/s0197-4580(02)00234-8 (2003).

73 Shear, D. A., Galani, R., Hoffman, S. W. & Stein, D. G. Progesterone protects against necrotic damage and behavioral abnormalities caused by traumatic brain injury. *Exp Neurol* **178**, 59-67, doi:10.1006/exnr.2002.8020 (2002).

74 Pettus, E. H., Wright, D. W., Stein, D. G. & Hoffman, S. W. Progesterone treatment inhibits the inflammatory agents that accompany traumatic brain injury. *Brain Res* **1049**, 112-119, doi:10.1016/j.brainres.2005.05.004 (2005).

75 Roof, R. L., Duvdevani, R. & Stein, D. G. Gender influences outcome of brain injury: progesterone plays a protective role. *Brain Res* **607**, 333-336, doi:10.1016/0006-8993(93)91526-x (1993).

76 Djebaili, M., Guo, Q., Pettus, E. H., Hoffman, S. W. & Stein, D. G. The neurosteroids progesterone and allopregnanolone reduce cell death, gliosis, and functional deficits after traumatic brain injury in rats. *J Neurotrauma* **22**, 106-118, doi:10.1089/neu.2005.22.106 (2005).

77 Djebaili, M., Hoffman, S. W. & Stein, D. G. Allopregnanolone and progesterone decrease cell death and cognitive deficits after a contusion of the rat pre-frontal cortex. *Neuroscience* **123**, 349-359, doi:10.1016/j.neuroscience.2003.09.023 (2004).

78 Wright, D. W. *et al.* ProTECT: a randomized clinical trial of progesterone for acute traumatic brain injury. *Ann Emerg Med* **49**, 391-402, 402.e391-392, doi:10.1016/j.annemergmed.2006.07.932 (2007).

79 Hardy, J., Duff, K., Hardy, K. G., Perez-Tur, J. & Hutton, M. Genetic dissection of Alzheimer's disease and related dementias: amyloid and its relationship to tau. *Nat Neurosci* **1**, 355-358, doi:10.1038/1565 (1998).

80 Cleary, J. P. *et al.* Natural oligomers of the amyloid-beta protein specifically disrupt cognitive function. *Nat Neurosci* **8**, 79-84, doi:10.1038/nn1372 (2005).

81 Pike, C. J., Walencewicz, A. J., Glabe, C. G. & Cotman, C. W. Aggregation-related toxicity of synthetic beta-amyloid protein in hippocampal cultures. *Eur J Pharmacol* **207**, 367-368, doi:10.1016/0922-4106(91)90014-9 (1991).

82 Lorenzo, A. & Yankner, B. A. Beta-amyloid neurotoxicity requires fibril formation and is inhibited by congo red. *Proc Natl Acad Sci U S A* **91**, 12243-12247, doi:10.1073/pnas.91.25.12243 (1994).

83 Simmons, L. K. *et al.* Secondary structure of amyloid beta peptide correlates with neurotoxic activity in vitro. *Mol Pharmacol* **45**, 373-379 (1994).

84 Lambert, M. P. *et al.* Diffusible, nonfibrillar ligands derived from Abeta1-42 are potent central nervous system neurotoxins. *Proc Natl Acad Sci U S A* **95**, 6448-6453, doi:10.1073/pnas.95.11.6448 (1998).

85 Schumacher, M. *et al.* Steroid hormones and neurosteroids in normal and pathological aging of the nervous system. *Prog Neurobiol* **71**, 3-29, doi:10.1016/j.pneurobio.2003.09.004 (2003).

86 Jaffe, A. B., Toran-Allerand, C. D., Greengard, P. & Gandy, S. E. Estrogen regulates metabolism of Alzheimer amyloid beta precursor protein. *J Biol Chem* **269**, 13065-13068 (1994).

87 Xu, H. *et al.* Estrogen reduces neuronal generation of Alzheimer beta-amyloid peptides. *Nat Med* **4**, 447-451, doi:10.1038/nm0498-447 (1998).

88 Yaffe, K., Sawaya, G., Lieberburg, I. & Grady, D. Estrogen therapy in postmenopausal women: effects on cognitive function and dementia. *JAMA* **279**, 688-695, doi:10.1001/jama.279.9.688 (1998).

89 Vincent, B. & Smith, J. D. Effect of estradiol on neuronal Swedish-mutated beta-amyloid precursor protein metabolism: reversal by astrocytic cells. *Biochem Biophys Res Commun* **271**, 82-85, doi:10.1006/bbrc.2000.2581 (2000).

90 Carroll, J. C. *et al.* Progesterone and estrogen regulate Alzheimer-like neuropathology in female 3xTg-AD mice. *J Neurosci* **27**, 13357-13365, doi:10.1523/JNEUROSCI.2718-07.2007 (2007).

91 Kipp, M., Amor, S., Krauth, R. & Beyer, C. Multiple sclerosis: neuroprotective alliance of estrogen-progesterone and gender. *Front Neuroendocrinol* **33**, 1-16, doi:10.1016/j.yfrne.2012.01.001 (2012).

92 Schumacher, M. *et al.* Progesterone synthesis in the nervous system: implications for myelination and myelin repair. *Front Neurosci* **6**, 10, doi:10.3389/fnins.2012.00010 (2012).

93 El-Etr, M. *et al.* Progesterone and nestorone promote myelin regeneration in chronic demyelinating lesions of corpus callosum and cerebral cortex. *Glia* **63**, 104-117, doi:10.1002/glia.22736 (2015).

94 Noorbakhsh, F., Baker, G. B. & Power, C. Allopregnanolone and neuroinflammation: a focus on multiple sclerosis. *Front Cell Neurosci* **8**, 134, doi:10.3389/fncel.2014.00134 (2014).

95 Tennekoon, G. I., Cohen, S. R., Price, D. L. & McKhann, G. M. Myelinogenesis in optic nerve. A morphological, autoradiographic, and biochemical analysis. *J Cell Biol* **72**, 604-616 (1977).

96 Schmitt, S., Castelvetri, L. C. & Simons, M. Metabolism and functions of lipids in myelin. *Biochim Biophys Acta* **1851**, 999-1005, doi:10.1016/j.bbalip.2014.12.016 (2015).

97 Dobson, R. & Giovannoni, G. Multiple sclerosis - a review. *Eur J Neurol* **26**, 27-40, doi:10.1111/ene.13819 (2019).

98 Le Goascogne, C. *et al.* Neurosteroid progesterone is up-regulated in the brain of jimpy and shiverer mice. *Glia* **29**, 14-24 (2000).

99 Orefice, N. *et al.* Assessment of neuroactive steroids in cerebrospinal fluid comparing acute relapse and stable disease in relapsing-remitting multiple sclerosis. *J Steroid Biochem Mol Biol* **159**, 1-7, doi:10.1016/j.jsbmb.2016.02.012 (2016).

100 Schumacher, M. *et al.* Local synthesis and dual actions of progesterone in the nervous system: neuroprotection and myelination. *Growth Horm IGF Res* **14 Suppl A**, S18-33, doi:10.1016/j.ghir.2004.03.007 (2004).

101 El-Etr, M. *et al.* Steroid hormones in multiple sclerosis. *J Neurol Sci* **233**, 49-54, doi:10.1016/j.jns.2005.03.004 (2005).

102 Labombarda, F. *et al.* Effects of progesterone on oligodendrocyte progenitors, oligodendrocyte transcription factors, and myelin proteins following spinal cord injury. *Glia* **57**, 884-897, doi:10.1002/glia.20814 (2009).

103 Garay, L. *et al.* Protective effects of progesterone administration on axonal pathology in mice with experimental autoimmune encephalomyelitis. *Brain Res* **1283**, 177-185, doi:10.1016/j.brainres.2009.04.057 (2009).

104 De Nicola, A. F. *et al.* Progesterone treatment of spinal cord injury: Effects on receptors, neurotrophins, and myelination. *J Mol Neurosci* **28**, 3-15, doi:10.1385/JMN:30:3:341 (2006).

105 Kashani, I. R. *et al.* Progesterone Enhanced Remyelination in the Mouse Corpus Callosum after Cuprizone Induced Demyelination. *Iran J Med Sci* **40**, 507-514 (2015).

106 Ghoumari, A. M. *et al.* Progesterone and its metabolites increase myelin basic protein expression in organotypic slice cultures of rat cerebellum. *J Neurochem* **86**, 848-859 (2003).

107 Salazar, M., Lerma-Ortiz, A., Hooks, G. M., Ashley, A. K. & Ashley, R. L. Progestin-mediated activation of MAPK and AKT in nuclear progesterone receptor negative breast epithelial cells: The role of membrane progesterone receptors. *Gene* **591**, 6-13, doi:10.1016/j.gene.2016.06.044 (2016).

108 Saher, G. *et al.* High cholesterol level is essential for myelin membrane growth. *Nat Neurosci* **8**, 468-475, doi:10.1038/nn1426 (2005).

109 Schumacher, M. *et al.* Novel perspectives for progesterone in hormone replacement therapy, with special reference to the nervous system. *Endocr Rev* **28**, 387-439, doi:10.1210/er.2006-0050 (2007).

110 Petersen, S. L. *et al.* Nonclassical progesterone signalling molecules in the nervous system. *J Neuroendocrinol* **25**, 991-1001, doi:10.1111/jne.12060 (2013).

111 Hartley, M. D., Altowaijri, G. & Bourdette, D. Remyelination and multiple sclerosis: therapeutic approaches and challenges. *Curr Neurol Neurosci Rep* **14**, 485, doi:10.1007/s11910-014-0485-1 (2014).

112 Xiao, L. *et al.* Diosgenin promotes oligodendrocyte progenitor cell differentiation through estrogen receptor-mediated ERK1/2 activation to accelerate remyelination. *Glia* **60**, 1037-1052, doi:10.1002/glia.22333 (2012).

113 Narayanan, S. P., Flores, A. I., Wang, F. & Macklin, W. B. Akt signals through the mammalian target of rapamycin pathway to regulate CNS myelination. *J Neurosci* **29**, 6860-6870, doi:10.1523/JNEUROSCI.0232-09.2009 (2009).

114 Fyffe-Maricich, S. L., Schott, A., Karl, M., Krasno, J. & Miller, R. H. Signaling through ERK1/2 controls myelin thickness during myelin repair in the adult central nervous system. *J Neurosci* **33**, 18402-18408, doi:10.1523/JNEUROSCI.2381-13.2013 (2013).

115 Stanojlović, M. *et al.* Effects of chronic cerebral hypoperfusion and low-dose progesterone treatment on apoptotic processes, expression and subcellular localization of key elements within Akt and Erk signaling pathways in rat hippocampus. *Neuroscience* **311**, 308-321, doi:10.1016/j.neuroscience.2015.10.040 (2015).

116 Sagare-Patil, V., Vernekar, M., Galvankar, M. & Modi, D. Progesterone utilizes the PI3K-AKT pathway in human spermatozoa to regulate motility and hyperactivation but not acrosome reaction. *Mol Cell Endocrinol* **374**, 82-91, doi:10.1016/j.mce.2013.04.005 (2013).

117 Norrmén, C. & Suter, U. Akt/mTOR signalling in myelination. *Biochem Soc Trans* **41**, 944-950, doi:10.1042/BST20130046 (2013).

118 Narayan, N. *et al.* The macrophage marker translocator protein (TSPO) is down-regulated on pro-inflammatory 'M1' human macrophages. *PLoS One* **12**, e0185767, doi:10.1371/journal.pone.0185767 (2017).

119 Vercellino, M. *et al.* Demyelination, inflammation, and neurodegeneration in multiple sclerosis deep gray matter. *J Neuropathol Exp Neurol* **68**, 489-502, doi:10.1097/NEN.0b013e3181a19a5a (2009).

120 Franklin, R. J. Why does remyelination fail in multiple sclerosis? *Nat Rev Neurosci* **3**, 705-714, doi:10.1038/nrn917 (2002).

121 Vavasour, I. M. *et al.* Global loss of myelin water over 5 years in multiple sclerosis normal-appearing white matter. *Mult Scler*, 1352458517723717, doi:10.1177/1352458517723717 (2017).

122 Lassmann, H., Brück, W., Lucchinetti, C. & Rodriguez, M. Remyelination in multiple sclerosis. *Mult Scler* **3**, 133-136, doi:10.1177/135245859700300213 (1997).

123 Scolding, N. *et al.* Oligodendrocyte progenitors are present in the normal adult human CNS and in the lesions of multiple sclerosis. *Brain* **121 (Pt 12)**, 2221-2228 (1998).

124 Lucchinetti, C. *et al.* A quantitative analysis of oligodendrocytes in multiple sclerosis lesions. A study of 113 cases. *Brain* **122 (Pt 12)**, 2279-2295 (1999).

125 Chang, A., Tourtellotte, W. W., Rudick, R. & Trapp, B. D. Premyelinating oligodendrocytes in chronic lesions of multiple sclerosis. *N Engl J Med* **346**, 165-173, doi:10.1056/NEJMoa010994 (2002).

126 Woodruff, R. H., Fruttiger, M., Richardson, W. D. & Franklin, R. J. Platelet-derived growth factor regulates oligodendrocyte progenitor numbers in adult CNS and their response following CNS demyelination. *Mol Cell Neurosci* **25**, 252-262, doi:10.1016/j.mcn.2003.10.014 (2004).

127 Ye, J. N. *et al.* Progesterone alleviates neural behavioral deficits and demyelination with reduced degeneration of oligodendroglial cells in cuprizone-induced mice. *PLoS One* **8**, e54590, doi:10.1371/journal.pone.0054590 (2013).

128 Ibanez, C. *et al.* Systemic progesterone administration results in a partial reversal of the age-associated decline in CNS remyelination following toxin-induced demyelination in male rats. *Neuropathol Appl Neurobiol* **30**, 80-89 (2004).

129 Vázquez, F. *et al.* Progesterone regulates proliferation of endothelial cells. *J Biol Chem* **274**, 2185-2192 (1999).

130 Taraborrelli, S. Physiology, production and action of progesterone. *Acta Obstet Gynecol Scand* **94 Suppl 161**, 8-16, doi:10.1111/aogs.12771 (2015).

131 Stekovic, S. *et al.* The neuroprotective steroid progesterone promotes mitochondrial uncoupling, reduces cytosolic calcium and augments stress resistance in yeast cells. *Microb Cell* **4**, 191-199, doi:10.15698/mic2017.06.577 (2017).

132 Kipp, M., Hochstrasser, T., Schmitz, C. & Beyer, C. Female sex steroids and glia cells: Impact on multiple sclerosis lesion formation and fine tuning of the local neurodegenerative cellular network. *Neurosci Biobehav Rev* **67**, 125-136, doi:10.1016/j.neubiorev.2015.11.016 (2016).

133 Huang, C. C., Shih, M. C., Hsu, N. C., Chien, Y. & Chung, B. C. Fetal glucocorticoid synthesis is required for development of fetal adrenal medulla and hypothalamus feedback suppression. *Endocrinology* **153**, 4749-4756, doi:10.1210/en.2012-1258 (2012).

134 Perrin, J. S. *et al.* Sex differences in the growth of white matter during adolescence. *Neuroimage* **45**, 1055-1066, doi:10.1016/j.neuroimage.2009.01.023 (2009).

135 Stikov, N. *et al.* In vivo histology of the myelin g-ratio with magnetic resonance imaging. *Neuroimage* **118**, 397-405, doi:10.1016/j.neuroimage.2015.05.023 (2015).

136 Rojas, J. I. *et al.* Structural sex differences at disease onset in multiple sclerosis patients. *Neuroradiol J* **29**, 368-371, doi:10.1177/1971400916666560 (2016).

137 Meyer, M. *et al.* The progesterone receptor agonist Nestorone holds back proinflammatory mediators and neuropathology in the wobbler mouse model of motoneuron degeneration. *Neuroscience* **308**, 51-63, doi:10.1016/j.neuroscience.2015.09.007 (2015).

138 Waubant, E. *et al.* Environmental and genetic risk factors for MS: an integrated review. *Ann Clin Transl Neurol* **6**, 1905-1922, doi:10.1002/acn3.50862 (2019).

139 Castelnovo, L. F., Magnaghi, V. & Thomas, P. Expression of membrane progesterone receptors (mPRs) in rat peripheral glial cell membranes and their potential role in the modulation of cell migration and protein expression. *Steroids*, doi:10.1016/j.steroids.2017.09.009 (2017).

140 Hellwig, K. Pregnancy in multiple sclerosis. *Eur Neurol* **72 Suppl 1**, 39-42, doi:10.1159/000367640 (2014).

141 Popescu, C. D. Multiple sclerosis and pregnancy. *Rev Med Chir Soc Med Nat Iasi* **118**, 28-32 (2014).

142 Fabian, M. Pregnancy in the Setting of Multiple Sclerosis. *Continuum (Minneap Minn)* **22**, 837-850, doi:10.1212/CON.0000000000000328 (2016).

143 Gold, S. M. & Voskuhl, R. R. Pregnancy and multiple sclerosis: from molecular mechanisms to clinical application. *Semin Immunopathol* **38**, 709-718, doi:10.1007/s00281-016-0584-y (2016).

144 Dunn, S. E., Gunde, E. & Lee, H. Sex-Based Differences in Multiple Sclerosis (MS): Part II: Rising Incidence of Multiple Sclerosis in Women and the Vulnerability of Men to Progression of this Disease. *Curr Top Behav Neurosci* **26**, 57-86, doi:10.1007/7854_2015_370 (2015).

145 Confavreux, C., Hutchinson, M., Hours, M. M., Cortinovis-Tourniaire, P. & Moreau, T. Rate of pregnancy-related relapse in multiple sclerosis. Pregnancy in Multiple Sclerosis Group. *N Engl J Med* **339**, 285-291, doi:10.1056/NEJM199807303390501 (1998).

146 Heiman, M., Kulicke, R., Fenster, R. J., Greengard, P. & Heintz, N. Cell type-specific mRNA purification by translating ribosome affinity purification (TRAP). *Nat Protoc* **9**, 1282-1291, doi:10.1038/nprot.2014.085 (2014).

147 Doyle, J. P. *et al.* Application of a translational profiling approach for the comparative analysis of CNS cell types. *Cell* **135**, 749-762, doi:10.1016/j.cell.2008.10.029 (2008).

148 Stoppini, L., Buchs, P. A. & Muller, D. A simple method for organotypic cultures of nervous tissue. *J Neurosci Methods* **37**, 173-182 (1991).

149 Vartanian, T., Fischbach, G. & Miller, R. Failure of spinal cord oligodendrocyte development in mice lacking neuregulin. *Proc Natl Acad Sci U S A* **96**, 731-735, doi:10.1073/pnas.96.2.731 (1999).

150 Latendresse, J. R., Warbrittion, A. R., Jonassen, H. & Creasy, D. M. Fixation of testes and eyes using a modified Davidson's fluid: comparison with Bouin's fluid and conventional Davidson's fluid. *Toxicol Pathol* **30**, 524-533, doi:10.1080/01926230290105721 (2002).

151 Newbigging, S., Ward, J. M. & Bolon, B. in *Pathology of the Developing Mouse: A Systematic Approach* (ed Brad Bolon). 133-173 (CRC Press (Taylor & Francis), 2015).

152 Liu, L. *et al.* Clinically relevant progestins regulate neurogenic and neuroprotective responses in vitro and in vivo. *Endocrinology* **151**, 5782-5794, doi:10.1210/en.2010-0005 (2010).

153 Kumar, N. *et al.* Nestorone® as a Novel Progestin for Nonoral Contraception: Structure-Activity Relationships and Brain Metabolism Studies. *Endocrinology* **158**, 170-182, doi:10.1210/en.2016-1426 (2017).

154 Ghoumari, A. M., Baulieu, E. E. & Schumacher, M. Progesterone increases oligodendroglial cell proliferation in rat cerebellar slice cultures. *Neuroscience* **135**, 47-58, doi:10.1016/j.neuroscience.2005.05.023 (2005).

155 Hill, R. A., Medved, J., Patel, K. D. & Nishiyama, A. Organotypic slice cultures to study oligodendrocyte dynamics and myelination. *J Vis Exp*, e51835, doi:10.3791/51835 (2014).

156 Caprariello, A. V. *et al.* Apoptosis of Oligodendrocytes during Early Development Delays Myelination and Impairs Subsequent Responses to Demyelination. *J Neurosci* **35**, 14031-14041, doi:10.1523/JNEUROSCI.1706-15.2015 (2015).

157 Lydon, J. P., DeMayo, F. J., Conneely, O. M. & O'Malley, B. W. Reproductive phenotpes of the progesterone receptor null mutant mouse. *J Steroid Biochem Mol Biol* **56**, 67-77 (1996).

158 Bae, Y. J. *et al.* Reference intervals of nine steroid hormones over the life-span analyzed by LC-MS/MS: Effect of age, gender, puberty, and oral contraceptives.

J Steroid Biochem Mol Biol **193**, 105409, doi:10.1016/j.jsbmb.2019.105409 (2019).

159 Cerghet, M. *et al.* Proliferation and death of oligodendrocytes and myelin proteins are differentially regulated in male and female rodents. *J Neurosci* **26**, 1439-1447, doi:10.1523/JNEUROSCI.2219-05.2006 (2006).

160 González, S. L. & Coronel, M. F. Beyond reproduction: the role of progesterone in neuropathic pain after spinal cord injury. *Neural Regen Res* **11**, 1238-1240, doi:10.4103/1673-5374.189177 (2016).

161 Ryu, C. S., Klein, K. & Zanger, U. M. Membrane Associated Progesterone Receptors: Promiscuous Proteins with Pleiotropic Functions - Focus on Interactions with Cytochromes P450. *Front Pharmacol* **8**, 159, doi:10.3389/fphar.2017.00159 (2017).

162 Piel, R. B. *et al.* A Novel Role for Progesterone Receptor Membrane Component 1 (PGRMC1): A Partner and Regulator of Ferrochelatase. *Biochemistry* **55**, 5204-5217, doi:10.1021/acs.biochem.6b00756 (2016).

163 Connor, J. R. & Menzies, S. L. Relationship of iron to oligodendrocytes and myelination. *Glia* **17**, 83-93, doi:10.1002/(SICI)1098-1136(199606)17:2<83::AID-GLIA1>3.0.CO;2-7 (1996).

164 Kimura, I., Nakayama, Y., Zhao, Y., Konishi, M. & Itoh, N. Neurotrophic effects of neudesin in the central nervous system. *Front Neurosci* **7**, 111, doi:10.3389/fnins.2013.00111 (2013).

165 Shen, E. H., Overly, C. C. & Jones, A. R. The Allen Human Brain Atlas: comprehensive gene expression mapping of the human brain. *Trends Neurosci* **35**, 711-714, doi:10.1016/j.tins.2012.09.005 (2012).

166 Sun, F. *et al.* Pgrmc1/BDNF Signaling Plays a Critical Role in Mediating Glia-Neuron Cross Talk. *Endocrinology* **157**, 2067-2079, doi:10.1210/en.2015-1610 (2016).

167 Heintz, N. Gene expression nervous system atlas (GENSAT). *Nat Neurosci* **7**, 483, doi:10.1038/nn0504-483 (2004).

168 Kasubuchi, M. *et al.* Membrane progesterone receptor beta (mPRβ/Paqr8) promotes progesterone-dependent neurite outgrowth in PC12 neuronal cells via non-G protein-coupled receptor (GPCR) signaling. *Sci Rep* **7**, 5168, doi:10.1038/s41598-017-05423-9 (2017).

169 Jeffries, M. A. *et al.* ERK1/2 Activation in Preexisting Oligodendrocytes of Adult Mice Drives New Myelin Synthesis and Enhanced CNS Function. *J Neurosci* **36**, 9186-9200, doi:10.1523/JNEUROSCI.1444-16.2016 (2016).

170 Ishii, A., Fyffe-Maricich, S. L., Furusho, M., Miller, R. H. & Bansal, R. ERK1/ERK2 MAPK signaling is required to increase myelin thickness independent of oligodendrocyte differentiation and initiation of myelination. *J Neurosci* **32**, 8855-8864, doi:10.1523/JNEUROSCI.0137-12.2012 (2012).

171 Cooke, P. S., Nanjappa, M. K., Yang, Z. & Wang, K. K. Therapeutic effects of progesterone and its metabolites in traumatic brain injury may involve non-classical signaling mechanisms. *Front Neurosci* **7**, 108, doi:10.3389/fnins.2013.00108 (2013).

172 Micevych, P. & Sinchak, K. Estradiol regulation of progesterone synthesis in the brain. *Mol Cell Endocrinol* **290**, 44-50, doi:10.1016/j.mce.2008.04.016 (2008).

173 Lephart, E. D., Lund, T. D. & Horvath, T. L. Brain androgen and progesterone metabolizing enzymes: biosynthesis, distribution and function. *Brain Res Brain Res Rev* **37**, 25-37 (2001).

174 Ishrat, T., Sayeed, I., Atif, F., Hua, F. & Stein, D. G. Progesterone and allopregnanolone attenuate blood-brain barrier dysfunction following permanent focal ischemia by regulating the expression of matrix metalloproteinases. *Exp Neurol* **226**, 183-190, doi:10.1016/j.expneurol.2010.08.023 (2010).

175 VanLandingham, J. W. *et al.* Progesterone and its metabolite allopregnanolone differentially regulate hemostatic proteins after traumatic brain injury. *J Cereb Blood Flow Metab* **28**, 1786-1794, doi:10.1038/jcbfm.2008.73 (2008).

176 Wang, S. S. *et al.* Functional trade-offs in white matter axonal scaling. *J Neurosci* **28**, 4047-4056, doi:10.1523/JNEUROSCI.5559-05.2008 (2008).

177 Wirth, M. M. Beyond the HPA Axis: Progesterone-Derived Neuroactive Steroids in Human Stress and Emotion. *Front Endocrinol (Lausanne)* **2**, 19, doi:10.3389/fendo.2011.00019 (2011).

178 Mensah-Nyagan, A. G. *et al.* Neurosteroids: expression of steroidogenic enzymes and regulation of steroid biosynthesis in the central nervous system. *Pharmacol Rev* **51**, 63-81 (1999).

179 Chung, B. C. Steroid deficiency syndromes in mice with targeted disruption of Cyp11a1. *Endocr Res* **28**, 575, doi:10.1081/erc-120016842 (2002).

180 O'Hara, L., York, J. P., Zhang, P. & Smith, L. B. Targeting of GFP-Cre to the mouse Cyp11a1 locus both drives cre recombinase expression in steroidogenic

cells and permits generation of Cyp11a1 knock out mice. *PLoS One* **9**, e84541, doi:10.1371/journal.pone.0084541 (2014).

181 Dumbell, R. *et al.* Dissociation of Molecular and Endocrine Circadian Rhythms in Male Mice Lacking Bmal1 in the Adrenal Cortex. *Endocrinology* **157**, 4222-4233, doi:10.1210/en.2016-1330 (2016).

182 Gannon, A. L. *et al.* Ablation of glucocorticoid receptor in the hindbrain of the mouse provides a novel model to investigate stress disorders. *Sci Rep* **9**, 3250, doi:10.1038/s41598-019-39867-y (2019).

183 Hu, M. C., Hsu, H. J., Guo, I. C. & Chung, B. C. Function of Cyp11a1 in animal models. *Mol Cell Endocrinol* **215**, 95-100, doi:10.1016/j.mce.2003.11.024 (2004).

184 Shih, M. C. *et al.* Mutation of mouse Cyp11a1 promoter caused tissue-specific reduction of gene expression and blunted stress response without affecting reproduction. *Mol Endocrinol* **22**, 915-923, doi:10.1210/me.2007-0222 (2008).

185 Perez-Garcia, V. *et al.* Placentation defects are highly prevalent in embryonic lethal mouse mutants. *Nature* **555**, 463-468, doi:10.1038/nature26002 (2018).

186 Carbone, E., Borges, R., Eiden, L. E., García, A. G. & Hernández-Cruz, A. Chromaffin Cells of the Adrenal Medulla: Physiology, Pharmacology, and Disease. *Compr Physiol* **9**, 1443-1502, doi:10.1002/cphy.c190003 (2019).

187 Kim, S. J. *et al.* Retinopathy of prematurity: a review of risk factors and their clinical significance. *Surv Ophthalmol* **63**, 618-637, doi:10.1016/j.survophthal.2018.04.002 (2018).

188 Dupin, E., Creuzet, S. & Le Douarin, N. M. The contribution of the neural crest to the vertebrate body. *Adv Exp Med Biol* **589**, 96-119, doi:10.1007/978-0-387-46954-6_6 (2006).

189 Krull, C. E. *et al.* Interactions of Eph-related receptors and ligands confer rostrocaudal pattern to trunk neural crest migration. *Curr Biol* **7**, 571-580, doi:10.1016/s0960-9822(06)00256-9 (1997).

190 Vogel, K. S. & Weston, J. A. The sympathoadrenal lineage in avian embryos. II. Effects of glucocorticoids on cultured neural crest cells. *Dev Biol* **139**, 13-23, doi:10.1016/0012-1606(90)90274-m (1990).

191 De Rasmo, D. *et al.* PBMC of Multiple Sclerosis Patients Show Deregulation of OPA1 Processing Associated with Increased ROS and PHB2 Protein Levels. *Biomedicines* **8**, doi:10.3390/biomedicines8040085 (2020).

192 Barcelos, I. P., Troxell, R. M. & Graves, J. S. Mitochondrial Dysfunction and Multiple Sclerosis. *Biology (Basel)* **8**, doi:10.3390/biology8020037 (2019).

193 Su, K., Bourdette, D. & Forte, M. Mitochondrial dysfunction and neurodegeneration in multiple sclerosis. *Front Physiol* **4**, 169, doi:10.3389/fphys.2013.00169 (2013).

194 Warburton, D. *et al.* Lung organogenesis. *Curr Top Dev Biol* **90**, 73-158, doi:10.1016/S0070-2153(10)90003-3 (2010).

195 Provost, P. R. & Tremblay, Y. Genes involved in the adrenal pathway of glucocorticoid synthesis are transiently expressed in the developing lung. *Endocrinology* **146**, 2239-2245, doi:10.1210/en.2005-0077 (2005).

196 Orentas, D. M. & Miller, R. H. The origin of spinal cord oligodendrocytes is dependent on local influences from the notochord. *Dev Biol* **177**, 43-53, doi:10.1006/dbio.1996.0143 (1996).

197 Szu, J., Wojcinski, A., Jiang, P. & Kesari, S. Impact of the Olig Family on Neurodevelopmental Disorders. *Front Neurosci* **15**, 659601, doi:10.3389/fnins.2021.659601 (2021).

198 Bergles, D. E. & Richardson, W. D. Oligodendrocyte Development and Plasticity. *Cold Spring Harb Perspect Biol* **8**, a020453, doi:10.1101/cshperspect.a020453 (2015).

199 Vallstedt, A., Klos, J. M. & Ericson, J. Multiple dorsoventral origins of oligodendrocyte generation in the spinal cord and hindbrain. *Neuron* **45**, 55-67, doi:10.1016/j.neuron.2004.12.026 (2005).

200 Mathisen, P. M., Pease, S., Garvey, J., Hood, L. & Readhead, C. Identification of an embryonic isoform of myelin basic protein that is expressed widely in the mouse embryo. *Proc Natl Acad Sci U S A* **90**, 10125-10129, doi:10.1073/pnas.90.21.10125 (1993).

201 Berthois, Y., Katzenellenbogen, J. A. & Katzenellenbogen, B. S. Phenol red in tissue culture media is a weak estrogen: implications concerning the study of estrogen-responsive cells in culture. *Proc Natl Acad Sci U S A* **83**, 2496-2500, doi:10.1073/pnas.83.8.2496 (1986).

202 Gao, L. & Miller, R. H. Specification of optic nerve oligodendrocyte precursors by retinal ganglion cell axons. *J Neurosci* **26**, 7619-7628, doi:10.1523/JNEUROSCI.0855-06.2006 (2006).

203 Zhang, C. *et al.* The transcription factor NKX2-2 regulates oligodendrocyte differentiation through domain-specific interactions with transcriptional

corepressors. *J Biol Chem* **295**, 1879-1888, doi:10.1074/jbc.RA119.011163 (2020).

204 Neely, S. A. *et al.* New oligodendrocytes exhibit more abundant and accurate myelin regeneration than those that survive demyelination. *Nat Neurosci*, doi:10.1038/s41593-021-01009-x (2022).

205 Crawford, A. H., Tripathi, R. B., Richardson, W. D. & Franklin, R. J. M. Developmental Origin of Oligodendrocyte Lineage Cells Determines Response to Demyelination and Susceptibility to Age-Associated Functional Decline. *Cell Rep* **15**, 761-773, doi:10.1016/j.celrep.2016.03.069 (2016).

206 Kessaris, N. *et al.* Competing waves of oligodendrocytes in the forebrain and postnatal elimination of an embryonic lineage. *Nat Neurosci* **9**, 173-179, doi:10.1038/nn1620 (2006).

207 Jarjour, A. A. & Kennedy, T. E. Oligodendrocyte precursors on the move: mechanisms directing migration. *Neuroscientist* **10**, 99-105, doi:10.1177/1073858403260751 (2004).

208 Xia, W. & Fancy, S. P. J. Mechanisms of oligodendrocyte progenitor developmental migration. *Dev Neurobiol* **81**, 985-996, doi:10.1002/dneu.22856 (2021).

209 Tsai, H. H. *et al.* Oligodendrocyte precursors migrate along vasculature in the developing nervous system. *Science* **351**, 379-384, doi:10.1126/science.aad3839 (2016).

210 Mathews, E. S. & Appel, B. Cholesterol Biosynthesis Supports Myelin Gene Expression and Axon Ensheathment through Modulation of P13K/Akt/mTor Signaling. *J Neurosci* **36**, 7628-7639, doi:10.1523/JNEUROSCI.0726-16.2016 (2016).

211 Kuhn, S., Gritti, L., Crooks, D. & Dombrowski, Y. Oligodendrocytes in Development, Myelin Generation and Beyond. *Cells* **8**, doi:10.3390/cells8111424 (2019).

212 Barres, B. A. *et al.* Cell death and control of cell survival in the oligodendrocyte lineage. *Cell* **70**, 31-46, doi:10.1016/0092-8674(92)90531-g (1992).

213 Barres, B. A. & Raff, M. C. Axonal control of oligodendrocyte development. *J Cell Biol* **147**, 1123-1128, doi:10.1083/jcb.147.6.1123 (1999).

214 McKinnon, R. D., Matsui, T., Dubois-Dalcq, M. & Aaronson, S. A. FGF modulates the PDGF-driven pathway of oligodendrocyte development. *Neuron* **5**, 603-614, doi:10.1016/0896-6273(90)90215-2 (1990).

215 Pineda-Torra, I., Siddique, S., Waddington, K. E., Farrell, R. & Jury, E. C. Disrupted Lipid Metabolism in Multiple Sclerosis: A Role for Liver X Receptors? *Front Endocrinol (Lausanne)* **12**, 639757, doi:10.3389/fendo.2021.639757 (2021).

216 Berghoff, S. A., Spieth, L. & Saher, G. Local cholesterol metabolism orchestrates remyelination. *Trends Neurosci*, doi:10.1016/j.tins.2022.01.001 (2022).

217 Berghoff, S. A. *et al.* Dietary cholesterol promotes repair of demyelinated lesions in the adult brain. *Nat Commun* **8**, 14241, doi:10.1038/ncomms14241 (2017).

218 Berghoff, S. A. *et al.* Neuronal cholesterol synthesis is essential for repair of chronically demyelinated lesions in mice. *Cell Rep* **37**, 109889, doi:10.1016/j.celrep.2021.109889 (2021).

219 Hubler, Z. *et al.* Accumulation of 8,9-unsaturated sterols drives oligodendrocyte formation and remyelination. *Nature* **560**, 372-376, doi:10.1038/s41586-018-0360-3 (2018).

220 Niu, J. *et al.* Aberrant oligodendroglial-vascular interactions disrupt the blood-brain barrier, triggering CNS inflammation. *Nat Neurosci* **22**, 709-718, doi:10.1038/s41593-019-0369-4 (2019).